POLITECNICO DI MILANO

School of Industrial and Information Engineering
Master of Science in Mechanical Engineering

Investigation of using fiber laser and CMT technology in welding of Docol pipes

Under Supervision of: Prof. Barbara Previtali

Co-Advisor: ING. Bruno Valsecchi

Industrial Advisor: ING. Paolo Conca

M.Sc Thesis of:

Aref Bagheri Matr. 779564

Academic Year 2013-2014

Abstract

This thesis is a collaboration between Polytechnic university of Milan and ABB Company. The aim of this work is investigation on the deformation of DOCOL M pipes caused by welding. Conventional welding process often fails to provide adequate joint in high strength steel and also makes residual stress and deformation in the components, therefore welding with three different unconventional technologies are performed: Proximity laser welding, wobbling laser welding and CMT (Cold Metal Transfer) welding. Possibility and feasibility of these three technologies on three joints configuration (butt joint, flanged joint and lap joint) are studied.

The effects of main process parameters (mainly power and velocity) on the microstructure are studied as well. The planarity of pipes after final welding is measured. For Proximity laser welding the planarity is remained intact but Remote laser welding changes the planarity to some extent. Proximity and Wobbling Laser welding are carried out without filler metal. Therefore the joint has the same chemical composition as the base material and its microstructure consists of martensite. Solidification in the weld metal lead to formation of coarse grains, whereas the heat affected zone (HAZ) remained fine-grained. The HAZ width for proximity laser welding is insignificant and hardness does not change considerably. For wobbling laser welding larger HAZ obtained in respect of proximity laser welding and hardness changes more than the latter one. CMT welding produces acicular microstructure of bainite (corresponding to lower hardness) and very larger HAZ in compares to two other technologies.

The tolerance-cost is also modelled for different technologies. The welding cost is broadly classified in to two categories, namely fixed and variable cost. All in all the tolerance-cost per hour for laser is more than CMT welding.

Keywords: Laser welding, CMT welding, Wobbling, High Strength Steel, Deformation.

Sommario

Questa tesi è una collaborazione tra Politecnico di Milano e la Società ABB.
La giunzione degli acciai alto resistenziali presenta particolare difficoltà se eseguita con tecniche convenzionali, infatti l'alto impatto temrico di questi processi provoca elevate deformazioni e stress residui, particolarmente critici per le sollecitazioni a fatica. Per questo motivo le tecniche convenzionali di saldatura non sono in grado di assicurare, il più delle volte, una perfetta e durevole giunzione.
In tal senso questo lavoro ha come obiettivo principale l'investigazione della deformazione residua a seguito di saldature con basso impatto energetico, come quelle laser o le cosiddette cold metal transfer (CMT), il materiale preso in esame è un alto resistenziale, in particolare dei tubi di DOCOL M. Le tecnologie sopracitate sono state studiate per differenti tipologie di giunto così da poter capire anche quale geometria si adattasse meglio alla particolare tecnologia.

Verranno presentati gli effetti dei parametri principali di processo (potenza e velocità) sui giunti con un'analisi metallurgica ed in seguito calcolando le deformazioni ottenute su dei prototipo reali. L'analisi metallurgica sarà svolta ottenendo le sezioni del giunti e andandone a studiare la microstruttura a seguito di attacchi chimici, come è noto, la microstruttura delle saldatura laser rimarrà all'interno di quelle possibili per gli acciai alto resistenziali, in quanto questo tipo di saldatura è autogena (sena materiale d'apporto), Al contrario la saldatura CMT avrà una modificazione nella zona del cordone, proprio dovuta al filo d'apporto immesso con questo processo.

Un'altra caratteristica importante da sottolineare per il sistema laser è che sono state eseguite delle prove anche con la testa a scansione, ciò ha dato la possibilità di capire l'effettiva utilizzabilità delle nuove tecniche di woobling in presenza di gap.

In ultimo è stato sviluppato anche un modello di costo per quantificare in termini economici l'investimento relativo alle tecnologie usate, il modello è stato fatto in relazione al caso industriale affrontato

Parole chiave: Saldatura laser , Oscillante, Saldatura CMT, Acciaio alto-resistenziale,

Deformazione.

Acknowledgments

I would like to thank my dear Supervisor and Co-Advisor, Professor Barbara Previtali and Dr. Bruno Valsecchi for their full support throughout the entire duration of the project. Special thanks to Mr. Paolo Conca for the opportunity to perform technical work in ABB Company, and for his hospitality. I also would like to thank everybody in the company for the support, especially to Mr. Paolo Cepollaro.

I also want to thank Mr. Giovanni Riva and Dr. Ali Gokhan Demir for providing necessary information regarding the research. I would like also to thank my parents for supporting me during my whole life and my sisters who have always motivated me. At last but not least gratitude goes to all of my friends who directly or indirectly helped me to complete this thesis. I want to say a big thank you to my dear friends, Reza, Kian, and Lorenzo.

Table of Contents

Table of Figures

List of Tables

Chapter 1: Introduction

This research is collaboration between SITEC - Laboratory for laser applications of Politecnico di Milano, technical department of ABB Company and Socage Company. Socage Company's requirement is welding of joint in Docol pipes. Pipes are meant to be use in arm of Socage cranes. Conventional welding such as TIG and MIG welding fail to make a good weld on the pipes and often cause big deformation in pipes. In this thesis welding with different technologies which input less heat to the pipes are compared to each other. Laser welding is performed in SITEC-Laboratory and CMT welding is performed in ABB Company of Italy.

Experiment has been performed on DOCOL M cold reduced martensitic steel pipes. The HSS Docol 1200M, is a fully martensitic steel produced by water quenching from an elevated temperature in the austenitic range supplied by Swedish Steel Ltd. (SSAB). It was delivered as a 1.5mm thickness pipe from Socage Company. Docol M is largely used in the crash management systems. Because of their security function these types of products have to combine characteristics like light weight, high structural Performances and low costs.

The objective of this work is investigation and minimization of the pipes deformation caused by welding with three different technologies: Fiber Laser Welding, Wobbling Laser Welding and CMT (Cold Metal Transfer) welding. The pipes are meant to be used in the arm of Socage Crane. The previous welding problem with conventional methods was that pipes were deformed and the planarity of pipes changed a lot. This problem can be fixed using technologies which input less heat in to the components such as laser welding and CMT welding. The experiments related to laser welding are done in SITEC laboratory for laser applications in Politecnico di Milano. And CMT experiments were performed in ABB Company.

The power density in laser welding is extensive and about 4 orders of magnitude higher than in conventional welding methods. This is why its influence on the parent metal close to the weld is considerably lower and the microstructure degradation is minimal. CMT is also input less heat in compare to MAG and TIG welding which are commonly used in the industries. Thanks to its characteristic feature of alternating thermal arc pool, i.e. hot when

an arc is initiated and cold when the arc is extinguished and the wire is retracted. This alternating hot and cold treatment has been made possible by a new technological development from Fronius International LLC that incorporates the wire motions into the process control via a computer monitoring system. All these three technologies input less heat to the component in respect to conventional methods of welding such as TIG and MIG welding.

In this study also the effect of laser wobbling welding on the deformation and microstructure of the pipes is analyzed. Wobbling laser welding benefits from three major advantages over traditional laser welding with short focal length optics - the high-speed of the intra-weld beam movement contributes to a significant reduction of the cycle time, The long stand-off of the focusing head permits access to areas not accessible with short focal length, Whereas in conventional laser processing the work head is close to the work, with wobbling laser welding, there is a standoff distance.

Consequently, there is the ability to effectively move the beam around with mirrors far more efficiently than if the laser is on a stationary mechanism, such as a robot arm. Finally the most important characteristic which is used in the experiment is that it also benefits of stirring the spot dimension for compensating the gap. Since joints configurations are simple and linear, mostly the advantage of stirring the spot dimension in order to compensate the gap is taken.

The laser head used for this experiment is Scan fiber Laser Processing Head, a product of Electronic, Engineering group (El.En) company, with the high scanning speed and scanning acceleration. The work statement will be started by reviewing the state of arts which discusses the material's general and specific characteristics and welding methods carried out on it. These discussions continue by giving information regarding to weld bead quality which has been reported in literature. All the information in this chapter is based on accredited sources such as international standards and publications.

After comes the objectives of the work which are intended to be investigated, such as decreasing the pipes deformation and obtaining good weld property and also cost modeling are explained. Three joint configurations are analyzed: lap joint, butt joint and flanged joint. The most suitable configuration for proximity laser welding is the lap joint. Using high

power laser welding with high velocity makes it possible to make the deformation of pipes almost intact. The planarity of components measured before and after welding.

The difference between before and after welding planarity is negligible. Good penetration is obtained in this welding as well. Even if the big gap is present in the butt joint, using laser wobbling method is satisfactory in this case. The change in planarity of the pipe before and after welding using wobbling technique is more than proximity laser welding. CMT method is applied on the Butt joint as well.

The advantage of CMT technique is that it is not sensitive to the gap. The nature of CMT welding is a rule based task. Majority parameters are chosen with machines automatically and it is an easy applicable method of welding. On the contrary more heat affected zone and more deformation are presented in the pipes welded with CMT welding.

Chapter 2: State of the art

This chapter discusses the HSS welding methods particularly the fiber laser welding and CMT welding by providing the parameters affecting the weld, weld composition and quality. Laser welding and CMT welding process parameters and their effects on the weld bead are explained in this chapter as well. It also deals with a detail explanation of properties and metallurgical specification of HSS (high strength steel, DOCOL M) used in the experiment.

2.1 Material – DOCOL M

Advanced high strength steels (AHSS) are promising solutions for the production of lighter automobiles with increased passenger safety and reduced fuel consumption [1]. AHSS grades include: (a) Dual-phase (DP) steels, which consist of a dispersion of islands of hard martensite (5‑20% by volume) in soft ferrite matrix. These steels are characterized by high work hardening and are used in automobile components that require high strength, good crashworthiness and reasonable formability. (b) Transformation-induced plasticity (TRIP) steels that offer high strength and toughness combination with excellent uniform elongation. TRIP steels have the ability to absorb more energy during crash due to the delayed transformation of retained austenite to martensite. They have a microstructure consisting of various fractions of ferrite, martensite, bainite and retained austenite, giving them their unique balance of properties. However, the higher percentage of alloying content and thermal cycle in welding, limits its weldability resulting in inferior microstructure and mechanical properties of the weld. (c) Boron-alloyed (MN) steels, trademarked as USIBOR, which are more widely used by automakers today. Essentially this steel is hot stamped by heating the blank to austenitization temperature, press formed and die-quenched, resulting in very hard phases that give rise to extreme tensile strength of 1500 MPa.

The HSS Docol 1200M, is a fully martensitic steel produced by water quenching from an elevated temperature in the austenitic range [2], supplied by Swedish Steel Ltd [3]. It was delivered as a 1.5 mm thickness pipe from Socage Company.

These steels are manufactured using heat treatment in a continuous annealing line. The ultra-high strength is produced by fast water quenching from an elevated austenitic temperature range. Table 2-1 gives the nominal chemical composition of the material [3]. The nominal yield strength is reported from the manufacturer to be in the range from 950 Mpa to 1150 Mpa, while the nominal tensile strength is reported to be between 1200MPa and 1400 Mpa.

Steel grade	C %	Si %	Mn %	P %	S %	Alto %	Nb %	Ti %
Docol 1200M	0,11	0,20	1,70	0,010	0,002	0,040	0,015	0,025

Table 2-1 Chemical composition of Docol 1200M

The strength of weld joints with Docol M is higher than conventional high strength steels. In figure 1 the tensile strength of weld is compared with tensile strength of parent material.

Docol M is largely used in the crash management systems. Because of their security function these types of products have to combine characteristics like light weight, high structural performances and low costs. In the fallowing the general mechanical properties of DOCOL M is listed, the plots are taken from [4]. In the Figure 2-1 the tensile curve is reported.

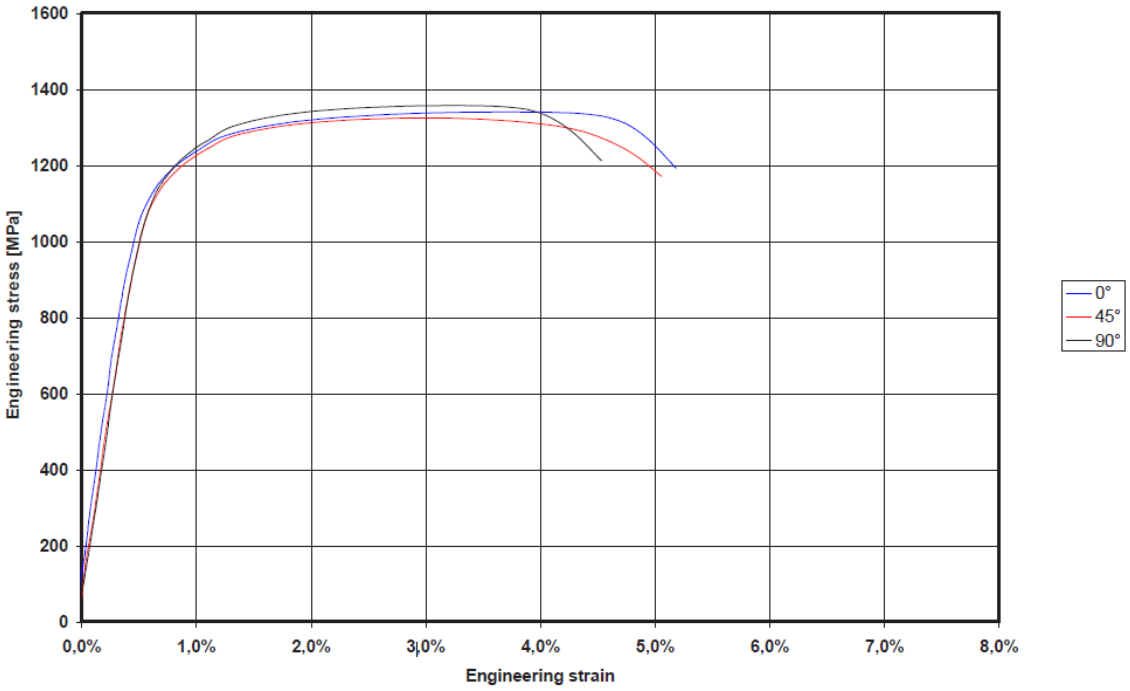

Figure 2-1 Stress-strain relationship for Docol 1200 M 1.5 mm thickness

In the Figure 2-2 the FLD curve is plotted. A forming limit diagram, also known as a forming limit curve, is used in sheet metal forming for predicting forming behavior of sheet metal [5]. The diagram attempts to provide a graphical description of material failure tests, such as a punched dome test.

In order to determine whether a given region has failed, a mechanical test is performed. The mechanical test is performed by placing a circular mark on the work piece prior to deformation, and then measuring the post-deformation ellipse that is generated from the action on this circle. By repeating the mechanical test to generate a range of stress states, the formability limit diagram can be generated as a line at which failure is onset

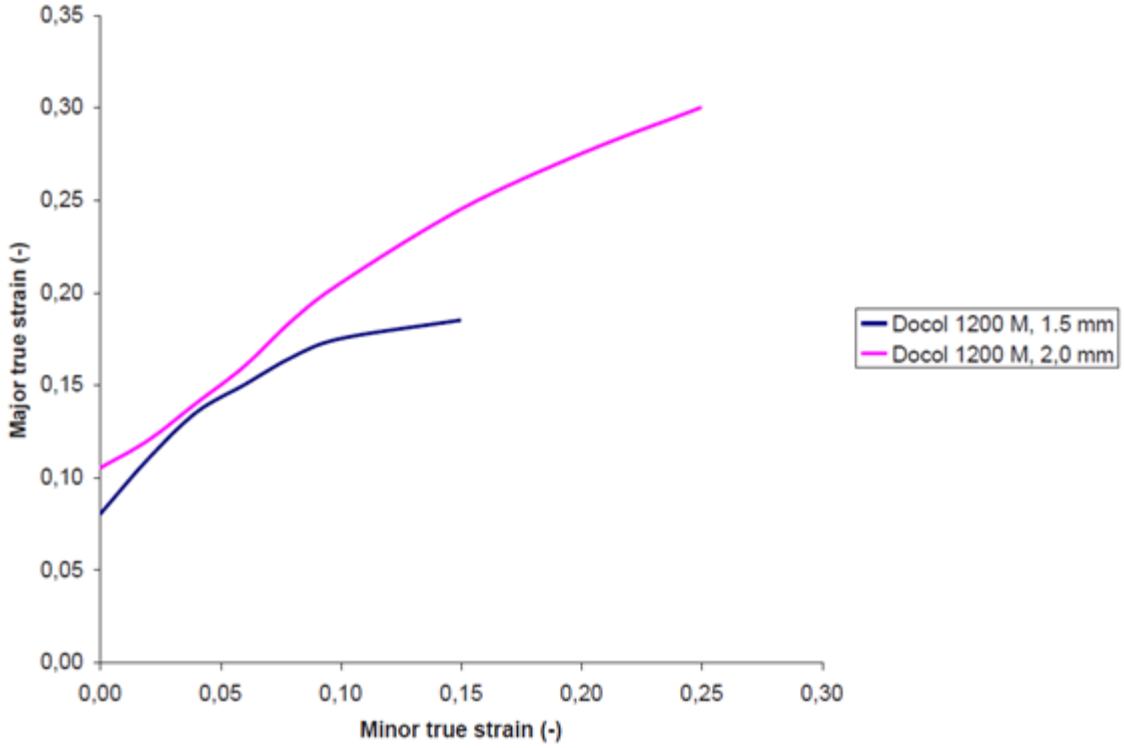

Figure 2-2 Forming limit curves for Docol 1200 M

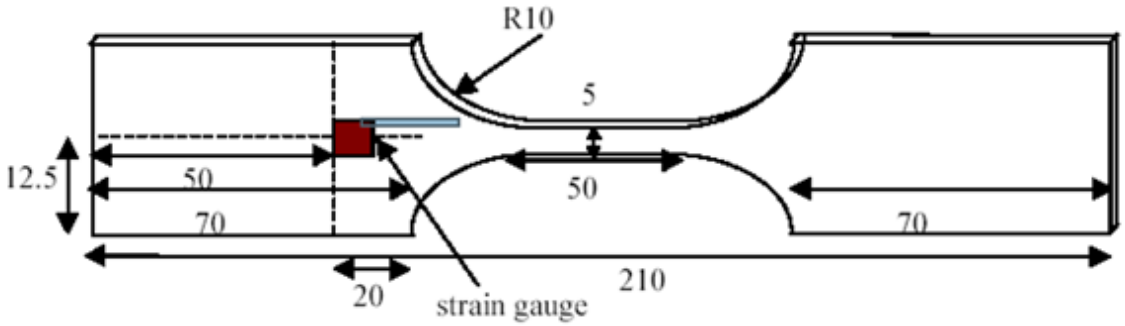

Figure 2-3 Tensile specimen geometry used in the test at both standard and high strain rate, values are in [mm]

True stress-strain curves from tensile tests performed on Docol 1200 M, 1.5 mm thickness. Blue lines Represent testing at standard strain rate and red lines represent testing at high strain rate. It is important to underline that this results are not so much different from the ones reported in Fig 2-4 taking into account that in this figures True stress and strain are shown while in the previous figure the engineering results are shown. The specimen used in the test at both standard and high strain rate is reported in Figure 2-3.

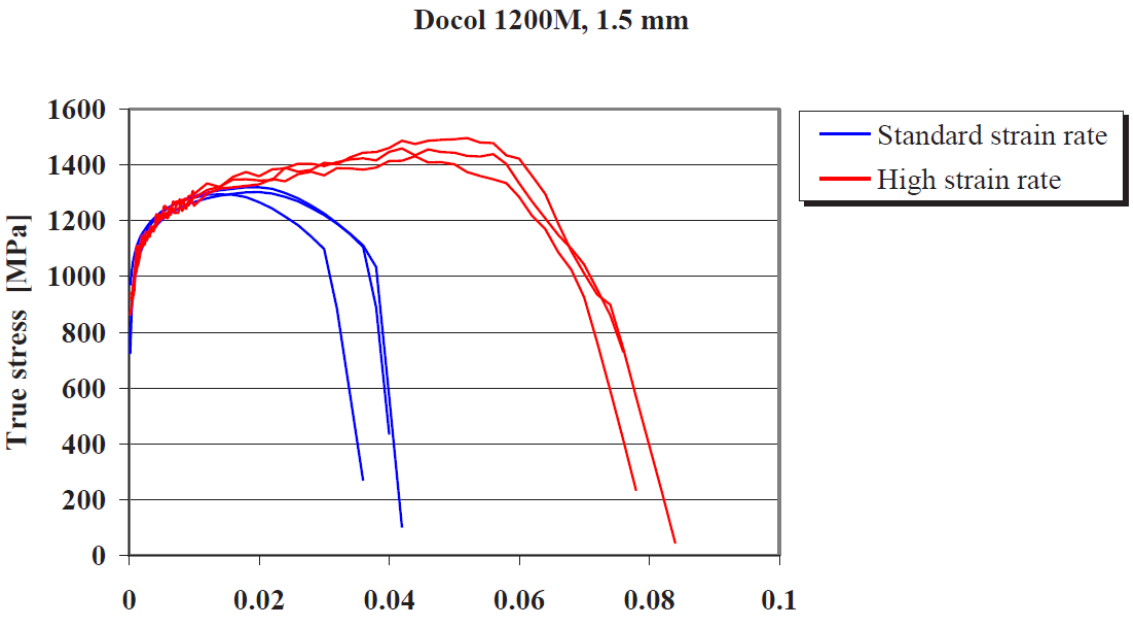

Figure 2-4 True stress-strain curves from tensile tests performed on Docol 1200M, 1.5 mm.
Blue lines represent testing at standard strain rate and red lines represent testing at high strain rate.

2.2 Description of joints

This chapter is dedicated to description of different mechanical joints which are used in the experiment. The American Welding Society defines a joint as “the manner in which materials fit together.” As shown in Figure 2-5, there are five basic types of weld joints: Butt joint, T-joint., Lap joint, Corner joint and Edge joint [6].

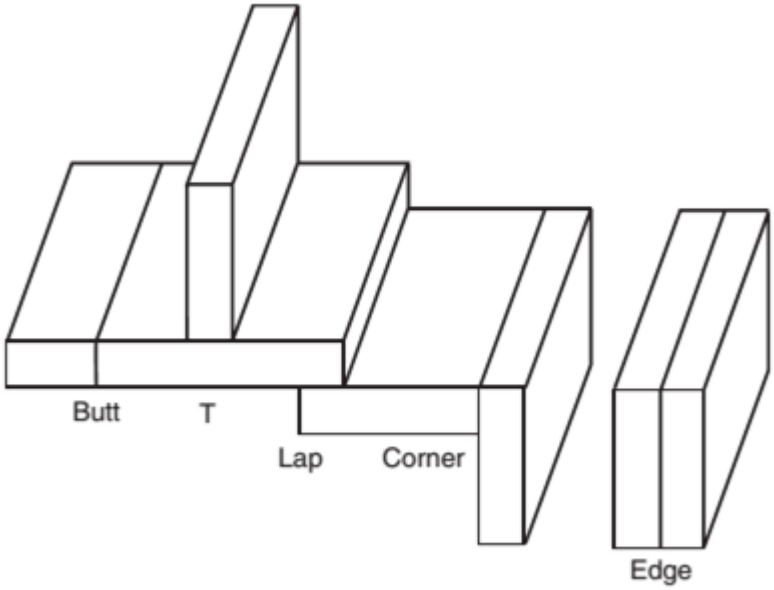

Figure 2-5 Five different joints which are used in welding

Three different joints are used in the study included: Butt joints, edge flange joints and lap joint. In this study Edge flange joint is simply called flange.

Butt welding is a welding technique used to connect parts which are nearly parallel and don't overlap. It can be used to run a processing machine continuously, as opposed to having to restart such machine with a new supply of metals. Butt-welding is an economical and reliable way of jointing without using additional components.

Usually, a butt-welding joint is made by gradually heating up the two weld ends with a weld plate and then joining them under a specific pressure. This process is very suitable for prefabrication and producing special fittings. Afterward, the material is usually ground down to a smooth finish and either sent on its way to the processing machine, or sold as a completed product.

This type of weld is usually accomplished with an arc or MIG welder. It can also be accomplished by brazing. With arc welding, after the butt weld is complete, the weld itself needs to be struck with a hammer forge to remove slag (a type of waste material) before any subsequent welds can be applied. This is not necessary for MIG welds however, as a

protective gas removes any need for slag to appear. Another advantage with a MIG welder is that a continuous copper wire is fed onto the stock, making the weld virtually inexhaustible [7]. Butt joints are used where high strength is required. They are reliable and can withstand stress better than any other type of weld joint. To achieve full stress value, the weld must have 100 percent penetration through the joint. This can be done by welding completely through from one side. The alternative is working from both sides, with the welds joining in the center. Different possible butt joints are shown in Figure 2-6.

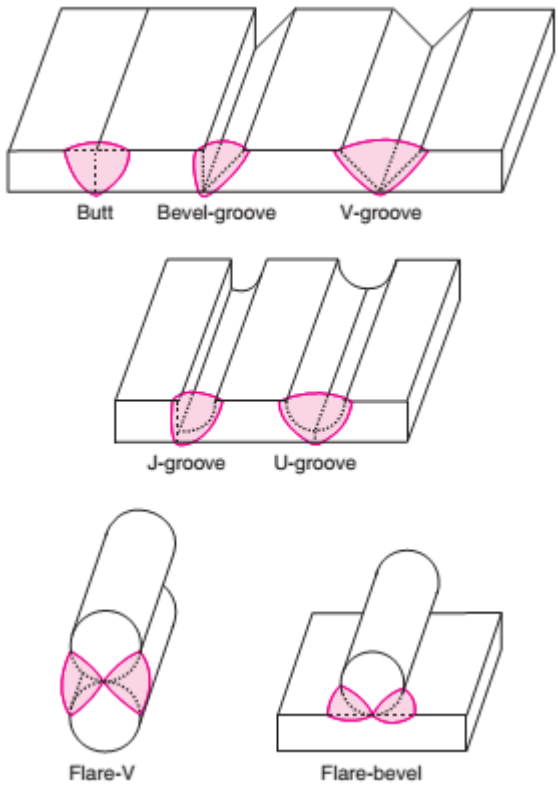

Figure 2-6 Different types of butt joint

Expansion of the base metal during welding often will cause a condition known as mismatch, Figure 2-7.

When mismatch occurs, the weld generally will not penetrate completely through the joint. Many specifications limit highly stressed butt joints to a 10 percent maximum mismatch of the joint thickness.

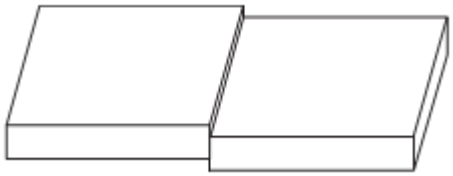

Figure 2-7 Welds made on mismatched joints often will fail below the rated load when placed in stress conditions

Whenever possible, butt joints should mate at the bottom, Figure 2-8. Joints of unequal thickness should be tapered in the weld area to prevent incomplete or inadequate fusion. When this cannot be done, the heavier piece may be tapered on the upper part of the joint as well.

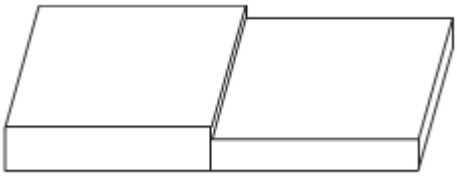

Figure 2-8 Mating the joint at the bottom equalizes the load during stress

Weld shrinkage, Butt welds always shrink across the joint (transversely) during welding. For this reason, a shrinkage allowance must be made if the “after welding” overall dimensions have a small tolerance.

Lap joints may be single fillet, double fillet, plug slot, or spot-welded. They require very little joint preparation. They are generally used in static load applications or in the repair of uni-body automobiles. Where corrosive liquids are involved, both edges of the joint must be welded. See Figure 2-9. One of the major problems with lap joint design is shown in Figure 2-10. Where the component parts are not in close contact, a bridging fillet weld must then be made. This leads to incomplete fusion at the root of the weld and oversize fillet

weld dimensions. When using this type of design in sheet or plate material, clamps or tooling must be used to maintain adequate contact of the material at the weld joint.

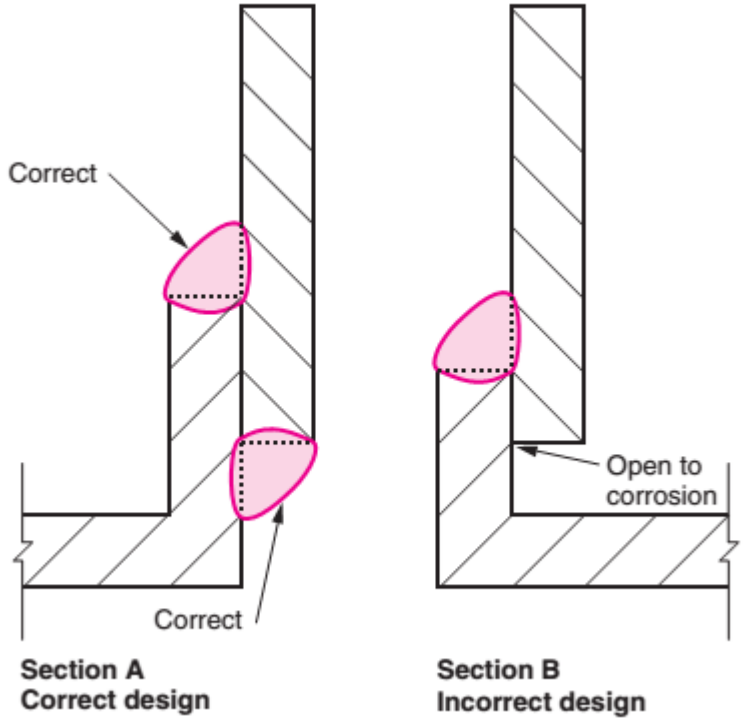

Figure 2-9 Corrosive liquid must not be allowed to enter the penetration side of weld joint

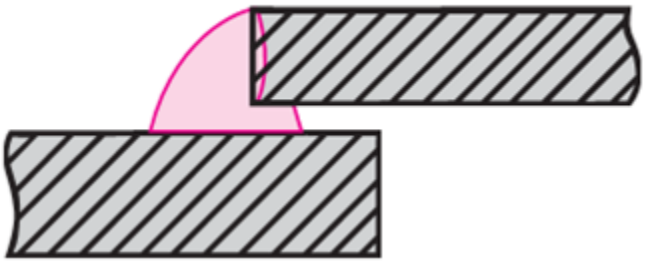

Figure 2-10 Lap joint problem areas that result from improper fit-up

Edge welds are used where the edges of two sheets or plates are adjacent and are in approximately parallel planes at the point of welding. Figure 2-11and 2-12 shows several types of edge weld designs. These designs are common only in structural use. Since the weld does not penetrate completely through the joint thickness, it should not be used in stress or pressure applications.

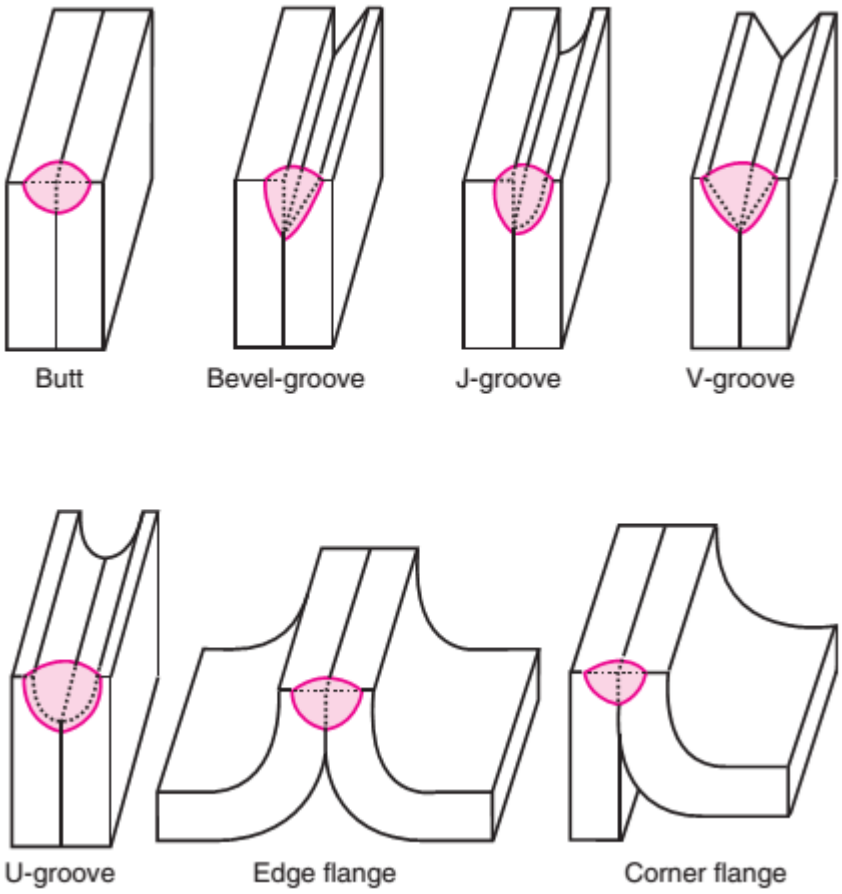

Figure 2-11 Types of weld that may be made with basic edge joint

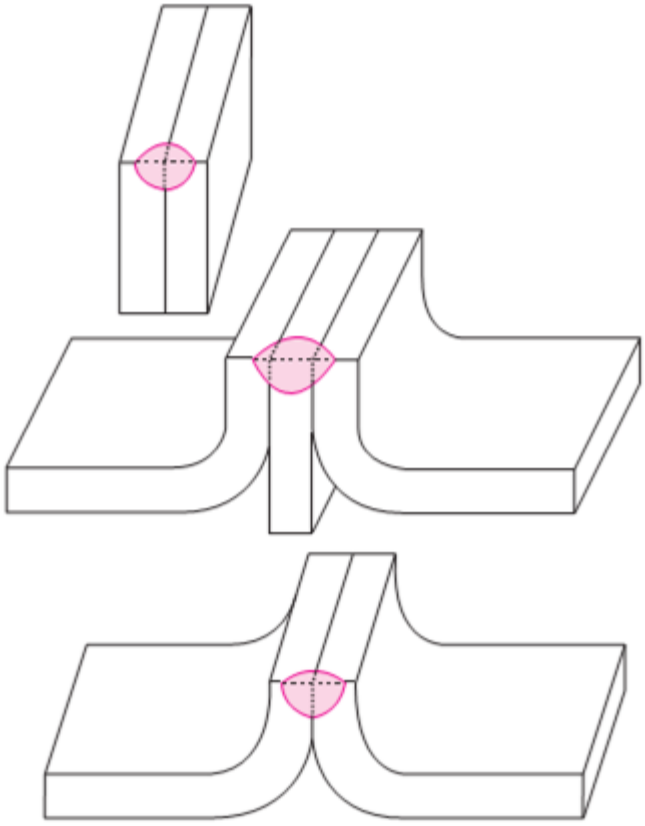

Figure 2-12 Common edge weld design that maybe used in fabrication

2.3 Laser welding of HSS

This section starts with introduction of laser welding and then it deals with a detail explanation of main process parameters which affects the weld quality for different laser technologies, proximity laser welding and wobbling laser welding technique used in the experiments.

2.3.1 Overview

Welding with laser beams is a process that takes place in a series of steps. Laser beam welding (LBW) is a welding technique used to join multiple pieces of metal through the use of a laser. The beam provides a concentrated heat source, allowing for narrow, deep

welds and high welding rates. The steps involved are inherently multidisciplinary, requiring knowledge from several branches of physics. A brief summary of the nature of laser beam interactions with materials and how heat is delivered from the beam into the part being welded is presented in ASM Handbook, "Laser Beam Welding, Welding Fundamentals and Process [8].

Laser interactions with metals are dominated by the effects of conduction (free) electrons at the metal surface. Absorption of the laser energy by these electrons occurs very rapidly, on the order of 10^{-13} s, and in a very shallow region of the metal surface, 10 to 100 nm, which is shorter than the wavelength of the laser. The photon energy excites the free electrons and gives them excess kinetic energy.

The excess kinetic energy is then transferred to the metal atoms through large numbers of elementary collisions and various energy-transfer mechanisms, creating heat as the excited electrons deposit their excess energy into the atomic lattice. This process of converting the laser energy into heat is called thermalization, and it produces a highly localized heat pulse on the surface of the metal where irradiation occurred. The thermalized heat can then macroscopically flow from this region into the remaining portion of the substrate, as described by classical heat-flow methods (conduction, convection, and radiation heat-transfer mechanisms).

During laser welding, the energy rise must be sufficient to melt the surface, and during keyhole welding, the energy rise must be sufficient to vaporize the substrate. Under the conditions where vapors are being created, the laser interaction becomes more complicated, because it must pass through this vaporized column to reach the metal surface.

The hot vapor column becomes partially ionized and can absorb photons through interactions with the thermally excited atoms and through the ions or free electrons in the ionized plasma. There are two different modalities to perform laser welding process, in function of the irradiance, Conduction mode for all the types of material Deep penetration mode: Key-hole only for metallic materials, this two modalities are discussed in the fallowing section.

Lasers are capable of both conduction-mode welding and deep-penetration welding.

- ✓ Conduction-Mode Welding

Momentum transfer or convection dominates conduction-mode welding. High power density (10^5 to 10^7 W/cm2) in laser welding produces a temperature gradient of the order of 10^6 K/cm, which in turn leads to surface-tension-driven thermo capillary flow (Marangoni convection) with surface velocities of the order of 1 m/s. Convection is the single most important factor affecting the geometry of the laser melt pool (that is, pool shape, aspect ratio, and surface ripples) and can result in defects such as variable penetration, porosity, and lack of fusion. Convection is also responsible for mixing, and it therefore affects the composition of the melt pool during laser welding.

- ✓ The pool configuration.

In conduction-mode laser welding is a function of the Prandtl number of the materials (Prm)-defined as the ratio of kinematic viscosity to molecular.

- ✓ Diffusivity

In materials with low Prandtl numbers (for example, aluminum with Prm = 0.02), the pool shape is more spherical and is dominated by conduction heat transfer. In contrast, a material with a high Prandtl number (for example, steel with Prm = 0.1) results in a pool shape that is shallow and wide, because it is dominated by the surface-tension-driven flow. Free surface deformation leading to defects such as undercuts is also influenced by convection. A small amount of surface reactant elements (for example, sulfur or oxygen) can change the convection direction. For most metals, thermo capillary flow drives the hot metal to the cold side, but the addition of sulfur changes the sign of the temperature-dependence function of the surface tension and drives the liquid metal to the center of the pool [9].

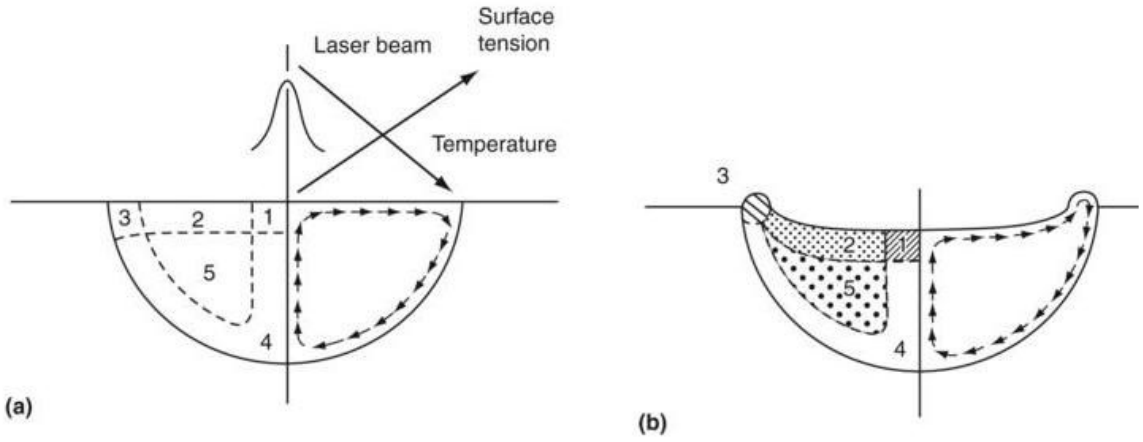

Figure 2-13 Schematic showing effect of convection on laser beam welding melt pool configuration

In Figure 2-13 spherical shape with flat surface typical of low-Prm materials. (b) Shallow and undercut free surface characteristic of high-Prm materials. Numbers in the Figure identify specific regions: 1, stagnation flow region; 2, free surface boundary-layer region; 3, cooled corner region; 4, solid-liquid interface boundary-layer region; 5, isothermal in viscid core.

- ✓ Deep-Penetration-Mode Welding

The mechanism of deep-penetration welding by a laser beam is very similar to that encountered with an electron beam (that is, energy transfer is via “keyhole” formation). This keyhole may be produced when a beam of sufficiently high power density causes vaporization of the substrate and the pressure produced by the vapor in the crater causes displacement of the molten metal upward along the walls of the hole (Figure 2-14). This hole acts as a blackbody, aiding the absorption of the laser beam as well as distributing the heat deep in the material. The energy in most conventional welding processes is deposited at the surface of the work piece and brought in to the interior by conduction.

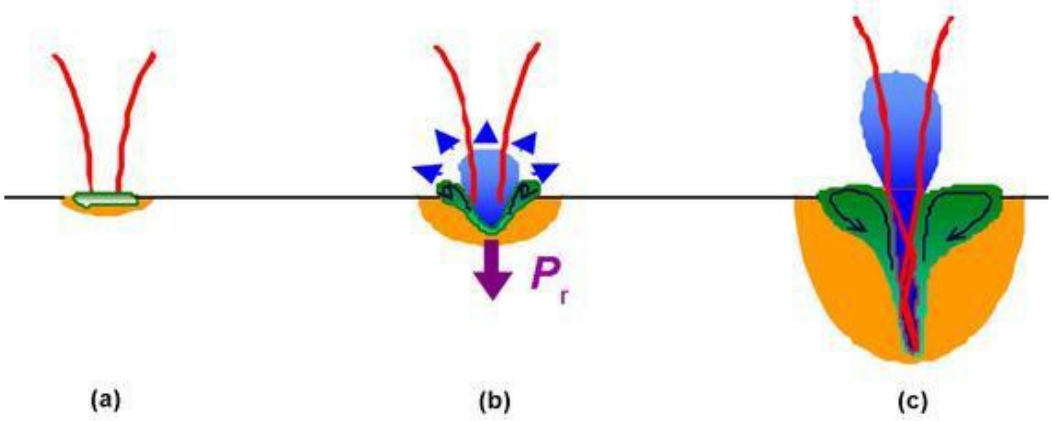

Figure 2-14 Forming of a narrow and deep capillary of vapor, or a keyhole

The keyhole or cavity is formed only if the beam has sufficient power density. The keyhole is filled with gas or vapor created by continuous vaporization of wall material by the beam. This Cavity is surrounded by liquid that, in turn, is surrounded by solid. The flow of the liquid and the surface tension tend to obliterate the cavity, while the vapor, which is continuously generated, tends to maintain the cavity. There is a continuous flow of Material out of the cavity at the point where the beam enters. For a moving beam, this keyhole achieves a steady state (that is, the cavity and the beam associated with the molten zone move forward at the speed set by the advance of the beam).

In viscid with no viscosity the material lost by vaporization shows up as a depression in the solidified melt as porosity, as an inward deformation of the work piece, or possibly as a combination of these effects. The Requirement that sufficient vapor be produced to maintain a steady state leads to a minimum Advance speed for a steady state. While the cavity moves through the solid and liquid material at a speed determined by the motion of the beam, materials must be moved continuously from the Region ahead of the cavity to the region behind it.

Figure 2-15 shows how the laser beam Interaction with the work piece produces keyhole plasma in the work piece and surface plasma above the work piece. The relative positions of the HAZ, weld pool, and convection pattern within the weld are also shown.

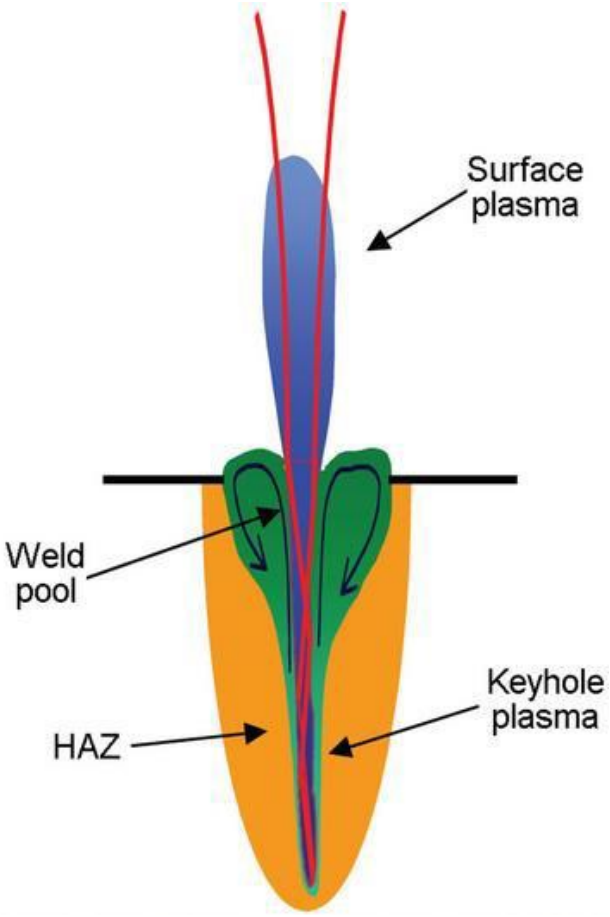

Figure 2-15 Schematic of keyhole plasma and surface plasma, HAZ, and heat-affected zone

2.3.2 Laser welding process parameters and their effects

They are a lot of independent process variables for laser welding such as incident laser power, material dependent absorptivity, beam product parameter, shielding gas, depth of penetration and microstructure and metallurgical properties, laser beam power and welding speed.

The effects of some of the important variables are discussed comprehensively in ASM [8]. However this Study regards mainly to effect of laser beam power and welding speed on the weld quality and deformation of the components. These two process parameters are explained in the following:

- ✓ Laser Beam Power

The depth of penetration with laser welding is directly related to the power density of the laser Beam and is a function of incident beam power and beam diameter. For a constant beam diameter, penetration typically increases as the beam power is increased. The penetration Increases almost linearly with incident laser power. It is generally observed that for LBW of a Particular thickness, a minimum threshold power is required to initiate melting and form a weld Pool. Laser power divided by spot area size is called irradiance.

$$I = \frac{P}{S}$$ *I*: Power density [W/cm²] (Irradiance)

- ✓ Welding Speed

The correlation of penetration depth relative to welding speed with both LBW and EBW Processes was studied by Duley [7]. The penetration in the laser weld is consistently less than that obtained with an electron beam, but the relative difference between the two penetrations Depths diminishes as the welding speed is increased. However, Duley found this somewhat surprising because the time to form a void or keyhole depends on the laser beam illumination Time for a particular area on the surface of the work piece as the welding speed is increased.

When this occurs, the average power dissipated in the sheet is expected to drop because the Keyhole is no longer a completely effective trap for the incident laser radiation. For an electron Beam, absorptivity of the material is independent of the shape and extent of the keyhole. Hence the total power dissipated in the work piece is less dependent on the welding speed. However for Very low welding speeds, the penetration depth of laser welds becomes significantly less than that attainable with the electron beam. This can be attributed to the formation of a plasma cloud, which attenuates the incident beam.

2.3.3 Fiber lasers welding

Fiber lasers essentially consist of a doped fiber where the laser is produced, an excitation source, and a beam delivery system. The fiber laser is unique in that the lasing media is contained within an optical fiber. Broad area multimode pump diodes surrounding the fiber

are then used to invoke the doped fiber to produce photons [10]. A general schematic of these components is shown in Figure 2-16. The diode laser is used to excite the doped fiber and produce the emission of photons which, due to the fiber's refractive nature, are contained within the strand and propagate back and forth along its length. To prevent the uncontrolled escape of photons in the fiber ends, Bragg gratings are created in the fiber.

These gratings are created by intense ultra-violet light that writes a periodic change in the refractive properties of the affected area. [11]. The Bragg gratings act as high-efficiency mirrors in the fiber and can be modified for a specific desired wavelength which allows fiber laser beams to be created with a range of wavelengths. The reflection within the fiber between the two sets of Bragg gates set up a resonance similar to the two previous laser systems that produce a single phase collimated beam with a wavelength between 1060 and 1070 nm. The output laser generally goes through additional beam collimators to eliminate any residual aberrant elements and to focus the beam to the final desired spot size.

Fiber lasers have only recently become viable as high-power laser sources [12]. Initial equipment expenses are more than offset over the laser's life cycle due to the fact that it requires almost no maintenance,

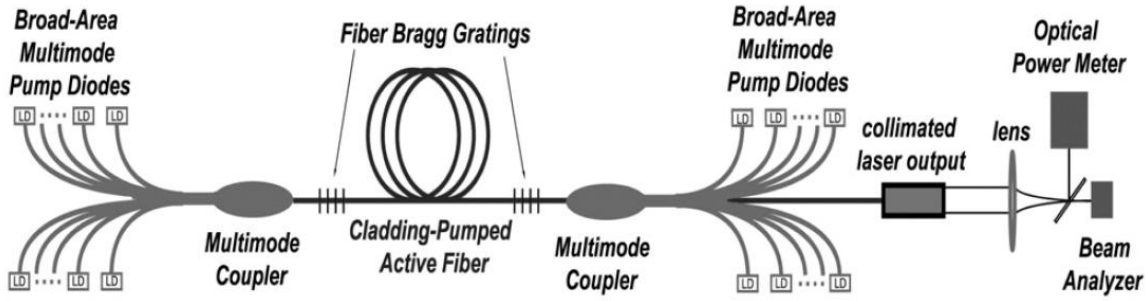

Figure 2-16 Schematic of a general fiber laser set up[10]

It does not require additional cooling, and has one of the highest wall-plug efficiencies of any laser beam process (between 25 and 30%). Also, the resulting beam experiences less divergence than other comparable laser beams [10]. How- ever, with the mature and industrialization of fiber laser technology, a new generation of high power laser–fiber laser has obtained rapid development due to its advantages of high power, high beam quality and high efficiency to produce deep penetration welds at high welding speeds [13]. High

power fiber laser welding process has the potential for high productivity. The low heat input used, minimize welding risks like cold cracking and excessive extensions of the heat affected zones. [14] has studied the characterization of fiber laser welds on X100 high strength steel. A systematic study on overlap welding properties of auto body galvanized steel is conducted by [15] using the late-model fiber laser and CO 2 laser respectively.

The welding joints surface formation, cross-sectional weld shape and mechanical properties of the two types of lasers are compared, and it is analyzed whether dissimilar laser sources would impact the welding quality, so as to control and optimize the craft quality of laser welding automobile body. The results show that under the test conditions, the weld fusion width presents wide at the top and narrow at the bottom and the cross-sections of overlap joints take a ‘‘Y’’ shape by using CO2 laser welding, while those by using fiber laser welding have shape like ‘‘I’’ which was mean the fusion widths of the upper and lower surface are almost the same. And the anti-shearing force of fiber laser welding joints was stronger due to its larger inter-sheet joint connection width. In addition, under certain conditions, the fiber laser welding could result in more uniform and finer joints, higher strength and hardness, and better mechanical properties. The active medium of a fiber is a core of the fiber doped with a rare earth. Most commonly, this is a single-mode fiber laser made of silica. The pump beam is launched longitudinally along the fiber length and it may be guided by either the core itself, as occurs for the single-mode lasers or by an inner cladding around this core (double-clad fiber laser) as shown in Fig 2-17.

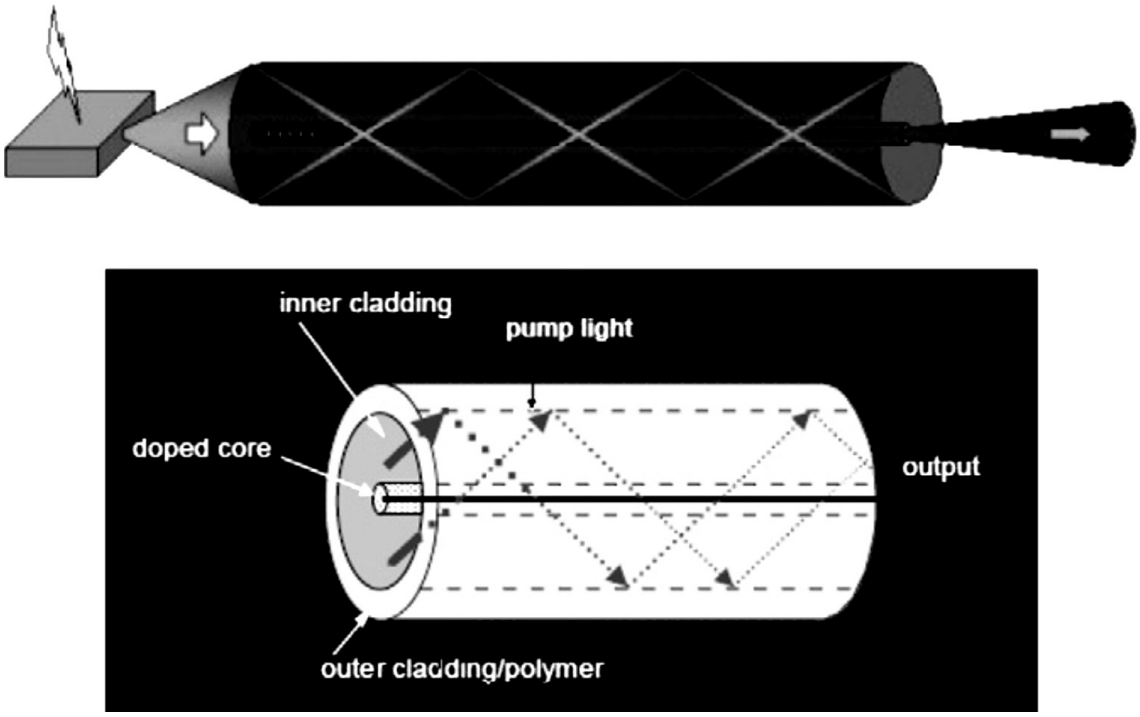

Figure 2-17 Double clad fiber laser

In a fiber laser, a silica ‘‘active’’ fiber doped with erbium, ytterbium, neodymium or thallium, is excited by a diode laser source. Two Bragg gratings, which reflect a predetermined narrow or broad range of wavelengths of light incident on the grating while passing all other wavelengths of the light, are written into the fiber generating the laser emission and result in an efficient, compact laser source with high beam quality. The outer cladding is made of glass or polymeric material, with low refraction coefficient, in order to prevent the signal attenuation [4].

The high power fiber lasers in the market are based on active fibers with a patented pumping technique that allows the utilization of broad area multimode diodes rather than diode bars. Typically, a device made from coils of ytterbium- doped multi-clad fiber with an emission wavelength of 1.07–1.08 lm is used. Alternatively, it may be thallium doped with a wavelength of 1.8–2.0 lm or erbium doped with a wavelength of 1.54–1.56 lm. The diode pumped energy is delivered to the active medium via multimode fibers that are

spliced to the multi-clad coil. The laser cavity is created directly in the active fiber. The laser emission exits the fiber laser through a passive single-mode fiber. The resulting laser beam is essentially diffraction limited and, when fitted with an integral collimator, produces a beam that is extremely parallel. For example, the 100-W single- mode fiber laser has a full angle divergence of 0.13 mrad at half angle when collimated to 5 mm diameter. A 1-kW unit would be made up of 10 individual fiber lasers integrated into a common cabinet. Although the beam is no longer single-mode, the resulting M2 of 7–10 is better than high-power Nd-YAG lasers.

The beam from a 6 kW fiber laser can be delivered via a 200–300 lm fiber. The ytterbium fiber laser has a wall plug efficiency of 16–20%. Erbium and thulium fiber lasers demonstrate lower wall plug efficiency, but they are still more efficient than typical YAG lasers. Fiber laser technology offers several benefits to the industrial user. The ‘‘footprint’’ area of a 4 kW fiber laser unit is 0.5 m2 versus 11 m2 for a conventional lamp pumped Nd:YAG. The dimensions of 8 kW fiber laser are 1.5*0.8*1.5 m, approximately. Maintenance needs are reduced in comparison with other laser because there is no need to replace flash lamps or diodes. The high electrical efficiency greatly reduces operating costs.

Better beam quality, with very low divergence, allows the user to produce spot diameters substantially smaller than conventional lasers producing longer working distances. A 1-kW laser can be focused to 50 lm spot size with a 100 mm focal length lens. An 8 kW can be focused to a spot size of 0.6 mm with a 250 mm focal length lens. The cost for fiber laser technology up to 1 kW output power is below or comparable with lamp-pumped YAG lasers. The cost of a fiber laser greater than 1 kW is higher. However, when all factors are accounted for these lasers, namely, floor space, chillers and maintenance, they should be more cost effective than equivalent power rod-type Nd: YAG lasers. Fig 2-18 shows calculated operating costs over an 8 year period, indicating that for intensive use, fiber lasers are projected to have a lower operating cost than either CO2 or Nd: YAG lasers (see Figure 2-18).

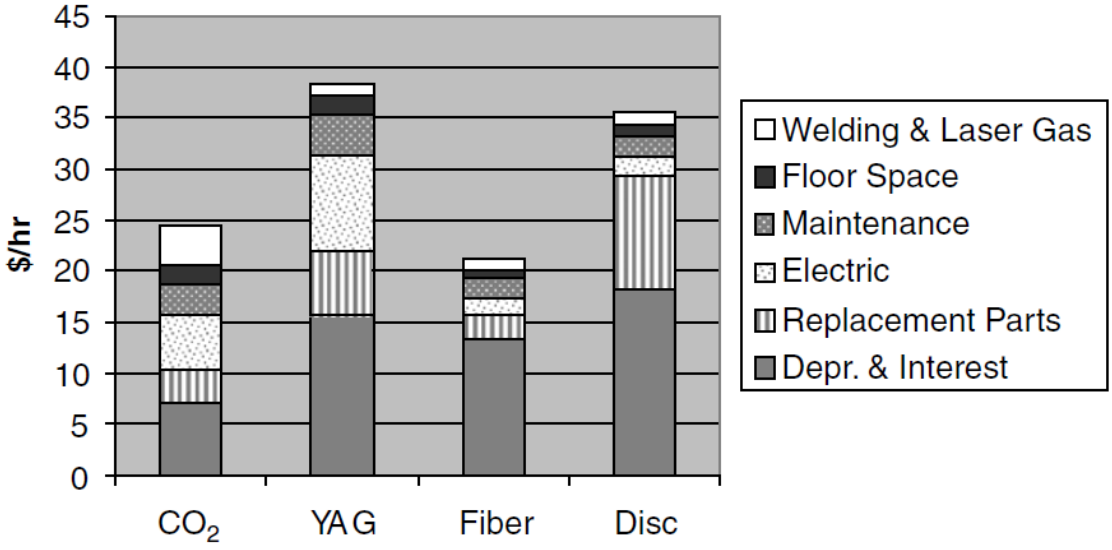

Figure 2-18 Estimated laser operating costs (8 years average)[16]

.

2.3.4 Wobbling laser welding

Wobbling technique is born from remote laser welding (RLW); this paragraph includes discussing the technological background and reviewing related literature of remote laser welding including a very new technology: wobbling technique. One of the most significant current technological trends in car body making is the spreading application of remote laser welding technology. RLW operations are performed from a distant point, by means of a laser beam that is emitted from a scanner mounted on the arm of an industrial robot. In contrast to traditional resistance spot welding (RSW), this contactless technology has to comply with much less accessibility constraints and can, at the same time, operate at higher speed. However, the new technology is much more expensive. Hence, replacing RSW with RLW technology is feasible only if the cycle time of the products can be considerably decreased [17, 18].

RLW is performed from a distance, usually with a scanner that uses mirrors and lenses to set the orientation and focal length of the beam. These components can act very fast (i.e., have a larger control bandwidth due to their small inertia) which can speed up the entire process (both tracing the welding locations, as well as repositioning between seams). Also, welding can take place with all robot joints and scanner elements continuously moving,

resulting in smaller control transients, implying energy savings and allowing faster operation. Nevertheless, laser welding does have its specific application constraints, resulting from the nature of the welding beam and the properties of the scanner head: Full visibility has to be ensured for the entire length of the seam. This has to be taken in consideration for the planning of fixtures, robot motion (avoiding occluding segments), and layout of potential visibility obstacles (even parts of the work piece).

Due to surface penetration properties, the beam-to surface inclination angle has to remain within technologically prescribed bounds. Scanner heads may be very limited in beam deflection angle and focal length—this has to be observed when the rest of the robot motion is calculated. The costs of an RLW cell are one more application constraint of a different kind. Switching to this new technology is only justified if expected advantages like reduction of cycle time or quality improvement balance out the costs in the given manufacturing context [19].

There are three basic preconditions for remote welding: First, a solid state laser is needed as the beam source. Solid state lasers enable delivery of the laser beam through a highly flexible fiber optic cable, which is required when joining components in 3D space with a Multiaxis robot.

Second, a laser with excellent beam quality and the appropriate power is required. Beam quality is the measure of focusability of a laser, and the long focal lengths required for remote welding necessitate superior beam quality (i.e. 4-8 mm-mrad) in order to achieve the appropriate focused spot size (i.e. about 0.6 mm) at the workpiece. For remote welding in automotive body production, typically about 3-6 kilowatts of laser power is used.

The third essential is precise positioning of the weld seams, which requires axis synchronization between the robot and the scanner control. This allows the weld shape programmed in the scanner control, let’s say a “C” shape, to really be a “C” shape with the robot moving at various speeds over the part to be welded. Some control architectures use “time” synchronization. The problem here is that if the robot speed is changed for any reason, the weld shape will also change because the axes are not synchronized.

Several Studies have been done about weldability of AHSS with fiber laser. [20]has reported the weldability of AHSS expressing penetration, weld profile, weld defects, micro hardness and melting efficiency. Microhardness measurements indicated a substantial

increase in hardness in the weld zones, attesting the superiority of laser welding. Analyses revealed that the typical melting efficiency is on the order of 50‑70% for full penetration welding. Tensile test results confirmed the high quality of the welds obtained. defects, microhardness and melting efficiency[21] Laser welding offers the benefits of low heat input per unit volume, small heat affected zone (HAZ), low thermal distortion of the work piece, fewer welding defects, high welding speed, and, deep and narrow weld profiles. In addition, it allows easy automation while welding complex joint configurations and dissimilar materials.

Like other welding techniques, laser welding has its share of drawbacks that include the need for almost press fitting of parts due to its small focused spot size, high equipment and operating costs, lower welding speeds for joints with a gap greater than 0.5 mm, low electrical efficiency of the laser and, in cases of certain lasers, difficulty in welding high reflective materials like aluminum [22] has made an extensive analysis of the comparison of four lasers (CO2, Nd:YAG, fiber and disk) for welding mild steel in the power range of 4‑5 kW. He suggests that with the emergence of high-power disk and fiber lasers, the competitive landscape has expanded. Fiber lasers exhibit multi-kilowatt powers in continuous wave mode, high efficiency, compact design and excellent beam quality that produce deep penetration welds at high-welding speeds. [23]Explains that the high electrical efficiency of the fiber laser greatly reduces operating costs while resulting in better beam quality, with very low divergence, allowing small spot diameters.

They present initial data on welding of X100 pipeline steel with 8 kW laser and obtained high melting efficiencies.[24] used a 6 kW fiber laser to obtain deep penetration welds with narrow widths in 8 mm thick plate at a high welding speed of 4.5 m/min, and later used a 2.5 kW laser beam to weld Zr55Al10Ni5Cu30 metallic glass at very high speeds of 72 m/min. Yb:YAG disk is the most widely used lasing medium for fiber lasers because of its long radiative life time, high thermal conductivity and good mechanical properties. Unlike Nd:YAG rod types, the disk has no thermal lensing, resulting in absence of optical distortion and keeping constant beam quality over the entire power range. It is expected that the disk and fiber lasers eventually replace conventional laser systems due to their higher quality[25]. Fiber laser is rapidly gaining momentum in the industry because of the cost effectiveness compared to Nd:YAG and improved quality of welded joints (Figure 2-19).

Operating and maintenance costs lasers (Ream, 2005).

Expenses ($/h)	CO_2	Nd:YAG	Fiber
Depreciation and interest	$7.50	$15.30	$13.20
Replacement parts	$3.10	$6.80	$1.90
Electric	$4.70	$8.90	$2.10
Maintenance	$3.30	$3.80	$2.10
Floor space	$1.90	$2.10	$0.70
Welding and laser gas	$3.80	$1.70	$1.40
Total	$24.30	$38.60	$21.40

Figure 2-19 Comparison between operating and maintenance costs of different lasers

Sharma has reported travel speed versus efficiency for different types of laser technology in welding of mild steel (see Figure 2-20) [20].

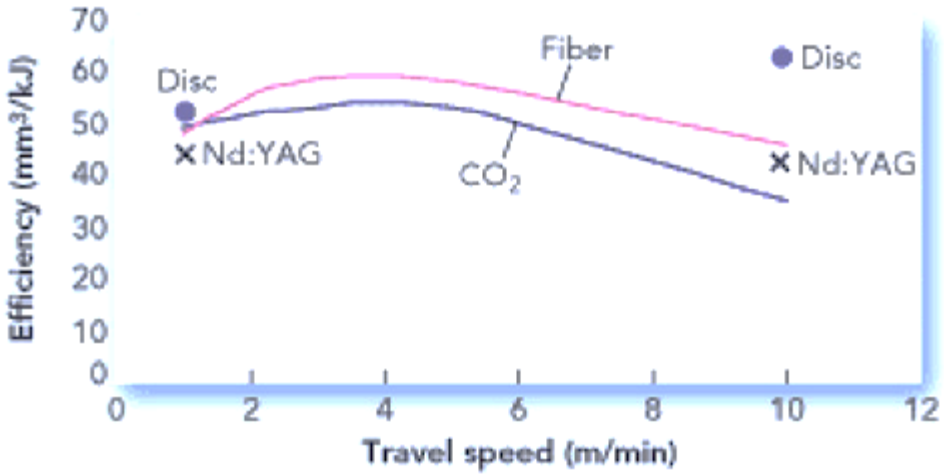

Figure 2-20 Travel speed versus efficiency for different types of laser technology

Heat transfer characteristics during laser welding are of great interest to researchers. Several models ranging from simple analytical models involving moving line heat-source to elegant numerical models which account for fluid dynamics and laser-plasma interaction have been proposed in the literature. [26] provide a simple theory that provides a good description of penetration welding for both electron beams and lasers.

[27] provide an analytical form for the temperature distribution; they have estimated weld profiles and compared them with examples of actual welds. [28] have considered the interaction of conditions in the liquid metal surrounding the keyhole formed and have developed a model for the energy interface and vapor flow in the keyhole. They have then used the model to calculate keyhole shapes and the variation of depth of the related quantities.

[29] has developed a model taking into account a point-by-point determination of the energy balance at the keyhole wall, deriving a formula for heat conduction from the model of a moving line source of heat, modeling the absorption mechanism and also considering the thermodynamics and the flow of metal vapor inside the keyhole.

[30] studied the effect of joint geometry – bead-on-plate, V groove and square groove – on the absorption of laser energy with the same laser power and found better absorption of laser beam energy in grooved joints.

All these models predict different results due to various assumptions and use of a number of different parameters such as keyhole size, material properties and absorptivity. The model proposed by [31] relates the penetration depth to the incident laser power and the Peclet number, the latter being a function of the welding speed, the keyhole radius and thermal diffusivity. The relative importance of conduction and convection in the overall transport of heat in the weld pool can be assessed from the value of the Peclet number. For steel keyhole welding, Peclet number is much greater than 1 implying that convection of melt pool is more dominant than conduction [32].

2.4 CMT welding of HSS

This section Starts with introduction of CMT welding and how it was born from evolution of GMAW processes, the advantages of this very new technology are discussed and effects of changes in process variables on weld attributes are taken in to account. At the end also usage of CMT welding in welding of dissimilar Metals including steel is reported.

2.4.1 Overview

Until now, aircraft engine manufacturers have faced a choice between GTAW or GMAW as a low cost option for arc welding gas turbine components during manufacturing and repair. GTAW has successfully captured much of the market, as the limiting factors of traditional GMAW have always been the joining of unique material types (including non-ferrous materials) and consistent quality (i.e. the weld spatter inherent in traditional GMAW). Fronius International LLC, a European market leader in arc-welding technology, introduced the concept of CMT welding to the public in 2005. By incorporating the traditional concepts of the GMAW method – that is, applying a wire consumable – Fronius was able to produce a process of arc welding with high levels of accuracy on various materials which were typically reserved for GTAW welding. The CMT is a fully digital, micro-processor-controlled inverter welding process that results in the introduction of a reduced amount of residual heat to the work piece and produces a virtually spatter free weld. The improved weld quality is obtained via a digital process-control that detects a short circuit, and then retracts the wire being feed so as to help detach and deposit a single molten droplet at a time, as shown in Figure 2-21. This figure shows one cycle of the CMT wire retraction process using high-speed photography. It is important to note the short duration of arcing period, approximately 1/3 of the total cycle time (14.31ms) [33].

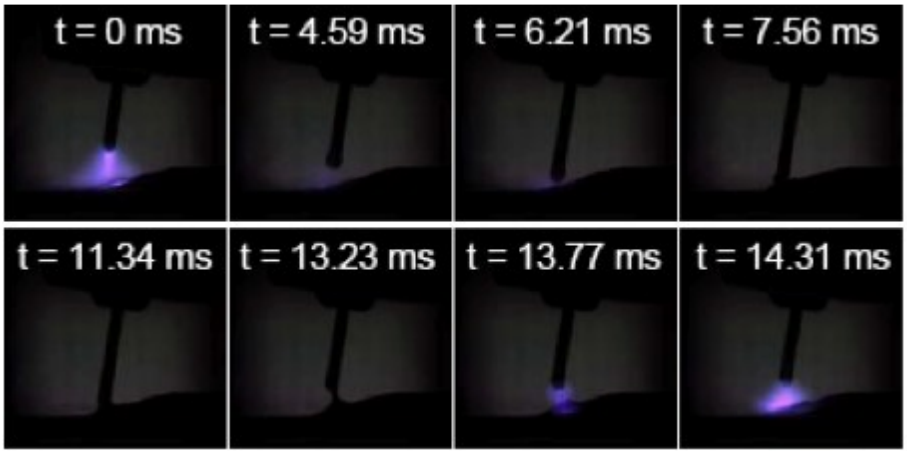

Figure 2-21 High-speed photography image a CMT cycle with real time stamps

While it is well known that GTAW is the industry standard, it also requires a highly skilled operator when performed manually. The process typically necessitates an operator to use both hands to execute the weld: one for holding the torch and the other for feeding in filler to ensure maximum precision. GTAW also uses a tungsten electrode from which an arc is generated to provide the heat for the addition of the filler material, creating a large temperature differential between the filler and the work piece.

Additionally, there is a potential for transfer of molten tungsten from the electrode to the weld causing contamination, resulting in a hard and brittle inclusion. However, the CMT uses a consumable electrode that acts not only as the filler, but also the heat conductive electrode. This coupled to the computer controlled wire retraction mechanism results in a process that greatly reduces the amount of heat applied to the work piece during joining. Additionally, the thermal input levels of CMT are much lower and more controllable than conventional GMAW or GTAW welding, since each of these processes cannot go below a certain heat level to create an arc. Speed and spatter control are the two key benefits of Fronius' CMT. CMT welding offers a speed that is four to five times faster than conventional GTAW, with levels of consistent quality matching those of robotic automation [33].

CMT stands for Cold Metal Transfer. Of course, the term "cold" has to be understood in terms of a welding process: when set against conventional GMAW, CMT is indeed a cold process with its characteristic feature of alternating thermal arc pool, i.e. hot when an arc is initiated and cold when the arc is extinguished and the wire is retracted. This alternating hot and cold treatment has been made possible by a new technological development from Fronius International LLC that incorporates the wire motions into the process control via a computer monitoring system (see figure 2-1). Some of the other features that make this unit unique when compared to conventional GMAW units include: two separate wire-drives (front and rear) that are separated by the wire buffer. The front drive, located in the torch, (see Figure 2-22), moves the wire back and forth in a dabbing motion at a rate of up to 90 times per second.

Simultaneously, the rear drive pushes the wire directly from the filler spool located in the wire drive. It is important to note that both drives are digitally controlled by the process control. To ensure a constant wire feed, a wire buffer (see Figure 2-22) is interposed between the two drives to decouple them from one another [34].

a. The new tension-lever system in the welding torch ensures constant and reproducible contact pressure.b.The wire buffer decouples the front and rear wire-drives from one another and ensures smooth wire travel.
Figure 2-22 Fronius CMT process control contact pressure [34]

In the world of GMAW processes, there are essentially three types of metal transfer mechanisms that can be used: [24] short circuiting transfer, globular transfer and (3) spray transfer. The type of transfer is determined by a number of factors, the most influential of which include [24] magnitude and type of welding current, electrode diameter, (3) electrode composition, (4) electrode extension, and (5) shielding gas. CMTGMAW in its most elementary form can be considered a short circuit GMAW process. Short circuit GMAW consists of the lowest range of welding currents and electrode diameters associated with GMAW. This type of transfer produces a small, fast-freezing weld pool. During the arcing process, metal is transferred from the electrode to the work piece only during a short period when the electrode is in contact with the weld pool, hence the term “short circuiting transfer.” It is important to note that no metal is transferred across the arc gap [35, 36].

The sequence of events in the transfer of metal and the corresponding current and voltage for a typical short circuit transfer GMAW process can be seen in Figure 2-23. As the wire touches the weld metal, the current increases [(A), (B), (C) and (D)]. The molten metal at the wire tip pinches off at D and E, initiating an arc as shown in (E) and (F). It is here that the rate of current increase must be high enough to heat the electrode and promote metal transfer, yet low enough to minimize spatter caused by violent separation of the drop of metal (one of the major disadvantages of conventional short circuit GMAW). Finally, when the arc is established, the wire melts at the tip as the wire is fed forward towards the next short circuit at (G). Overall, the open circuit voltage of the power source must be low enough that the drop of molten metal at the wire tip cannot transfer until it touches the base metal [35, 36].

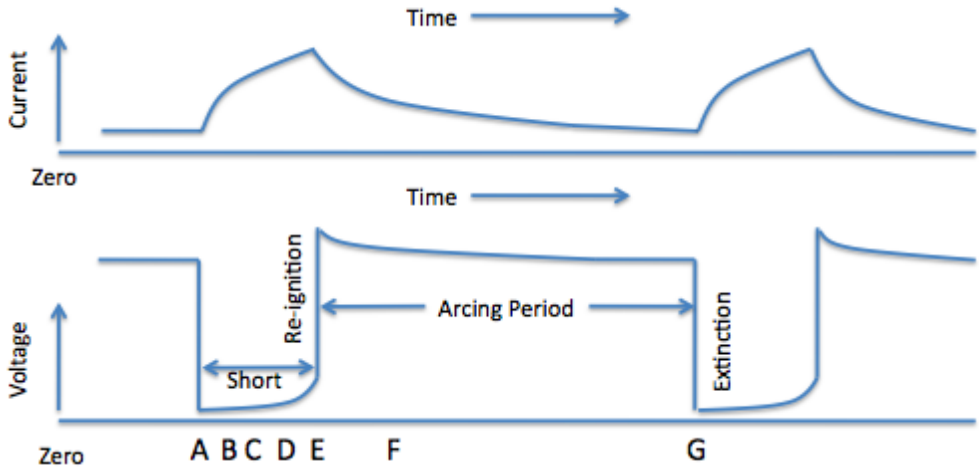

Figure 2-23 Schematic representation of short circuiting metal transfer [36]

Unlike its short circuit GMAW counterpart, CMT-GMAW incorporates a digital process-control that detects the short circuit at the work piece, and then mechanically retracts the wire to help detach the molten droplet. The wire retraction greatly reduces the spatter that is typically associated with conventional short circuit GMAW. Reduced spatter is the first essential difference from conventional short circuit GMAW processes; the second most notable difference is a reduction in thermal input since there is virtually current-free droplet detachment, hence the term "Cold Metal Transfer." Lastly, unlike conventional short circuiting GMAW -where there is a constant push motor driven system, the CMT-GMAW uses a two motor drive system that pushes the wire forward, and as soon as the short circuit occurs, it pulls it back (see Figure 2-24).

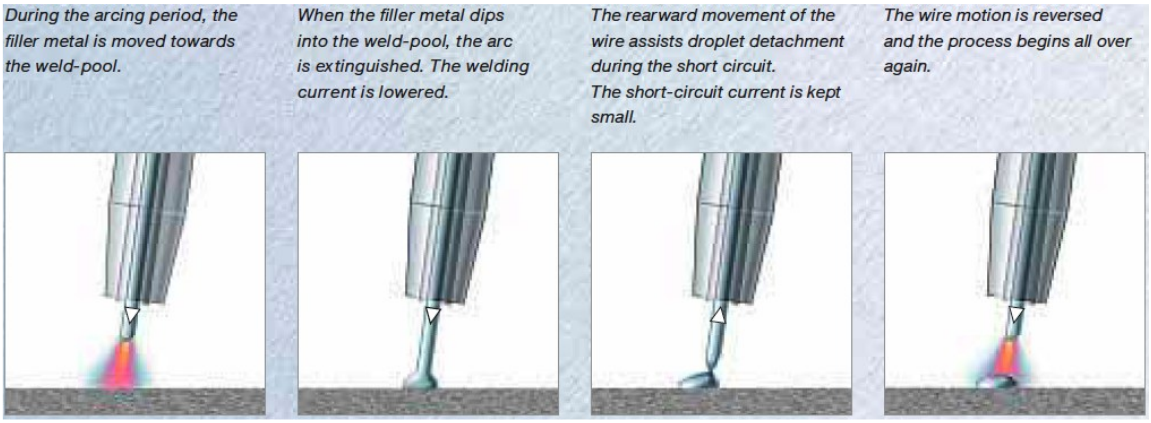

Figure 2-24 CMT-GMAW wire retraction process

The rearward movement of the wire assists droplet detachment during the short circuit. In this way, the arc itself only inputs heat very briefly during the arcing period.

The thermal input is immediately reduced after arc is extinguished, creating an oscillating hot/cold weld pool. During the CMT-GMAW process, the average current is kept very small by controlling the short circuit, resulting in virtually spatter free metal transfer. Figure 2-25 illustrates the reduced thermal input required for metal transfer as compared to other conventional metal transfer processes. Also worth mentioning, precision droplet detachment of the CMT-GMAW ensures that after every short circuit, a near-identical quantity of filler metal is melted off [37].

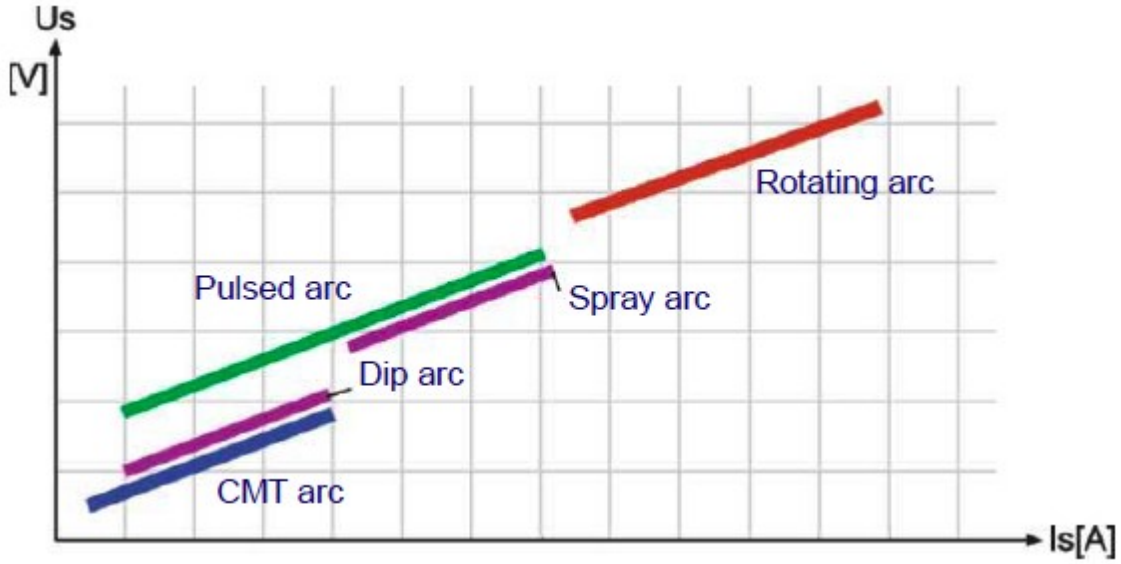

Figure 2-25 Comparative thermal inputs for various metal transfer processes

2.4.2 CMT welding process parameters and their effects

The most important variable of any GMAW process, including CMT-GMAW, which affects the weld penetration, bead geometry, and overall weld quality are: [24] welding current (wire feed speed), polarity, (3) arc voltage (arc length), (4) travel (traverse) speed, (5) electrode extension, (6) torch angle, and (7) electrode diameter.

Knowledge and control of these variables are essential in order to consistently produce welds of acceptable quality. However, changing one variable generally requires altering additional parameters to retain an acceptable quality weld because the variables are not completely independent of each other. The effects of these variables on deposit attributes are shown in Table 2-2 [38].

Welding variables to change	**Desired Changes**							
	Penetration		*Deposition rate*		*Bead size*		*Bead width*	
	Increase	*Decrease*	*Increase*	*Decrease*	*Increase*	*Decrease*	*Increase*	*Decrease*
Current and wire feed speed	Increase	Decrease	Increase	Decrease	Increase	Decrease	Little effect	Little effect
Voltage	No effect	No effect	Little effect	Little effect	Little effect	Little effect	Increase	Decrease
Travel speed	No effect	No effect	Little effect	Little effect	Decrease	Increase	Decrease	Increase
Electrode extension	Decrease	Increase	Increase (a)	Decrease (a)	Increase	Decrease	Decrease	Increase
Electrode diameter	Decrease	Increase	Decrease	Increase	Little effect	Little effect	Little effect	Little effect
Shield gas %	Increase	Decrease	Little effect	Little effect	Little effect	Little effect	Increase	Decrease
Torch angle	Drag	Push	Little effect	Little effect	Little effect	Little effect	Push	Drag

Table 2-2 Effect of changes in process variables on weld attributes, (a) Will result in desired weld if current levels are maintained by adjustment of wire feed speed

- ✓ Arc Length

Arc voltage and arc length are related terms that are often used interchangeably, however they are quite different in practice. Arc voltage is the electrical potential between the electrode and the work piece. Arc voltage is generally lower than the voltage measured directly at the power source because the voltage drops at the connections and along the length of the welding cable. Consequently, an increase in arc voltage will result in a longer arc length. It is also important to note that excessively high arc voltage can cause weld porosity, spatter, and undercut; therefore, arc length is a variable of interest and should be controlled as it can have a profound impact on the overall weld quality [36].

In conventional GMAW, the surface of the work piece (i.e. jagged or flat) and the welding speed can both have a marked effect on the stability of the arc. The arc length is acquired and adjusted mechanically with the CMT-GMAW. This means that the arc remains stable, regardless of the surface condition of one's work piece. In addition to a mechanical response, the CMT-GMAW utilizes a self-correction mechanism via a constant-potential power source as illustrated in Figure 2-26. Where L is the arc length, the length is between the melting electrode tip and the base metal. As the contact-to-work distance increases, the

arc voltage and arc length would tend to increase with a conventional GMAW power source. However, with the CMT-GMAW power source, the welding current decreases with a slight increase in voltage, while the mechanical drives in the torch adjust appropriately to maintain a consistent arc length. Conversely, if the distance is shortened, the lower voltage would be accompanied by an increase in current and a mechanical adjustment in wire feed speed to compensate for the shorter wire stick out [36].

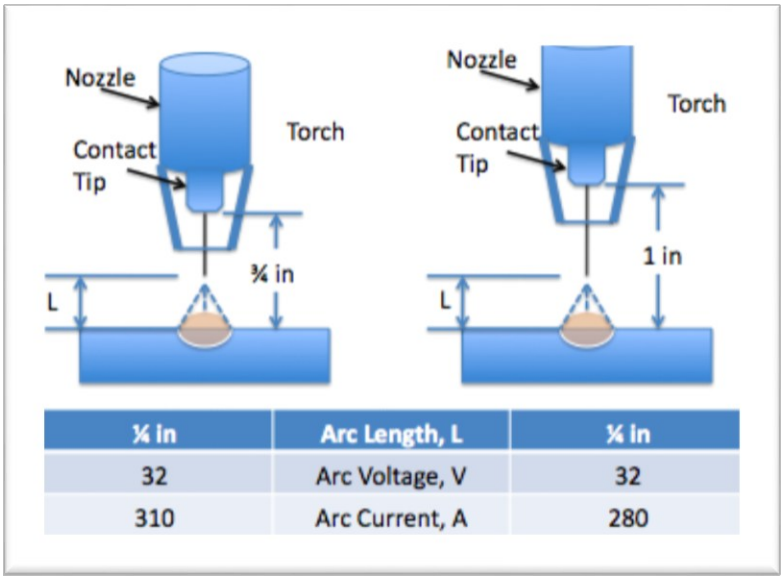

¾ in	Arc Length, L	¾ in
32	Arc Voltage, V	32
310	Arc Current, A	280

Figure 2-26 Constant-potential power source illustration

- ✓ Wire Feed Speed

In conventional GMAW welding, as the electrode feed speed (wire feed speed) is varied, the welding current varies in a similar manner with the arc length. This occurs because the current output of the power source fluctuates dramatically with the slight Changes in the arc voltage when alterations are made to the wire feed speed. If all other variables were held constant, an increase in welding current would result in the Following: [24] an increase in the depth and width of the penetration, an increase in the deposition rate, and (3) an increase in the size of the weld bead. [36] Unlike conventional GMAW units where current and voltage can be changed independently, these two key parameters are linked together in the CMT-GMAW via a digital process control, or an arc synergic line. An arc synergic line

is a linear Mathematical relationship (proprietary to Fronius International LLC) which incorporates the voltage and amperage process controls into the wire feed speed, and is dependent on the thermal and electrical resistivity properties of the material substrate/filler used. Therefore, each synergic line is uniquely different: that is, every synergic line consists of several points on a voltage current diagram (U-I diagram), which are formed from the connection of a series of certain current and pertinent voltage levels for any given wire composition and gas. Each point on the synergic line is recorded with the same Arc length, despite different performance, through the whole power range. An arc synergic line is experimentally determined via high-speed video techniques [37].

- ✓ Traverse Speed

As with any GMAW process, including CMT-GMAW, the traverse or travel Speed has a profound impact on the weld quality. Travel speed is the linear rate at which the arc is moved along the surface of the work piece. The filler metal deposition rate per unit length increases when the travel speed is decreased. The welding arc impinges on the molten weld pool rather than the base metal at very slow speeds, thereby reducing the effective penetration and resulting in a wider bead. As travel speed is increased, the thermal energy per unit length of weld transmitted to the base metal from the arc is at first increased because the arc acts more directly on the base material. However, further increases in travel speed impart less thermal energy to the base metal. Melting of the base metal therefore first rises and then decreases with increasing travel speed. As the travel speed increases, there is a tendency for undercutting along the edges of the weld bead because of insufficient deposition of filler metal to fill the path melted by the arc [37].

- ✓ Electrode Orientation

Electrode orientation affects bead shape and penetration to a greater extent than arc voltage and travel speed. The electrode orientation is described in two ways: [24] by the relationship of the electrode axis with respect to the direction of travel and the angle between the electrode axis and the adjacent work piece surface. When the electrode points in a direction opposite to the travel direction, it results in a trail angle, which is known as the backhand method. Similarly, when the electrode points in the direction of travel, it results in a lead angle and is called the forehand method. The electrode orientation and its effect on the width and penetration of the weld bead are illustrated in Figure 2-27 [36].

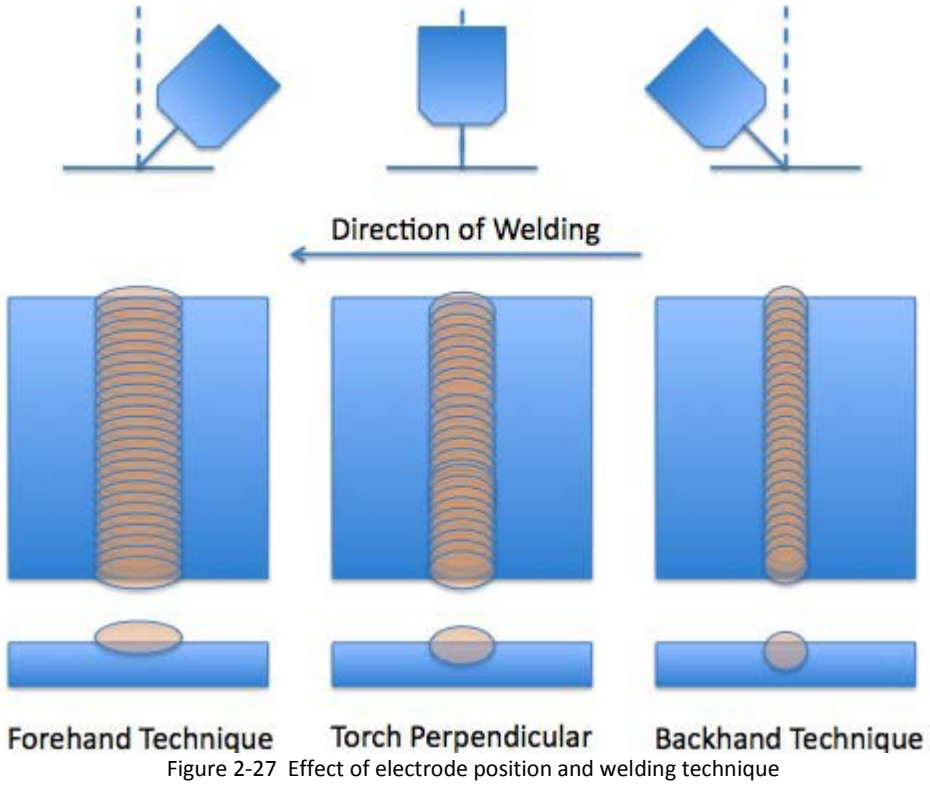

Figure 2-27 Effect of electrode position and welding technique

When the electrode is changed from perpendicular to the lead angle technique with all other conditions unchanged, the penetration decreases and the weld bead Exhibited is wider and flatter. Maximum penetration is obtained in the flat position with the drag technique, at a drag angle of about 25 degrees from perpendicular. The drag technique also produces a more convex, narrower bead, an increasingly stable arc, and fewer spatters on the work piece.

A few Studies have been done about weld ability of AHSS with CMT welding. [39] have studied on long term problem of joining steel and aluminum in the automotive industry. Focusing to the principle of CMT process, composition and description of the individual components welding sets and where is the most applicable. Because of the automatic welding robot it was created product for attachment welded materials. This enabled manufacturers to provide lapped materials against movement and still weld at one position after replacing the other samples [39].

Chapter 3: Aim of the thesis

The thesis aim is to reduce the deformation of DOCOL M pipes. The pipes are meant to be used in the arm of Socage Crane. The previous welding problem with conventional methods was that pipes were deformed and the planarity of pipes changed a lot. This problem can be fixed using technologies which input less heat in to the components such as laser welding and CMT welding. The most important factor which affects the deformation is the amount of heat which input to the component by welding. By using high power and high velocity types of welding such as Laser welding and CMT welding the value of heat which input to the component is considerably low.

This study intends to find the best combination of power and velocity to obtain as a minimum75% of penetration depth. Depth of penetration is one of the most critical parameters in laser welding, which users usually need to adjust for the material being welded. For a given beam diameter a range of combinations of laser power and travel speed can be used to achieve a desired depth of penetration. Alternatively, for a given combination of power and travel speed, different depths of penetration occur, if different beam diameters are used. Beam diameter is controlled by the laser properties and optical system and these may vary between laser systems.

This study means to compare microstructures and properties of DOCOL M (high strength steel) weld joints made by different technologies. Continuous improvement in properties of steels is tied to optimization of their chemical composition and thermal and mechanical treatment. These efforts lead to optimized microstructures with specific and defined sizes and distributions of microstructure constituents. One of the difficulties in welding of this material such as DOCOL M is existence of tempered martensite in the weld caused by extra heat. This work aims to find the best combination of process parameters in order to minimize the HAZ in the welding joint.

As it is mentioned the welding is performed by three new welding technologies: CMT (Cold Metal Transfer), Proximity laser welding and wobbling laser welding. The most important variable of any GMAW process, including CMT, which affects the weld penetration, bead geometry, and overall weld quality are: welding current (wire feed speed), polarity, (3) arc voltage (arc length), (4) travel (traverse) speed, (5) electrode

extension, (6) torch angle, and (7) electrode diameter. Knowledge and control of these variables are essential in order to consistently produce welds of acceptable quality. However, changing one variable generally requires altering additional parameters to retain an acceptable quality weld because the variables are not completely independent of each other. This work mainly analyses the effect of changing velocity for two different combination of current and voltage.

In this study also the effect of wobbling laser welding on the deformation and microstructure of the pipes is analyzed. Wobbling laser welding benefits from two major advantages of remote welding over traditional laser welding with short focal length optics - the high-speed of the intra-weld beam movement contributes to a significant reduction of the cycle time, The long stand-off of the focusing head permits access to areas not accessible with short focal length, Whereas in conventional laser processing the work head is close to the work, with wobbling laser welding, there is a standoff distance. Consequently, there is the ability to effectively move the beam around with mirrors far more efficiently than if the laser is on a stationary mechanism, such as a robot arm, but the most important benefit of wobbling laser welding is stirring the spot dimension for compensating the gap. Since in the experiment the joints configurations are simple and linear, in this study the advantage of stirring the spot dimension is mostly used in order to compensate the gap. .

At the end, this report compares between the costs for different techniques. The welding cost can be mostly sorted in to two categories, namely fixed and variable cost. For cost-tolerance, the fixed cost components, such as set-up cost, is ignored since they do not vary with the tolerance. Thus, only the variable cost components will be considered. Machining cost components used in this work are adopted from [40].

Chapter 4: Facilities

In this chapter the facilities which are used in different step of experiment and different technologies, (proximity laser welding, wobbling laser welding and CMT welding) are presented. The laser sources which are used for both wobbling laser welding and proximity laser welding is The YLS3000 Ytterbium fiber laser manufactured by IPG photonics.

Three different robot arms manufactured by ABB Company are used to move and hold the laser head and CMT torque. The main characterization of equipment is explained in the fallowing sections.

4.1 Laser welding facilities

During the experiment several devices have been used. They include devices and equipment used for welding, samples preparation, metallurgical preparation of the welded specimens and mechanical tests. In order to perform the proximity laser welding these set of devices and instruments are needed.

- ✓ Laser source
- ✓ Laser delivery

4.1.1 Laser source

The laser source used for welding is Ytterbium Fiber Laser System a 3KW Fiber Laser, manufactured by IPG photonics. The YLS3000 Ytterbium fiber laser was developed for the industrial use and research applications. This compact and efficient laser readily replace bulk and less efficient solid state lasers with the main target applications being welding, cutting and brazing.

The optical power randomly polarized 1070-1080 nm emission wavelength, ytterbium doped, red aiming diode with maximum available output fiber of 3kw. Table 4-1 represents some characteristics of the source; Operational modes are continuous and quasi continuous wave with random polarization.

Standard features	Randomly polarized, 1070-1080 nm emission wavelength, ytterbium doped, red aiming diode
Available Operating Modes	CW, QCW, SM
Max Available Output Power(watt)	3000
Feed Fiber Diameter(mm)	50 μm

Table 4-1 Laser Fiber Source Characteristics

4.1.2 Robot arm

The laser head is being hold and moved by the robot. Two different robot arms are used in laser welding which both are 6-axis anthropomorphic robots manufactured by ABB. The IRB 2400 is used for performing proximity welding and IRB 4400 is used for performing wobbling laser welding throughout the experiment.

Both products designed for manufacturing industries that use flexible robot-based automation, have an open structure that is adapted for flexible use and can communicate extensively with external systems. Robots are equipped with an operating system called BaseWare OS. BaseWare OS controls every aspect of the robot, like motion control, development and execution of application programs communication and can also be equipped with optional software for application support - gluing, arc welding for example, communication features - network communication - and advanced functions such as multitasking, sensor control etc. The IRB 2400 and IRB 4400 are schematically represented in Figure 4-1 also the datasheet of them is shown in Table 4-2.

Robot arm	IRB 2400	IRB 4400
Axes	6	6
H-Reach (mm)	1500	1500
Repeatability(mm)	0.06	0.19
Robot mass(Kg)	380	1040

Table 4-2 Robot arm specification

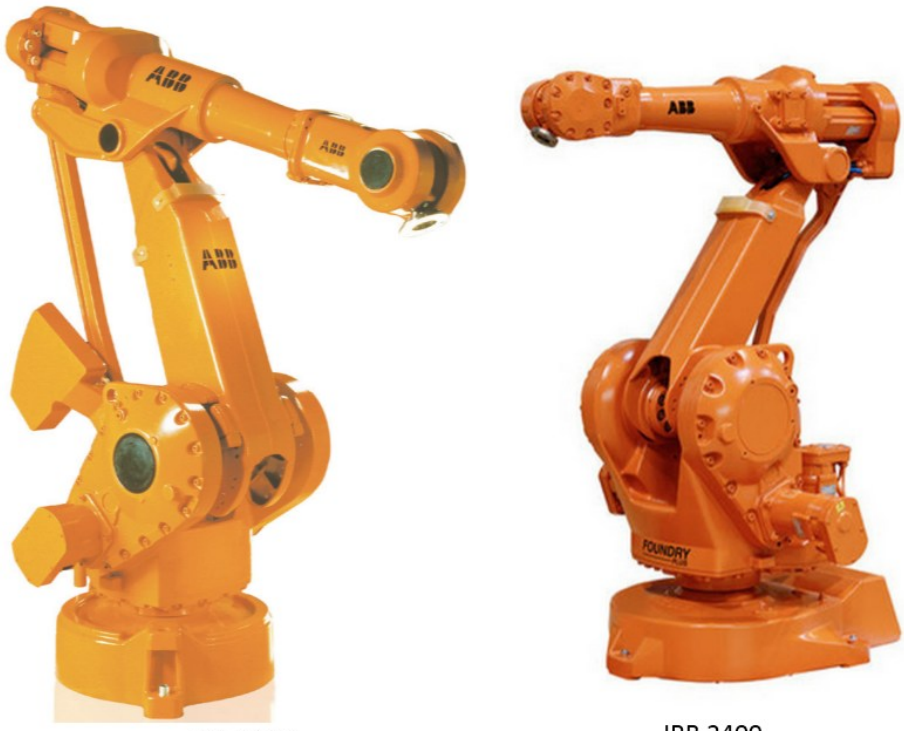

Figure 4-1 Robot arm used in laser welding

4.1.3 Laser delivery for proximity laser welding

The laser beam is delivered to the laser focusing system by means of optical fiber which has the diameter equal to 500µm.The optical fiber is connected directly from the laser source to the laser head, as the focusing system. The laser head used for the experiment is BIMO Laser Processing Head, a product of HIGHYAG laser technologies. This focusing length is 200mm for focusing system and 100mm for collimation system. The laser head is schematically represented in Figure 4-2 and Figure 4-3.

The processing head can be configured in individual and modular ways. This includes simple tasks, like focusing the laser light onto the work piece, as well as configuration of the entire turnkey subsystem of the laser processing head inside the laser cell. In the most advanced stage of expansion, the processing head provides, in addition to process-relevant

components, all accessories necessary for the integration into an automated production cycle. These include the proven modules for media guiding via a cable management system and the EPS electric-pneumatic installation system as interface with the system PLC and the media supplies.

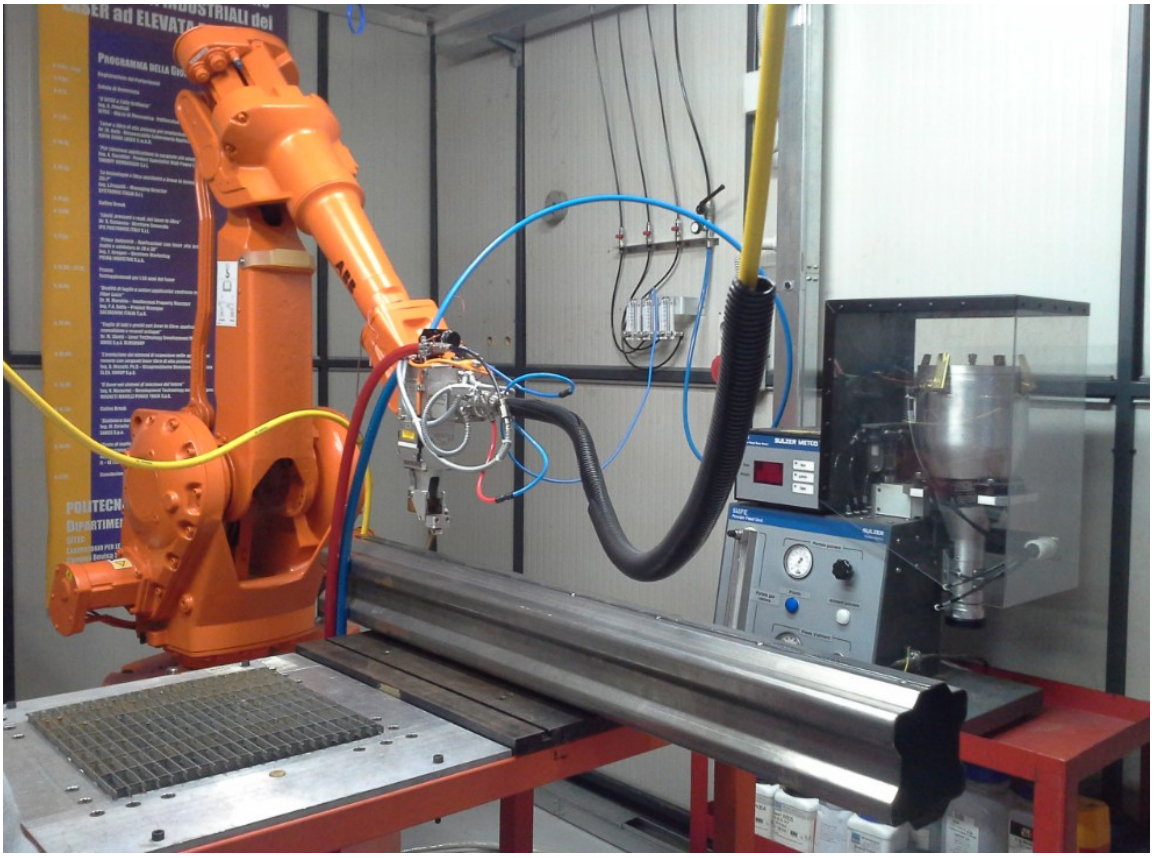

Figure 4-2 SITEC-Laboratory Set up of BIMO head on the robot arm

Figure 4-3 Laser Processing Head BIMO

4.1.4 Laser delivery for wobbling laser welding

The laser beam is delivered to the scanning fiber system by means of optical fiber which has the diameter equal to 50 μm. The optical fiber is connected directly from the laser source to the laser head, as the focusing system. The laser head used for the experiment is Scan fiber Laser Processing Head, a product of El.En (Electronic, Engineering group) company. The scanning speed is 35 ($\frac{rad}{s}$) and scanning acceleration is 30000 ($\frac{rad}{s^2}$). The scan head and its set up on the robot arm are schematically represented in Figure 4-4 and Figure 4-5. The datasheet is shown in Table 4-3.

Working field(mm)	250x250
Optical scanning deflection(mrad)	+/-350
Scanning speed($\frac{rad}{s}$)	35
scanning acceleration ($\frac{rad}{s^2}$)	30000
Positioning resolution(μrad)	20
Dimension $W * L * H$(mm)	213*240*220
Weight (kg)	13

Table 4-3 Datasheet of Fiber laser head

Figure 4-4 Scan Laser Head

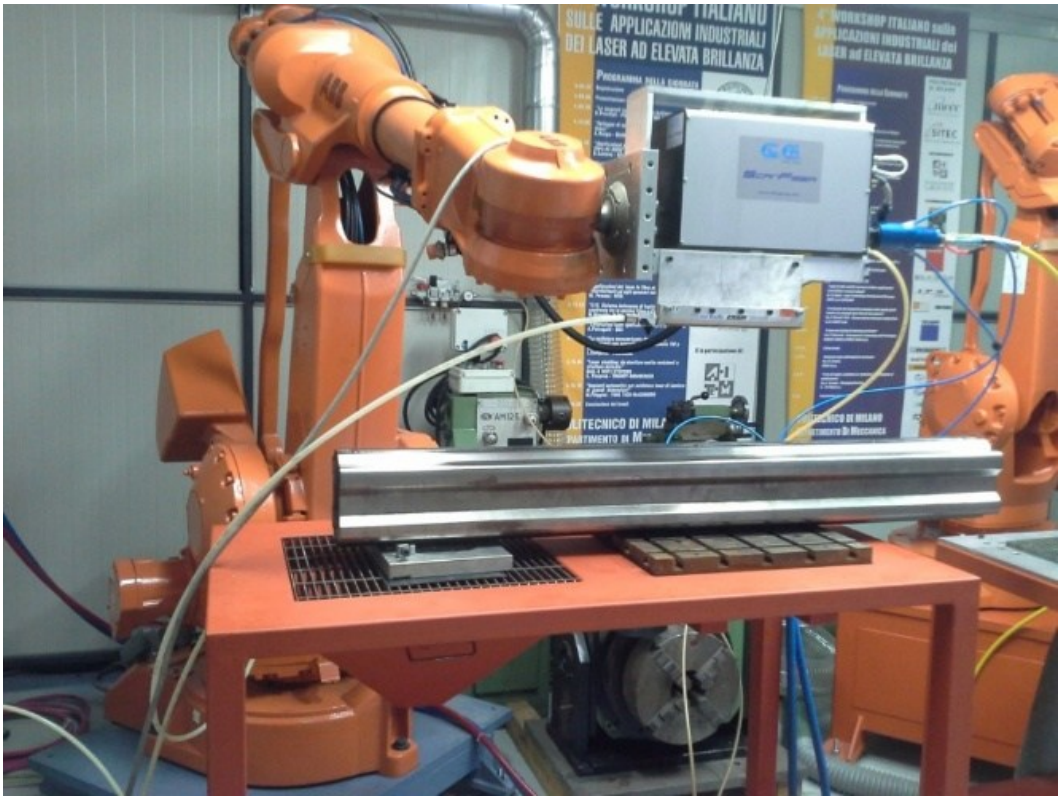

Figure 4-5 Set up of scan head on the robot arm

4.2 CMT welding instruments

In order to perform the CMT welding a set of devices and instruments are needed. Below you will see overviews of the system as a whole automated configuration (Figure 4-6):

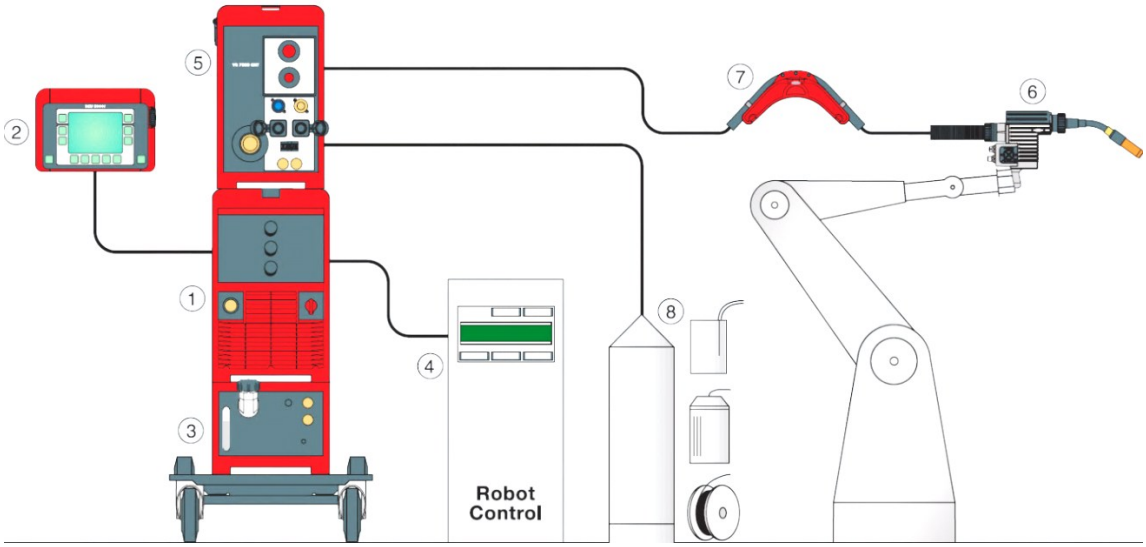

Figure 4-6 Welding System of CMT welding equipped for automated applications (Source: Fronius)

1. TPS 3200 / 4000 / 5000 CMT power source fully digitized, microprocessor-controlled and digitally regulated GMA inverter power source (320/400/500 A) with an integral functional package for the CMT process.

2. RCU 5000i remote-control unit Remote-control unit with full-text display, weld-data monitoring with Q-Master function, easy-to-follow user guidance, systematic menu structure, user administration features.

3. FK 4000 R cooling unit Sturdy and dependable, ensures optimum cooling of Water-cooled robot welding torches.

4. Robot interface Suitable for all customary robots, irrespective of whether these are addressed digitally, in analogue or via field-bus.

5. VR 7000 CMT wire feeder digitally controlled wire feeder for all common types of wire pack.

6. Robacta Drive CMT Compact robot welding torch with digitally controlled, gearless, highly dynamic AC servo motor. For precision wire feed and constant contact pressure.

7. Wire buffer decouples the two wire-drives from one another and provides additional storage capacity for the wire. For mounting on the balancer (preferably), or on the third axis of the robot.

8. Wire supply

9. TransPuls Synergic 2700 CMT power source Fully digitized, microprocessor-controlled and digitally regulated GMA inverter power source (270 A) with integral wire feeder and functional package for the manual CMT process.

10. PullMig CMT Compact, water-cooled high-performance welding torch for manual CMT applications. In conjunction with the wire buffer in the hose pack, the digitally controlled, high-dynamic AC servo motor permits rapid oscillating motions of the welding wire.

The robot which is used in this experiment is IRB 1600 M24, Which is a 6-axis anthropomorphic robot manufactured by ABB. The IRB 1600 M24 is used mainly for performing arc welding as in die casting, machine tending, material handling, injection molding, assembly and packaging. CMT welding have been performed in ABB Company. The robot and positioner are schematically represented in Figure 4-7 and Figure 4-8 and the datasheet is shown in Table 4-5.

Figure 4-7 IRBP 1600 M2004

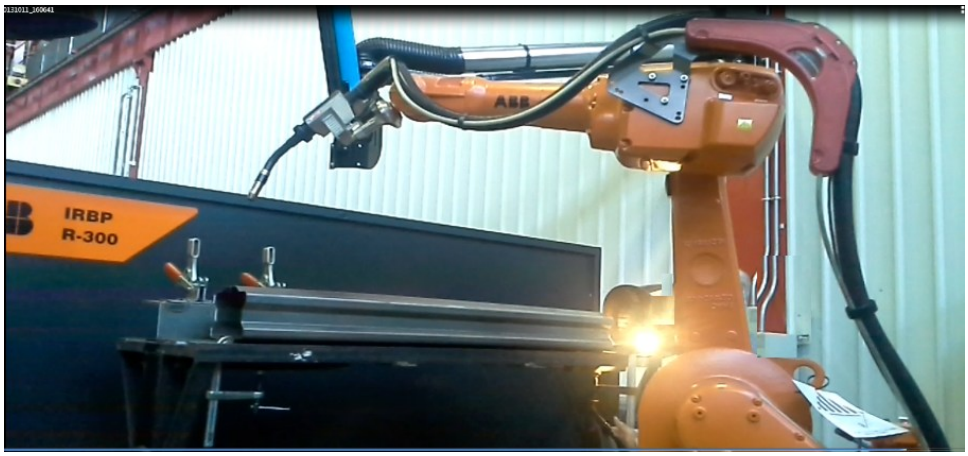

Figure 4-8 IRB 1600 M2004 robot and IRBP positioner set up

Axes	6
H-Reach (mm)	1450
Repeatability(mm)	0.005
Robot mass	250 kg

Table 4-4 Datasheet of IRB 1600 M2004

Chapter 5: Design of experiment

Experimental details of welding: AHSS (DOCOL M) with 1.5 mm thickness pipes prepared with Socage Company with length of 124mm are presented in this chapter. The pipes were made with three different joints. In welded joints, two components may be under the direct control of the designer, the weld type and the joint type. There are several different techniques for joining two pieces of material. Examples of these techniques are butt joints, lap joints, corner joints, edge joint, tee joints and flanged joint. In accordance with the joining type designed, the weld will have different properties. In our case we use 3 different joints in the experiments: 1.Lap joints 2. Butt joints 3.Falanged joints.

The specific fiber laser used was continuous wave type with a power capacity of 3 kW and beam quality of (8 mm-mrad). The laser beam was transmitted through optical fiber and focused on the specimen surface by the lens with 200 mm focal length. The spot diameter at the focal point was about 0.1 mm. The system comprises of the laser beam delivery system mounted on the robots end-effector and moving in 3D space, with the beam perpendicular to the work pieces for all Combinations except those involving with sealing the pipe.

5.1 Design of experiment for proximity laser welding

This section is dedicated to the all the experiment which are performed, including design of experiment for choosing best combination of power and velocity in order to have small HAZ and good penetration.

5.1.1 Preliminary experiment done with 1 Kw power

In first step the feasibility of welding is tested with 1 kW power for different joint types (Lap, Flanged and Butt) with two different velocities (5mm/s and 10mm/s) Table 5-1. Using 1 Kw power is an economical choice to start the experiment. According to literature the proper choice for laser welding with 1K laser source is in the range of 5-10 mm/s. Lap joint is the best joint configuration for proximity laser welding since the material is always available.

Number	Welding type	Joint type	Power(kw)	Velocity(mm/s)
1	Proximity	Lap	1	5
2	Proximity	Lap	1	10
3	Proximity	Flanged	1	5
4	Proximity	Flanged	1	10
5	Proximity	Butt	1	5
6	Proximity	Butt	1	10

Table 5-1 First preliminary test

These experiments can be helpful in choosing the defocus value and also the weld ability of the material. Each joint configuration has some characteristic that affect the weld quality.

5.1.2 Preliminary experiments done with bead on plate configuration

The second preliminary test is done with 3 kW power on the plate of sheets. With increasing the power from 1 to 3 kW and also increasing the velocity the overall ratio of P/v decrease so less heat enter to the material and it results directly to lower deformation in the pipes. Three step of velocities(100mm/s,150mm/s and 200 mm/s) and three different spot dimension (0.1mm,0.27mm and 0.5 mm) are tried. The parameters are reported in Table 5-2:

Number	**Welding type**	**Power(Kw)**	**Velocity(mm/s)**	**Defocus(mm)**	**Spot(mm)**
1	Proximity	3	100	0	0.1
2	Proximity	3	100	3	0.27
3	Proximity	3	100	6	0.5
4	Proximity	3	150	0	0.1
5	Proximity	3	150	3	0.27
6	Proximity	3	150	6	0.5
7	Proximity	3	200	0	0.1
8	Proximity	3	200	3	0.27
9	Proximity	3	200	6	0.5

Table 5-2 Third preliminary test

Experiment with bead on plate configuration (BOP) is a useful way for understanding the weld penetration and obtaining best configuration of velocity and power.

5.1.3 Welding on prototype

In the final step the welding is performed on the pipe with lap joint configuration. No gas was used as assistance. Butt joint configuration is not used because of presence of gap in the joint. Since full penetration is not obtained for flange joint, it is suggested in the standard, it should not be used in stress or pressure applications. Micro hardness is evaluated using a Vickers's hardness tester at a load of 1 KN (Table 5-3).

Number	Welding type	Joint type	Power(kw)	Velocity(mm/s)
2	proximity	Lap	3	200

Table 5-3 Final test

Micrographs and microhardness result of the final test are presented in chapter 7.1.3

5.2 Design of experiment for Wobbling laser welding

Remote welding with wobbling technique is used to compensate the gap and also the effects of main parameters are evaluated. The main objective of using laser welding with wobbling method (which is a very new and interesting technology of laser welding) in this experiment is studying the feasibility of using wobbling technique for different joint and also evaluating the effect of main parameters.

Three different joints are used in the experiments: 1.Lap joints 2. Butt joints 3.Falanged joints. The specific fiber laser used was continuous wave type with a power capacity of 3 kW and beam quality of 8.9 mm-mad.

The scanning head is mounted on the robot arm which makes it possible to wobble the spot during welding. The laser beam was transmitted through optical fiber and focused on the specimen surface by the lens with 290 mm focal length. The spot diameter at the focal point was about 0.3 mm.

5.2.1 Preliminary experiment for choosing proper velocity

In the first step bead-on-plate experiments were performed to obtain the appropriate laser parameters for welding with 3 kW power with the focus position on the surface. As it is mentioned using bead on plate configuration is helpful for understanding the penetration

and also weldability of the material. According to literature appropriate velocity range for 3 Kw power is between 100-200 mm/s, but lower levels of velocities are tried in order to input more energy to the material for providing enough energy for wobbling the spot dimension. The parameters are reported in Table 5-4:

Number	Welding type	P(kw)	V(mm/s)	wobbling
1	Wobbling	3	30	No
2	Wobbling	3	50	No
3	Wobbling	3	70	No

Table 5-4 First preliminary test

As it is mentioned in this experiment the velocity which drills slightly the material will be used, since for enlarging the spot dimension extra power is needed.

5.2.2 Preliminary experiment on different joint configuration

In this step the feasibility of welding on different joints is tested with 3kW power for different joint types (Lap, Flanged and Butt). Poorly fitting parts often have gaps at the joint line. Gaps are undesirable as they result in poor conduction of the heat energy from the lower layer to the upper layer at this point. Conduction is paramount in achieving adequate melt of both parts, therefore for knowing the effect of different joints on the weld quality three test is done on three different joints. Parameters are reported in Table 5-5:

Number	Welding type	joint	P(kw)	V(mm/s)	wobbling
1	Wobbling	Butt	3	30	No
2	Wobbling	Flanged	3	30	No
3	Wobbling	Lap	3	30	No

Table 5-5 Second preliminary test

5.2.3 Preliminary experiment with two levels of PLU

The third preliminary test weigh up the effect of wobbling with changing PLU from 20 to 40 on the three different joints (Flanged joints, Lap joints and Butt joints).The goal of this step is enlarging the spot dimension in order to compensate big gaps. Considerations should be made for access of the beam to the joint line. The effect of increasing the spot dimension will be evaluated in this experiment. Two main aim of this step are checking possibility of

compensating big gap with 20 PLU and 40 PLU as well as evaluating the weld quality with increasing the spot dimension. Parameters are reported in Table 5-6:

Number	Welding type	joint	P(kw)	V(mm/s)	wobbling
1	Wobbling	Flanged	3	30	20
2	Wobbling	Flanged	3	30	40
3	Wobbling	Lap	3	30	20
4	Wobbling	Lap	3	30	40
5	Wobbling	Butt	3	30	20
6	Wobbling	Butt	3	30	40

Table 5-6 The Third preliminary test

In the next step the max PLU is tried on the butt joint.

5.2.4 Welding on prototype

In the final attempt, in order to compensate the big gaps in Butt joint configuration, wobbling with 80 PLU is applied to a big gap dimensions (in respect to spot dimension of laser which is in order of tenths of mm). The parameters are reported in Table 5-7:

Number	Welding type	joint	P(kw)	V(mm/s)	wobbling
1	Wobbling	Butt	3	30	80

Table 5-7 Final test

5.3 Design of experiments for CMT welding

Knowledge and control of different parameters such as welding current, polarity, arc voltage and travel speed are essential in order to consistently produce welds of acceptable quality. However, changing on variable generally requires altering additional parameters to retain an acceptable quality weld because the variables are not completely independent of each other.

Since the nature of welding with Cold Metal Transformation (CMT) is a rule based task and it is not knowledge based, fewer experiments are done in this step. It is enough to choose the joint configuration, wire material and gas type for the CMT program which is especially made for steel, then machine automatically chooses other process parameters.

But these parameters are not always trustable and further investigation and test are required. The filler metal which we used in the welding is AWS/SFA A5.28 ER110 S-G (cod. 106010017). This filler metal deposits high-strength, very tough weld metal for critical applications. Originally developed for welding HY80 steels for military applications, it is also used for a variety of structural applications where tensile strength requirements exceed 100 ksi (690 MPa), and excellent toughness is required to temperatures as low as -60°F (-51°C) [41].

Chemical Composition Requirements for Solid Electrodes and Rods:

C	Mn	Si	P	S	Ni	Cr
0.08	1.25-1.80	0.20-0.55	0.010	0.010	1.40-2.10	0.30
Mo	V	Ti	Zr	Al	Cu	Total other
0.25-0.55	0.05	0.10	0.10	0.10	0.25	0.50

Table 5-8 Chemical composition of filler metal

5.3.1 Preliminary experiment with bead on plate configuration

In the first step of experiment after selecting the joint configuration, wire material and gas type for the program prepared especially for the steel, other parameters e.g. WS (Welding Speed), current, WFS (Wire Feed Speed) and the voltage values are suggested by the machine, parameters are shown in Table 5-9.

Number	Welding type	Joint	Voltage (volt)	Current(A)	V(mm/s)
1	CMT	BOP	12	175	10
2	CMT	BOP	14	205	15

Table 5-9 the first preliminary test

As it's presented two values of current are applied for welding. Increasing the current will directly increase the penetration, deposition rate and bead size but it has little effect on bead width.

Micrographs of the first experiment are shown in chapter 7.

5.3.2 Preliminary experiment for selecting the proper velocity

The main goal of second experiment step is modifying the travel speed in order to change the bead size and bead width. With increasing the travel speed both bead size and bead width decrease but it has no effect on penetration and little effect on the deposition rate. The parameters are reported in Table 5-10.

Number	Welding type	Joint	Voltage (volt)	Current(A)	V(mm/s)
1	CMT	Butt	12	175	15
2	CMT	Butt	12	175	20
3	CMT	Flanged	14	205	20
4	CMT	Flanged	14	205	25

Table 5-10 The second preliminary test

Due to the second preliminary test for obtaining the desired weld bead dimension an average value of velocities are chosen.

5.3.3 Welding on prototypes

The final test is performed on both butt joint and flanged joint configuration. Unlike laser welding, CMT welding is not sensitive to the gap, so it's applicable in different butt joints with bigger gap in respect to the fiber laser. The parameters are reported in Table 5-11.

Number	Welding type	Joint	Voltage (volt)	Current(A)	V(mm/s)
1	CMT	Butt	17	175	17
2	CMT	Flanged	22	205	22

Table 5-11 Final test

The micrographs and micro hardness test of final test are presented in chapter 7.

Chapter 6: Sample preparation process

In order to cut the pipes to the required dimension a sheet metal cutting Guillotine and an abrasive water jet system has been used (see Figure 6-1). The sheet metal cutting Guillotine was used to cut Small dimensions after performing of welding, while pipes and other bigger sheets have been cut by use of Abrasive water jet. The abrasive water jet system also has been used for cutting the welded specimens of lap-joint, butt joint and flanged joint configurations longitudinally in the middle of the weld.

To study the joints, once welded the sheets, it is necessary to make a Metallographic sample preparation. This preparation allows us to make a macro and micro examination of the welded joints. After these examination, and to conclude the study we must to carry out the hardness tests. Below it is showed the order to follow for the analysis of the samples, as well as a brief description of each step.

Metallographic is knowledge of material science and microscopy and also Knowledge about sample preparation in practice. By metallographic examination is possible identify and study the different structural elements and properties of each material. To study the structure of a material with an optical microscopy is necessary Carry out a careful sample preparation. The practical sample preparation may be divided into following steps:

- ✓ Cutting
- ✓ Mounting
- ✓ Planar grinding
- ✓ Fine grinding
- ✓ Polishing
- ✓ Etching

In our case the process for HSS has been used.

Cutting

Cutting, or sectioning, has performed with a Water jet machine and “abrasive cutter”.

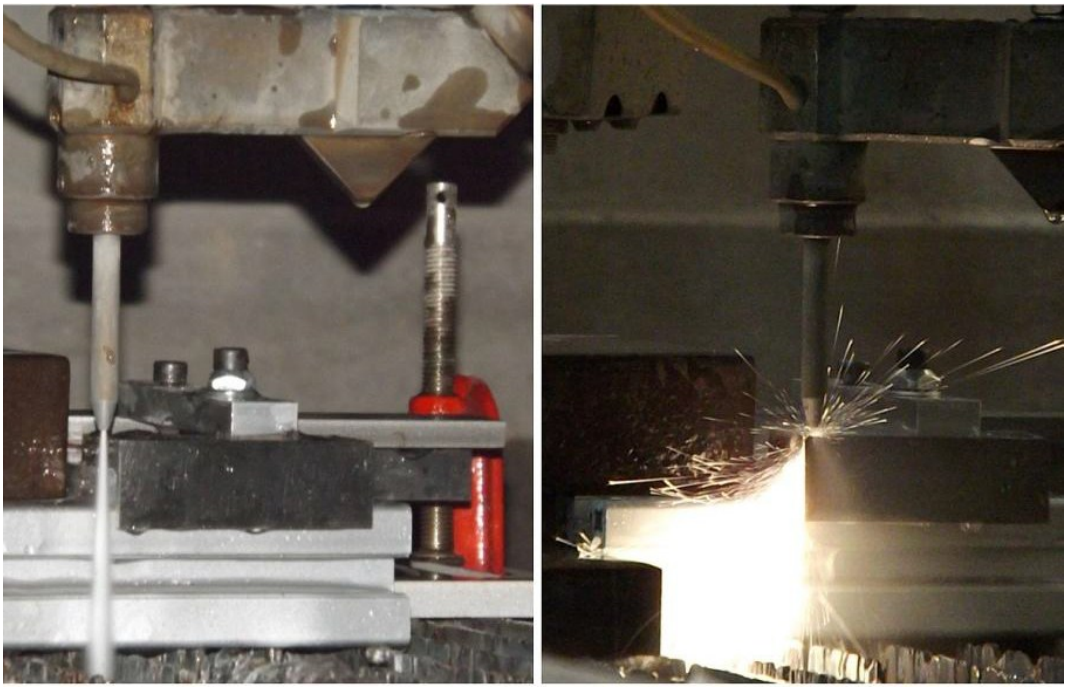

Figure 6-1 Cutting of pipes using water jet machine

Mounting

After cutting the sample are mounting with a “phenol powder”. This step is necessary to make the samples easier to handle and to protect edges or to reinforce weak or porous material.

Planar grinding

Grinding paper is used to carry out the planar grinding. In our case it has been performed in 8 steps, on 60,120,180,320, 600, 800, 1200 and 2500 grains size. It is compulsory to start with the paper of biggest grain size and finish with the finest one. Each step took about 3 minutes. It is important rotate 90o and washes the sample carefully between each step and also using ultra sound between each step in order to completely remove the abrasive grains of last step.

Polishing

It consists in 3 steps: 9μm (2 minutes), 3μm and 1μm (2 min each one) using diamond abrasives in aerosol on "TEXMET" cloths. "DP-Blue" is used for cooling and lubrication. The samples must be washed with soap and water between steps and after the last one.

Etching

This step is necessary in order to see the structure. 2% "Nital" (3% HNO3 in ethanol) is used. Is necessary clean again with methanol to avoid marks from the stains. Once Metallographic sample preparation has been finished, the samples are ready to perform the macro and micro examination in the microscopy, Figure 6-2.

Macro Examination

Macro Examination is a method of examination of large regions of the specimen surface or fractured section with the naked eye or under low magnification. During the examination, any defects on the sample may be assessed, as slag, porosity, lack of weld penetration or lack of sidewall fusion. As well as defects, is possible to determinate a large number of features, including weld run sequence.

Figure 6-2 Etched samples for micro examination

Micro examination

Micro examination is carried out for several purposes; the most clear is to analyze the structure of the material. It is also common to examine for metallurgical anomalies such as excessive grain growth, third phase precipitates, measuring HAZ and weld penetration as well as weld width and also different weld defects such as drop out and porosity. This process is performed with an optical microscopy with a high magnification.

Hardness test

Hardness is the property of a material that enables it to resist plastic deformation, usually by penetration. Hardness is not an intrinsic property of the material. The value of this property is the result of a defined measurement procedure, thus depending on the hardness method used; the hardness value will be different. All of the hardness tests involve the use of a specifically shaped indenter, significantly harder than the test sample. This indenter is pressed into the surface of the sample using a specific force. Either the depth or size of the indent is measured to determinate the hardness value.

Hardness measurements are widely used for the quality control of materials because they are quick and considered to be non-destructive tests when the marks or indentations produced by the test are in low stress areas. It this thesis Vickers hardness test has been used.

- ✓ Vickers hardness test

Vickers hardness is a measure of the hardness of a material, calculated from the Size of an impression produced under load by a pyramid-shaped diamond indenter. This indenter is a square-based pyramid with an angle of 136º between opposite faces, Figure 6-3.

The two diagonals of the indentation left in the surface of the material after removal of the load are measured using a microscope and their average calculated. The area of the surface of the indentation is calculated. The Vickers hardness is the value obtained by dividing the kg load by the square mm area of indentation. Load time is around 30 seconds. To cover all testing requirements the Vickers test has two different force ranges, Micro (10g. to 1000g) and Macro (1kg to 100kg). The advantages of the Vickers hardness test are that extremely accurate measures may be taken, and just one type of indenter is used for all types of metals and surface treatments [42].

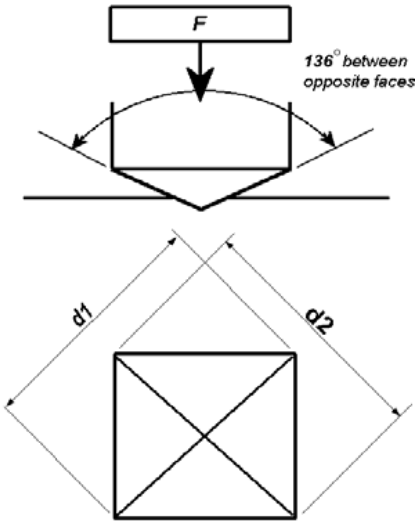

Figure 6-3 Vickers indenter

Chapter 7: Welding results and analysis

As cited in advance totally 43 specimens have been welded. Welding can be seen in the fallowing figures. .This section is dedicated to all the micrographs and hardness plot s of the welds which are performed, including Proximity laser welding experiments, wobbling laser welding experiments and CMT welding experiments for choosing best combination of power and velocity in order to have small HAZ and good penetration.

7.1 Proximity laser welding

In this section proximity welding welds are analyzed. In order to find the best combination of power and velocity micrograph of all preliminary tests are obtained. In the first step the fusibility of using proximity laser for welding DOCOL M is checked and in the second step by varying the velocity from 100mm/s, 150 mm/s and 200 mm/s and also changing the spot dimension the micrographs and micro hardness is evaluated.

7.1.1 Preliminary experiment done with 1 Kw power

Initially the feasibility of welding is tested with 1 kW power for different joint types (Lap, Flanged and Butt) with two different velocities (5mm/s and 10mm/s). The lap joints and flanged joints are the best joint configuration for proximity laser welding since in the experiment no filler material is used and the gap compensation is not possible in laser welding taking it in to account that the spot dimension is in order of tenth of millimeter. The first two figures show the welding on lap joint configuration. The macrograph is shown in Figure 7-1.

By increasing irradiance, the depth of the welded bead increases. But the increase of irradiance must be controlled and limited in the case of not through welding. If the irradiance is too high, porosity can be generated during the laser welding process because of the entrapment by plasma channel inside the bead. This results in a **porosity** defect. And also the other problem of high irradiance is **drop out** defect. This problem occurs in welding with high power and low velocity, such as experiment number one which is done with 1Kw and 5 mm/s velocity. See Figure 7-2.

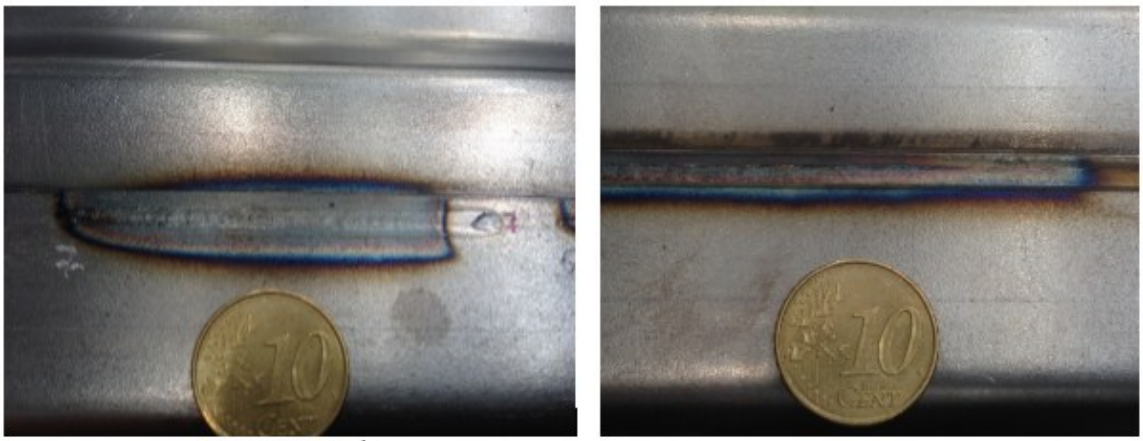

Figure 7-1 Proximity laser welding, spot dimension=0.1mm

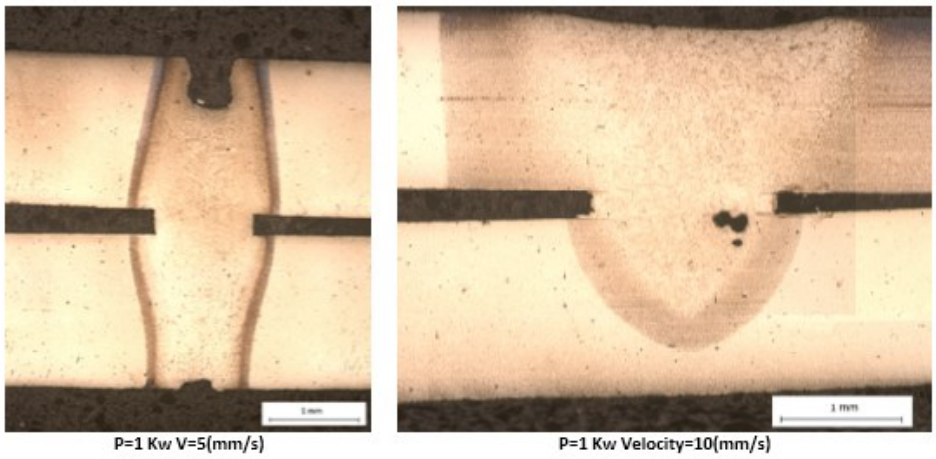

Figure 7-2 Proximity laser welding, spot dimension=0.1mm

In the fallowing figures micrographs of 1Kw proximity laser welding on the flanged component are reported. Flange joints can be welded with fiber laser in a good way, since no gap is present in the joints, Figure 7-3.

P=1, V=5 mm/s P=1 Kw, v=10 mm/s

Figure 7-3 Proximity laser welding, spot dimension=0.1mm

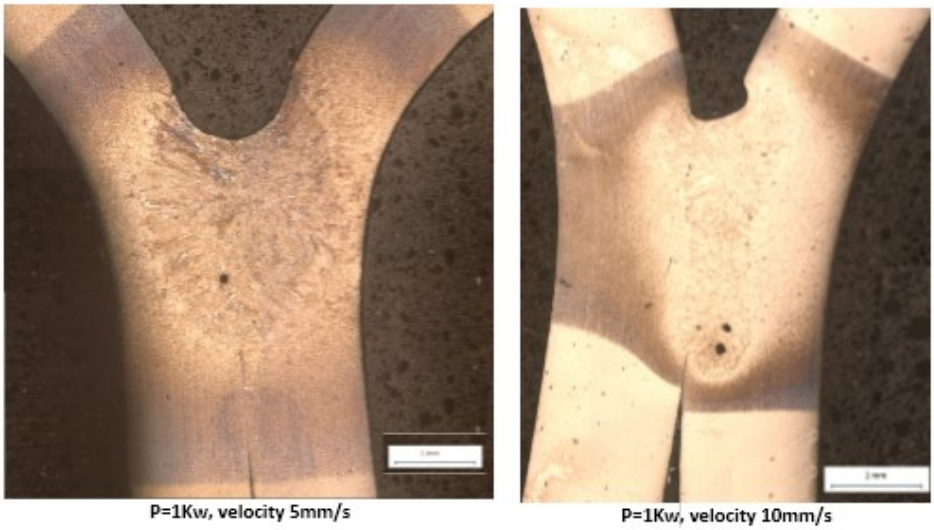

P=1Kw, velocity 5mm/s P=1Kw, velocity 10mm/s

Figure 7-4 Proximity laser welding, spot dimension=0.1mm

As it is shown in Figure 7-4 similar to ex-experiment due to the high irradiance, porosity is entrapped by and weld has **porosity** defect. And a large HAZ is present in the pictures.

Since proximity laser welding is sensitive to gap, it's not applicable to all kind of joints and a precise coupling is needed, In the case of present of big gap, the solution will be wobbling laser welding or CMT welding. In the fallowing figures micrographs of two experiment are showed, in the first figure the joint is precisely coupled and is welded properly on the contrary in the second one a gap is present and it is not welded in a good way, Figure 7-5.

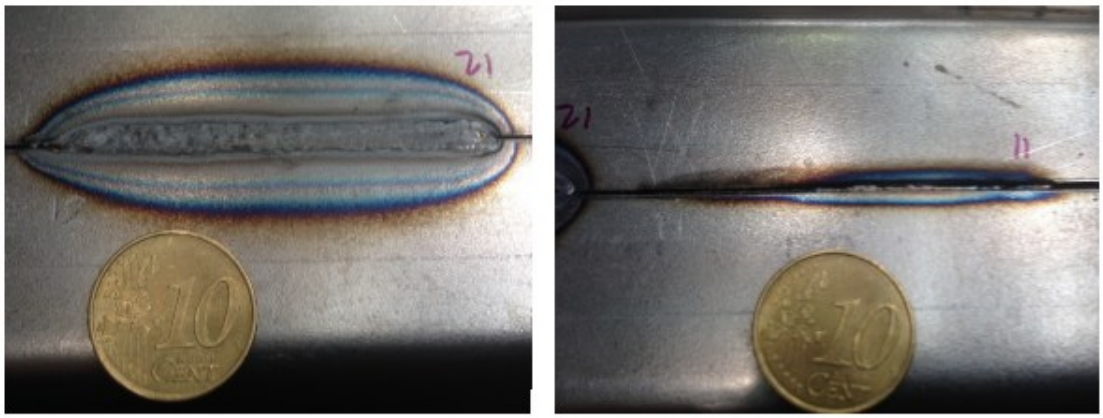

P=1Kw, V=5mm/s P=1 Kw, V=10(mm/s)

Figure 7-5 Proximity laser welding, spot dimension=0.1 mm

P=1Kw, velocity 5(mm/s)

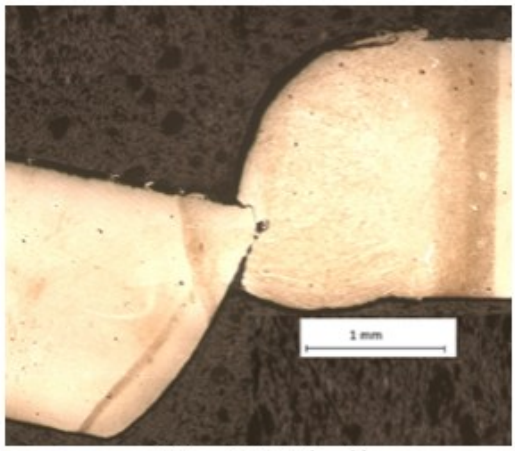

P=1Kw, velocity 10 (mm/s)

Figure 7-6 Proximity laser welding, spot dimension=0.1 mm

Large HAZ is present in sample welded with 5 mm/s (see Figure 7-6).

7.1.2 Preliminary experiments done with bead on plate configuration

The second preliminary test is done with 3 kW power on the plate of pipes. Welding on the plate is a logic way to understand the penetration of weld as well as the HAZ, in this part the micrographs of experiment which is done with 3 different powers and 3 different spot dimensions are showed. Also the hardness test of each sample is presented. With increasing the power from 1 to 3 kW and also increasing the velocity the overall ratio of P/v decrease so we input less heat to the material and it results directly to lower deformation in the pipes. The objective is obtaining process parameters in order to have 75% weld penetration with

max velocity in overlap joint configuration. Three different velocities (100mm/s, 150mm/s, 200mm/s) are tried with three different defocus values (no defocus, 3mm and 6mm defocus).

The first experiment is done with 3 Kw power and 100 mm/s velocity (number 1, 2 and 3 in Figure 7-7).

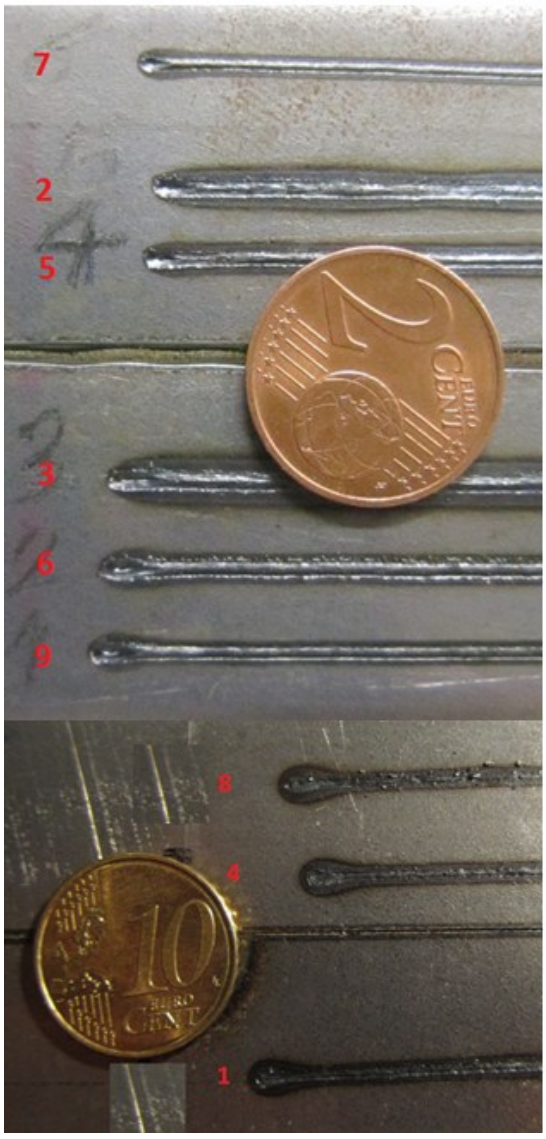

Figure 7-7 Second experiment P=1Kw

At slow speeds the pool is large and wide and results in drop out (Figure 7-8). The place which hardness test is performed is shown in all pictures with a rectangular on the Macrographs.

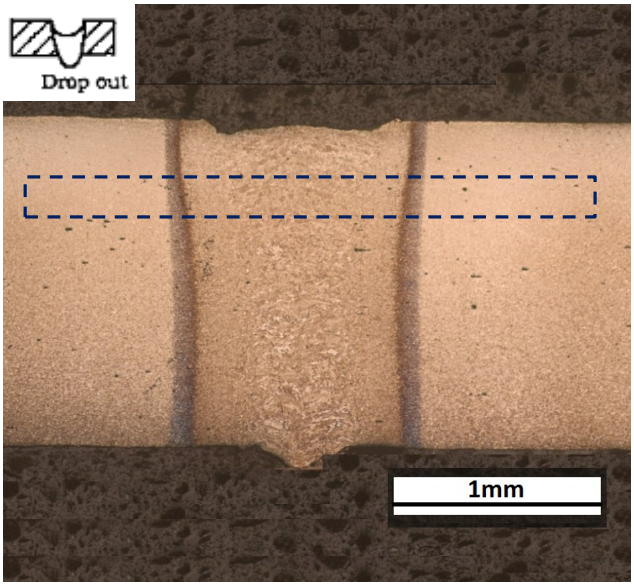

Figure 7-8 Velocity 100mm/s, spot dimension 0.1mm

Due to the high power density, full penetration is obtained and the micro hardness result is presented in Figure 7-9. The HAZ width is equal to 0.6 mm.

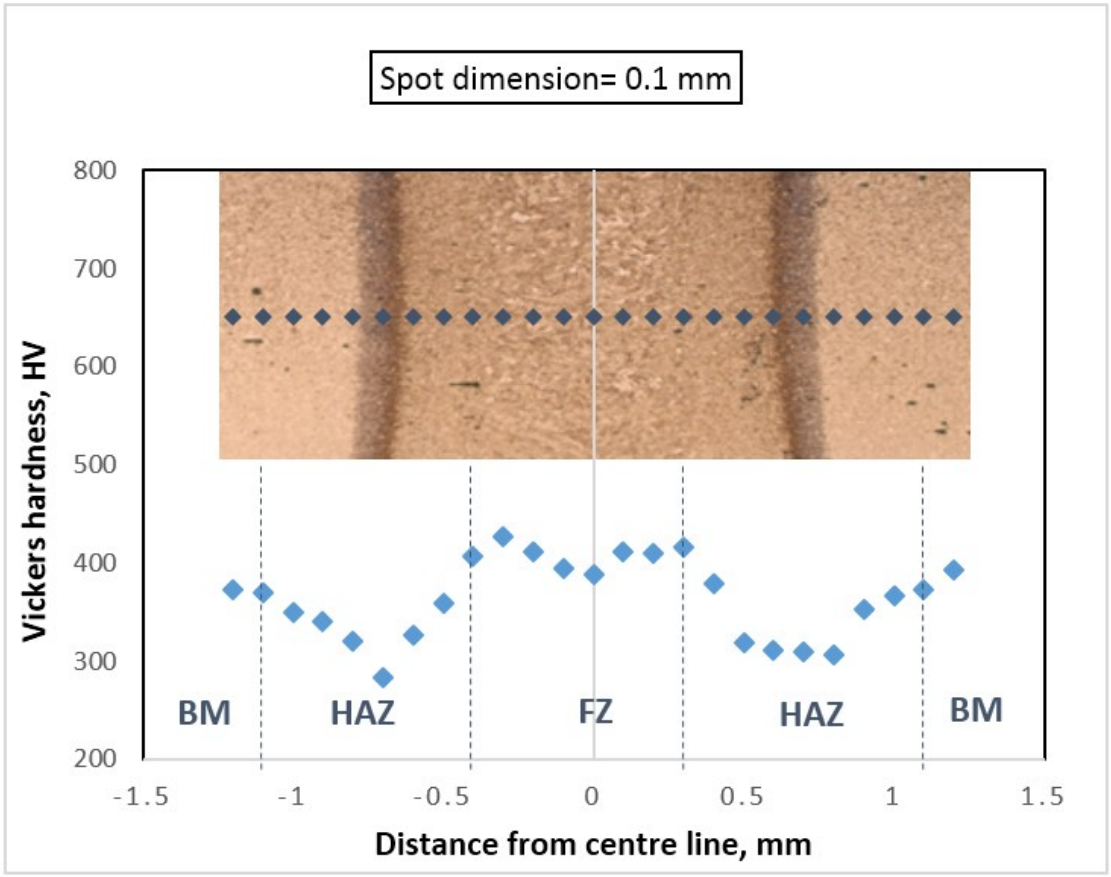

Figure 7-9 Spot dimension 0.1 mm

The second experiment is done with 3 Kw power and 100 mm/s velocity and 3mm defocus. Full penetration is obtained. The FZ, HAZ and based metal are presented in Figure 7-10 and Figure 7-11. The HAZ width is equal to 0.8mm.

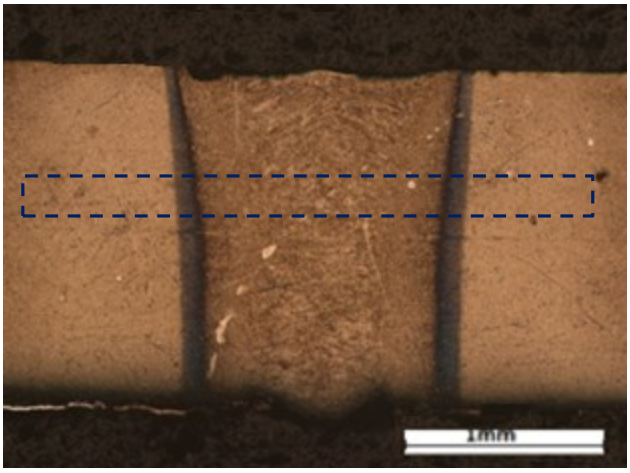

Figure 7-10 Velocity 100mm/s, spot dimension 0.27mm

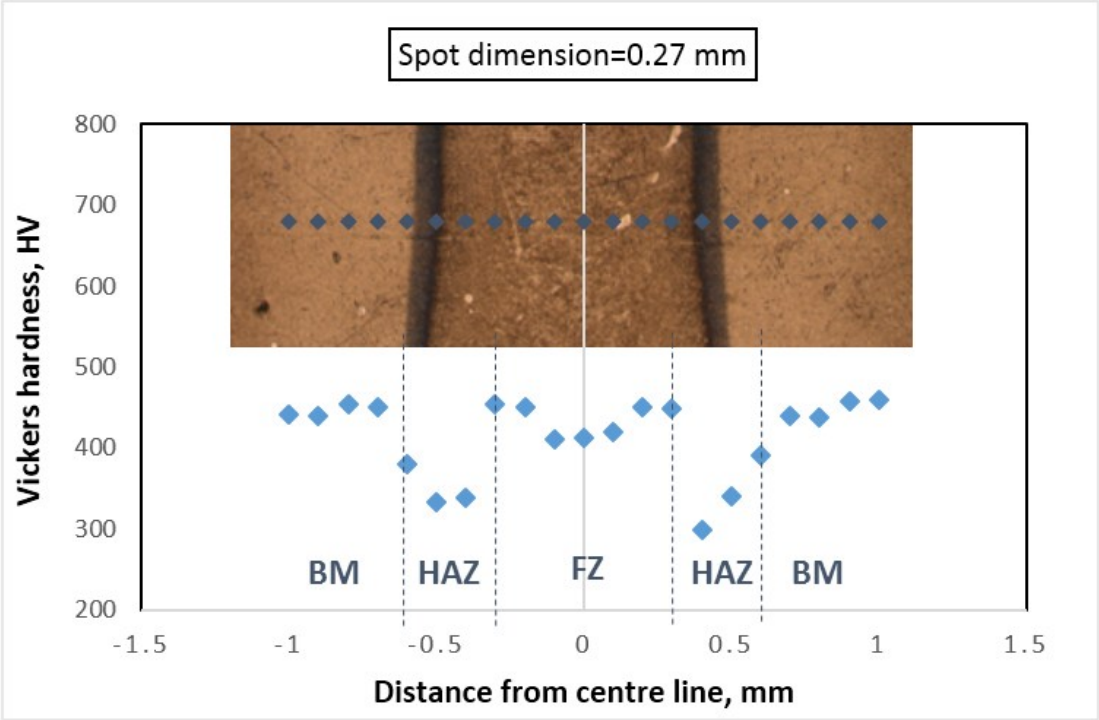

Figure 7-11 V=100 mm/s

The third experiment is done with 3 Kw power and 100 mm/s velocity and 6mm defocus. Also in this case Full penetration is obtained. The FZ, HAZ and based metal are presented in Figure 7-12 and Figure 7-13. The HAZ width is equal to 0.9 mm

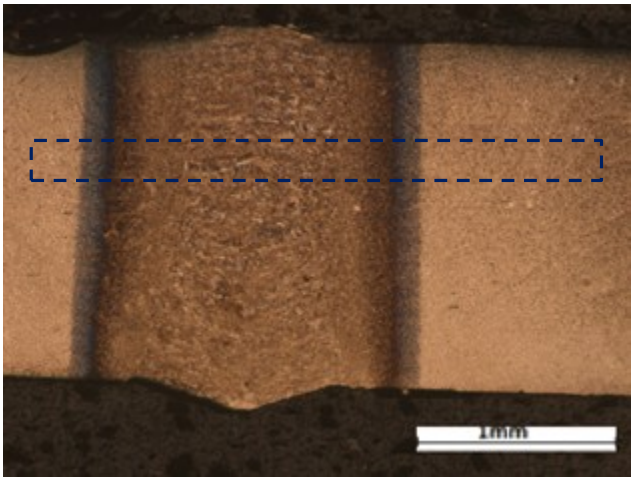

Figure 7-12 Velocity 100 mm/s, spot dimension 0.5mm

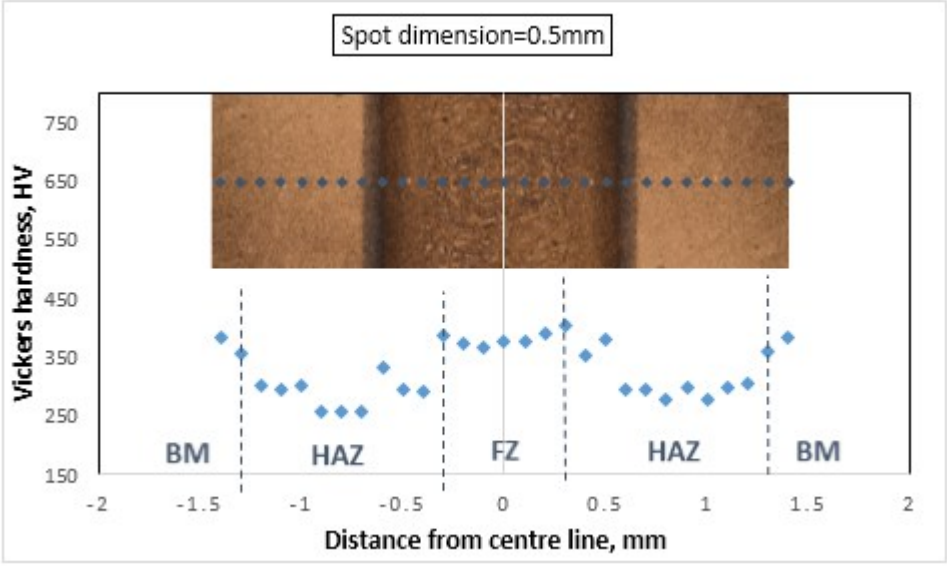

Figure 7-13 V=100 mm/s

In next step higher velocity (150 mm/s) is tested with 3Kw power, for all cases full penetration is obtained. The hardness and micrograph is shown in Figure 7-14 and Figure 7-15. The HAZ width is equal to 0.25mm.

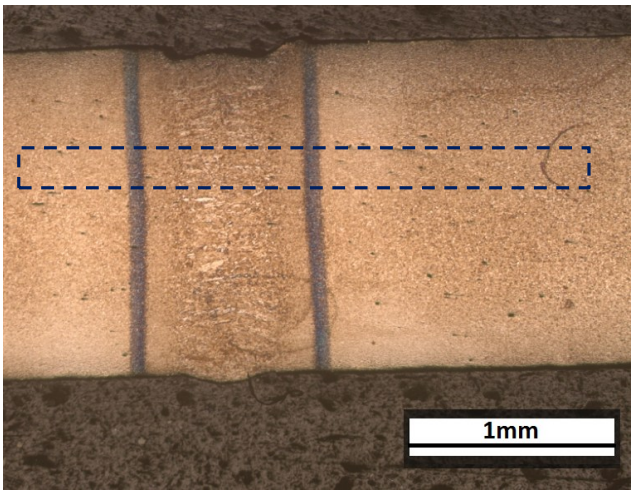

Figure 7-14 Velocity 150 mm/s, spot dimension 0.1mm

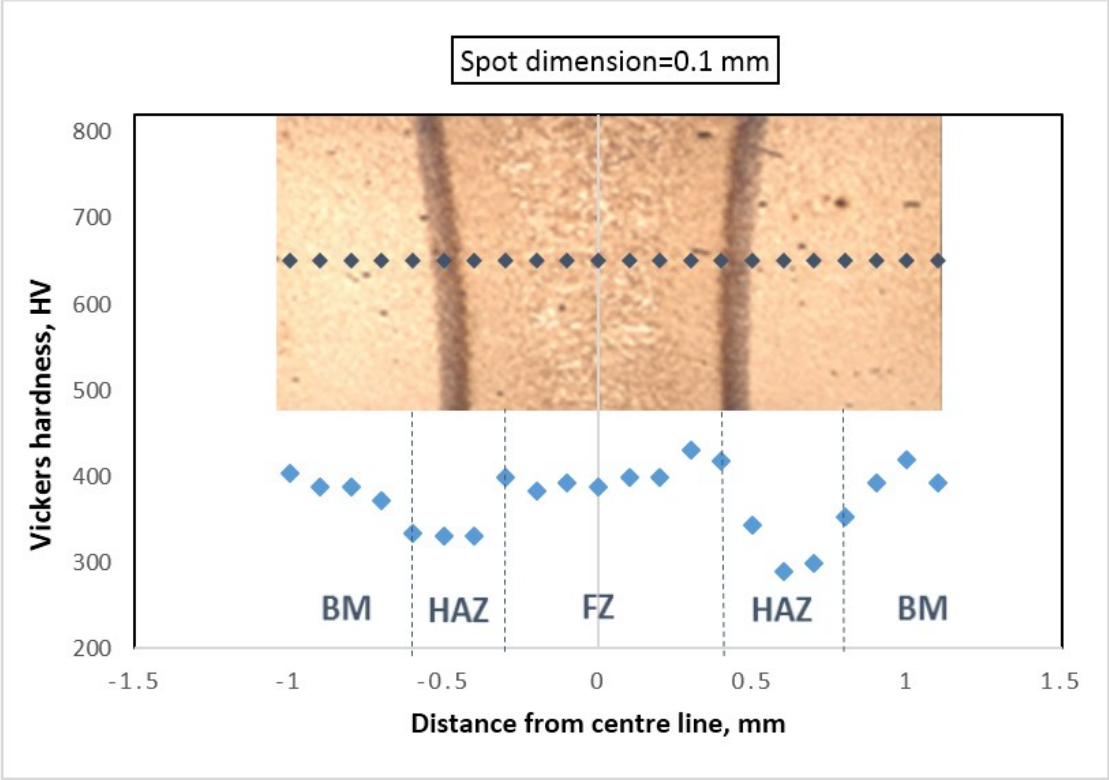

Figure 7-15 V=150 mm/s

Changing the spot dimension with defocus of 3mm does not affect the heat affected zone and fusion zone too much. The HAZ slightly increase to 0.3 mm as and full penetration is obtained, Figure 7-16 and Figure 7-17.

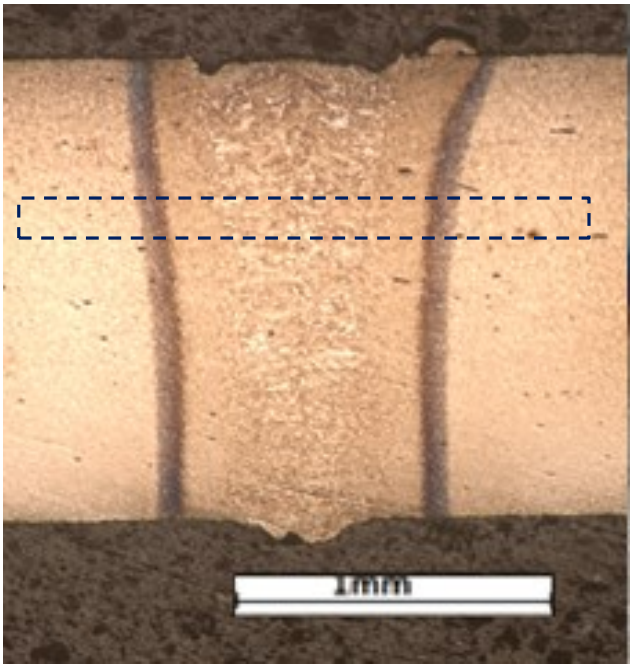

Figure 7-16 Velocity 150 mm/s, spot dimension 0.27mm

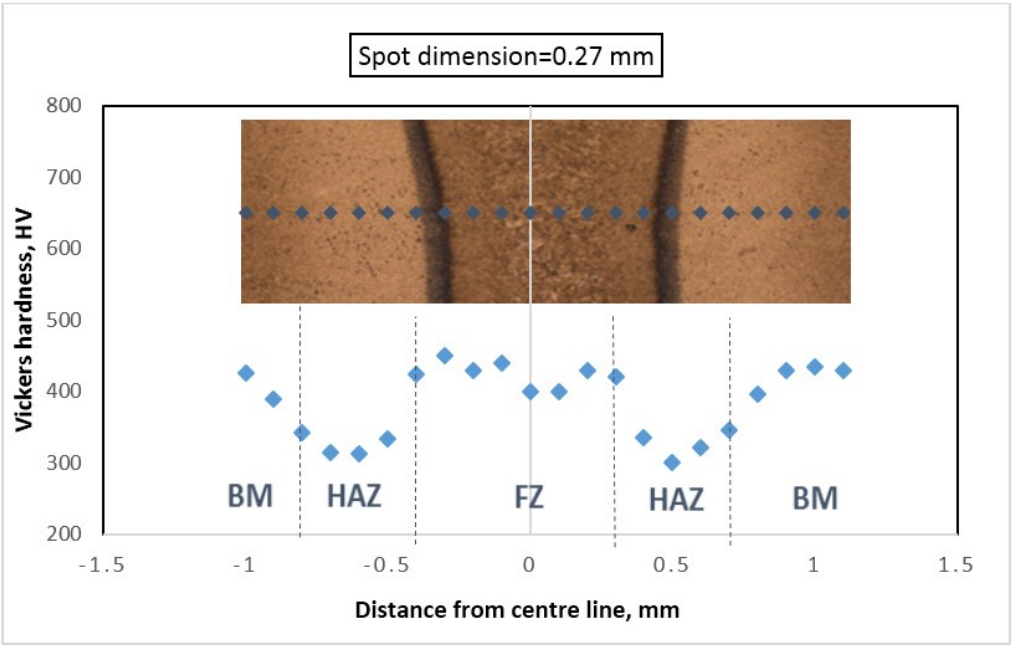

Figure 7-17 V=150 mm/s

By increasing the spot dimension to 0.5 mm, again full penetration is obtained, as it's presented the hardness of HAZ slightly decreased, the HAZ is equal to 0.4mm. Figure 7-18 and Figure 7-19.

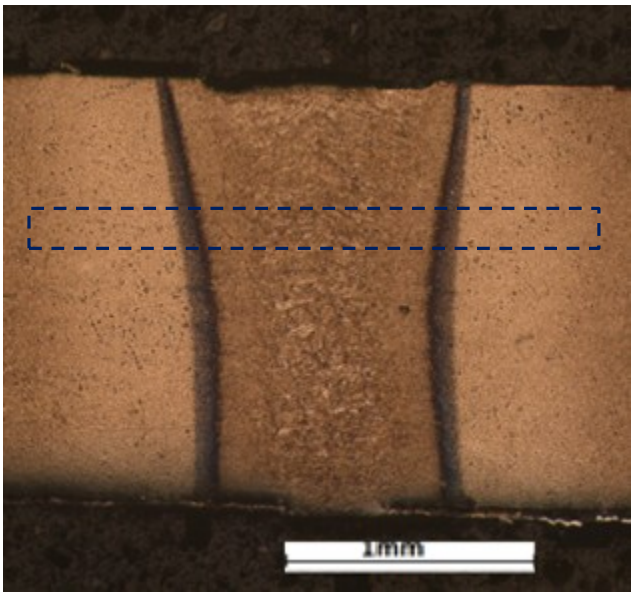

Figure 7-18 Velocity 150 mm/s, spot dimension 0.5mm

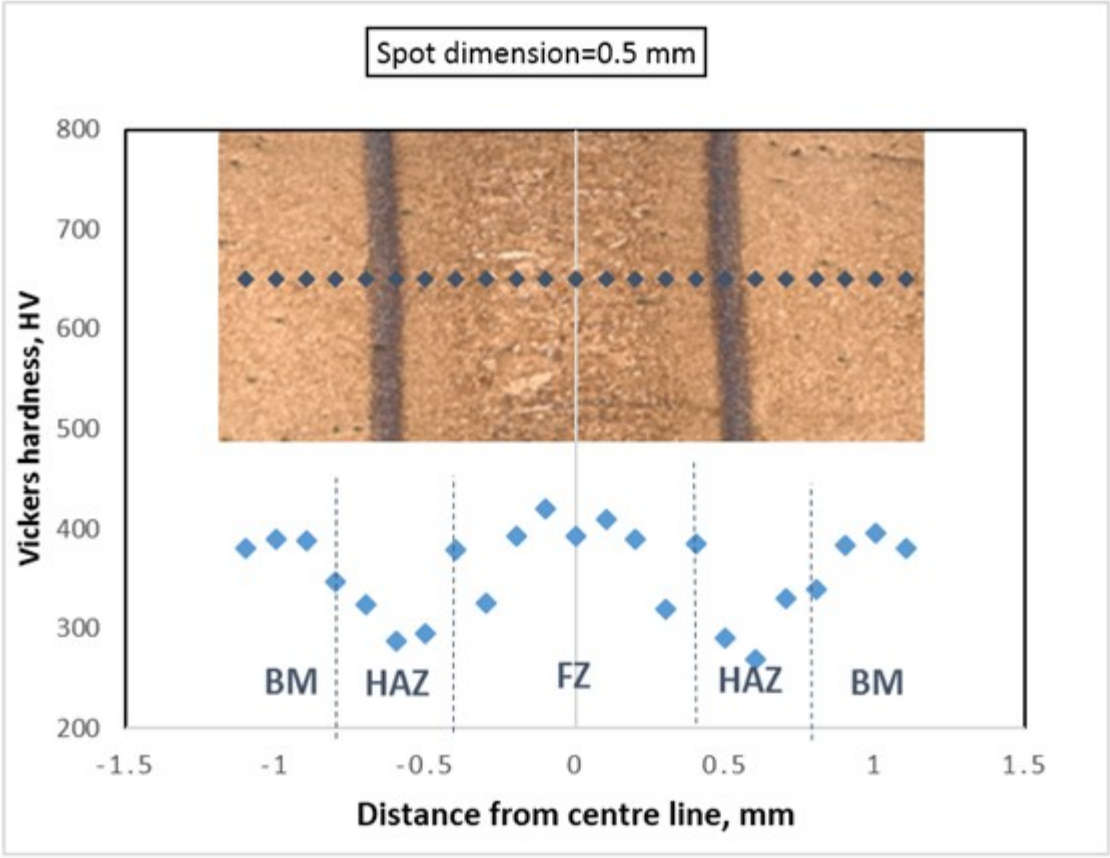

Figure 7-19 V=150 mm/s

The welding speed is one of the most important factors in laser welding. This variable affects the geometrical and micro-structural characteristics of the welding bead. The higher welding speed produces the lower bead dimension (thickness and width).In this experiment, finally the velocity is increased to 200 mm/s. A smaller width of in lower part of weld is obvious. It's presented in the graph that heat affected zone is decreased to 0.1 mm, and again in this case full penetration weld is obtained, Figure 7-20 and Figure 7.21.

At higher speeds, the strong flow towards the center of the weld in the wake of the keyhole has no time to redistribute and is hence frozen as an undercut at the sides of the weld. The HAZ is equal to 0.2 mm.

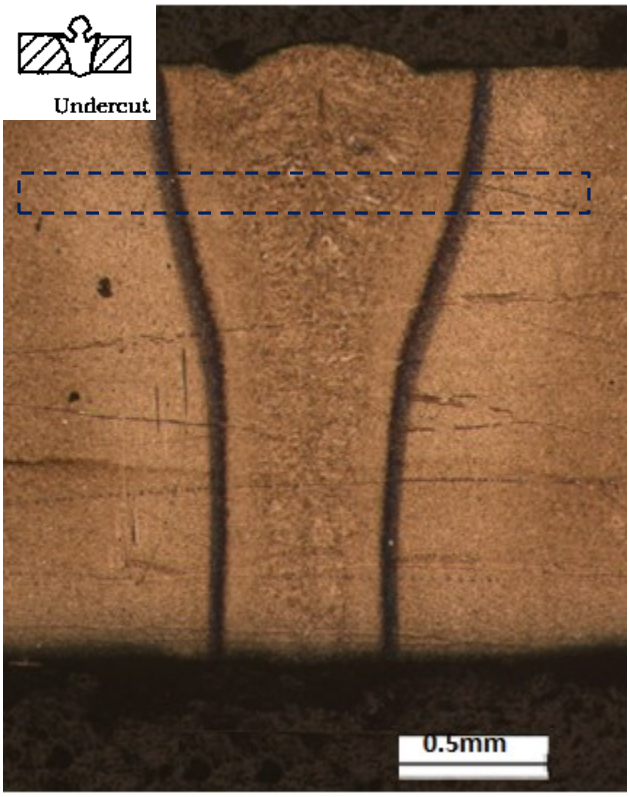

Figure 7-20 Velocity 200 mm/s, spot dimension 0.1mm

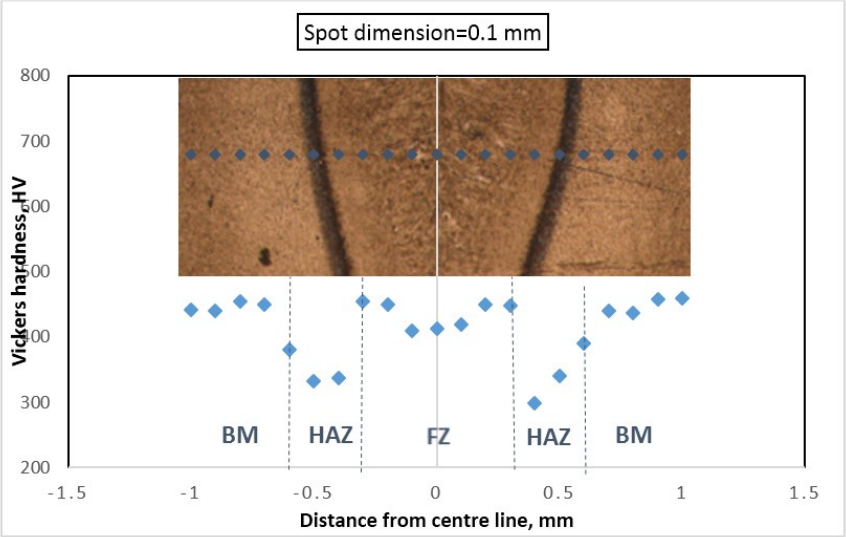

Figure 7-21 V=200 mm/s

The test is done with 0.27 mm spot dimension, the power density is not enough to obtain full penetration, 70% penetration is obtained and HAZ is equal to o.3 mm. Figure 7-22 and Figure 7-23.

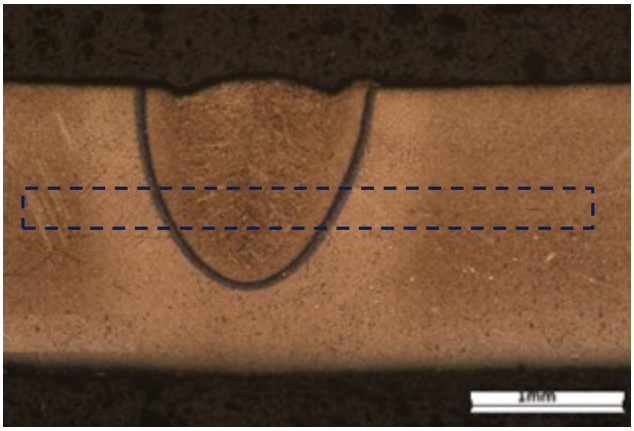

Figure 7-22 Velocity 200 mm/s, spot dimension 0.27mm

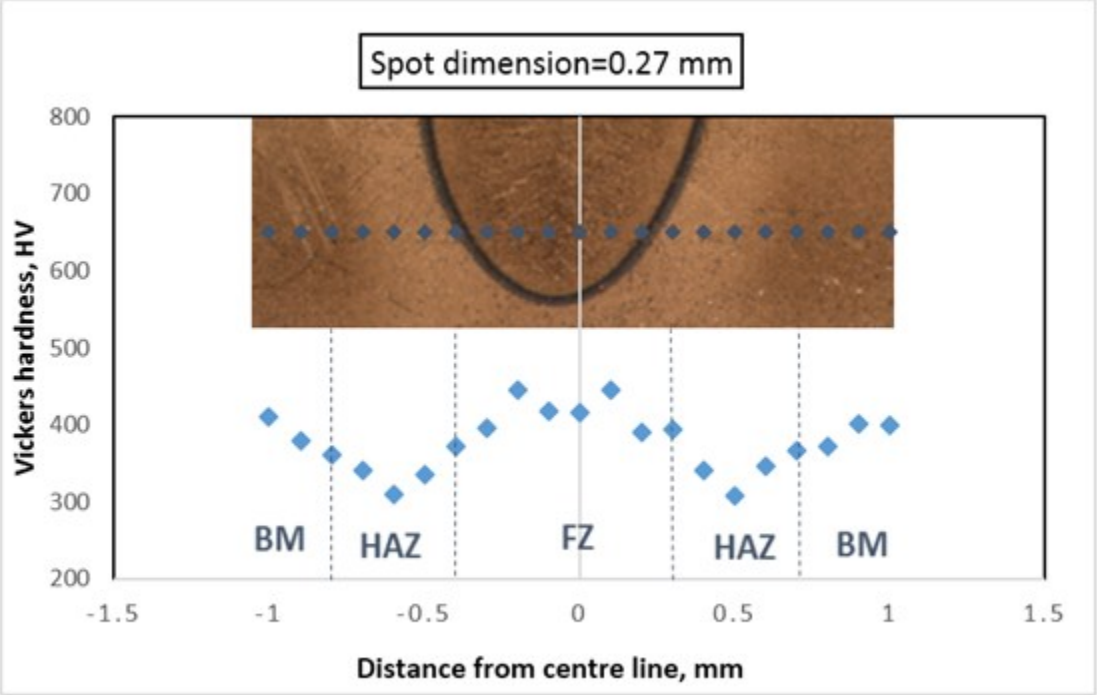

Figure 7-23 V=200 mm/s

As it's mentioned increasing the spot dimension, directly decrease the power density, when irradiance decrease, the depth of the welded bead decrease as well. To weld with 0.5 spot dimension results in 50% penetration depth. HAZ is equal to 0.4 mm. See Figure 7-24 and 7-25.

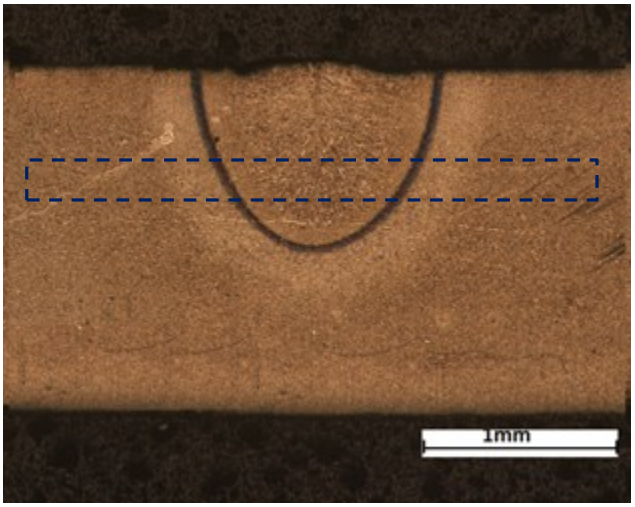

Figure 7-24 Velocity 200mm/s, spot dimension 0.5mm

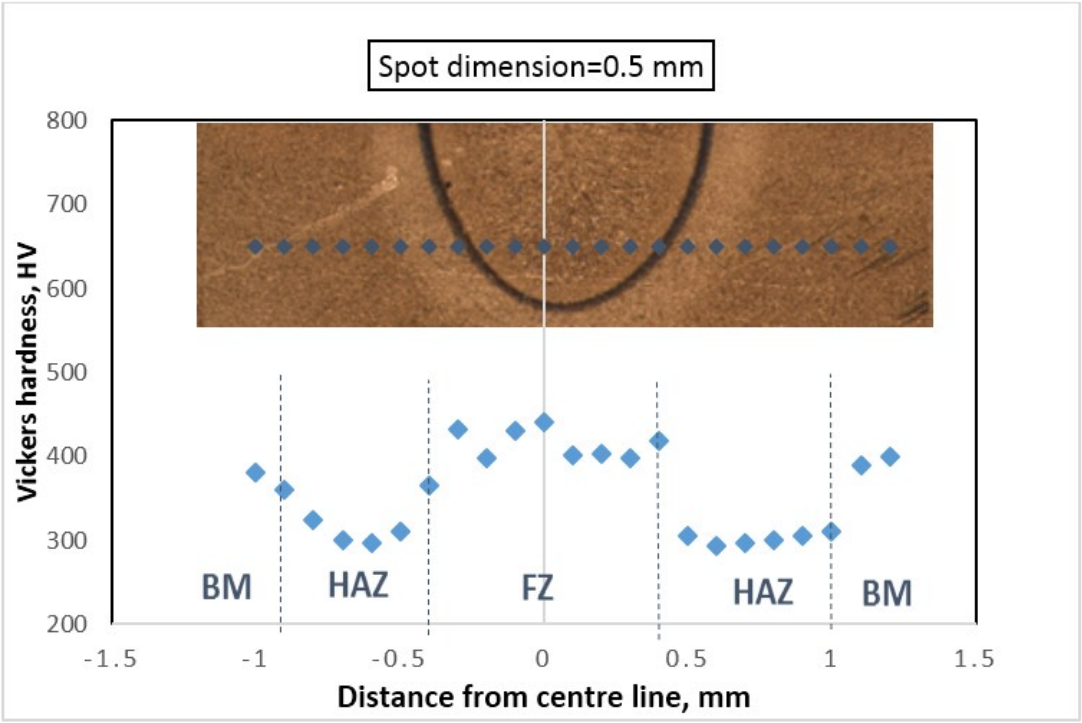

Figure 7-25 V=200 mm/s

In the fallowing both HAZ width and FZ width of second preliminary experiments which are performed with bead on plate configuration are plotted. By increasing the velocity both HAZ and FZ width decrease. Also increasing the spot dimension (D=0.1mm, D=0.27mm and D=0.5mm) the HAZ width and FZ width increase as well. See Figure 7-26 and Figure 7-27.

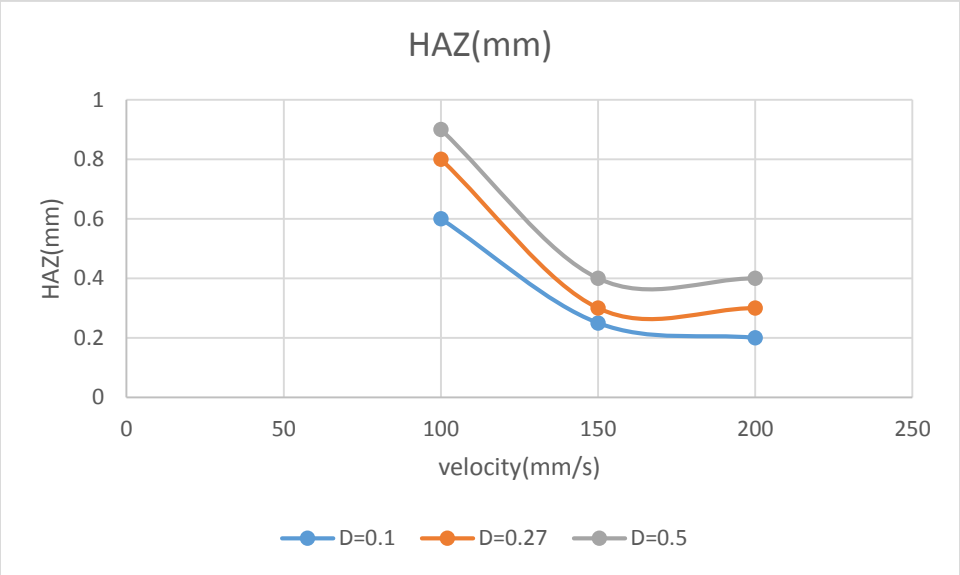

Figure 7-26 HAZ width-Velocity, P=3Kw

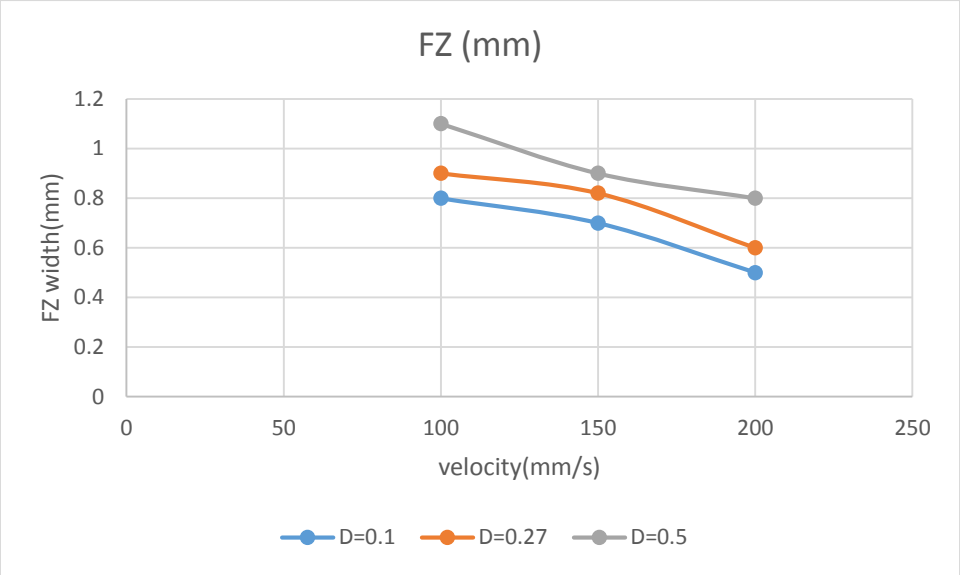

Figure 7-27 FZ width-velocity, P=3 Kw

7.1.3 Results and analysis of weld joint of prototype

In the final step the welding is performed on the pipe with lap joint configuration. For obtaining full penetration and at the same time high productivity the test is performed with 3 Kw power and 200 mm/s velocity. The focus is chosen on the surface of the plate. Values of hardness measured in the weld are shown in the following figures. Hardness of base metal is in range of 370-430 HV. Laser welds contain martensitic microstructure with a corresponding hardness of about 440 HV which is slightly more than base metal. Hardness of the HAZ did not significantly decrease. A very small area of material affected with heat HAZ=0. mm, Figure 7-28.

Figure 7-28 P=3 Kw, Spot dimension= 0.1 mm

Lap joint problem areas that result from **improper fit-up** is visible in Figure 7-29.

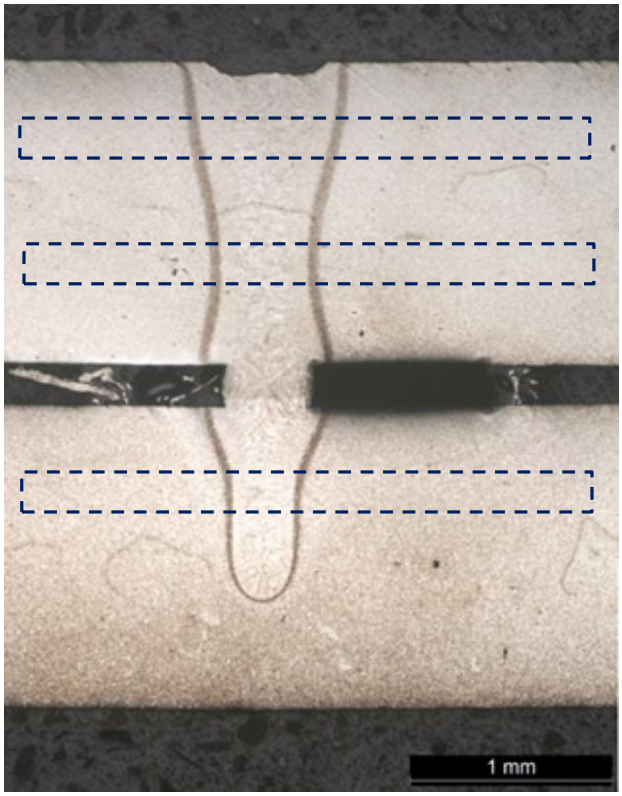

Figure 7-29 P=3Kw, Spot dimension=0.1 mm

The hardness test is performed in 3 different levels in the final samples. Results of hardness of upper side of the weld are presented in Figure 7-30. The area of base metal, heat affected zone and fusion zone are presented as well.

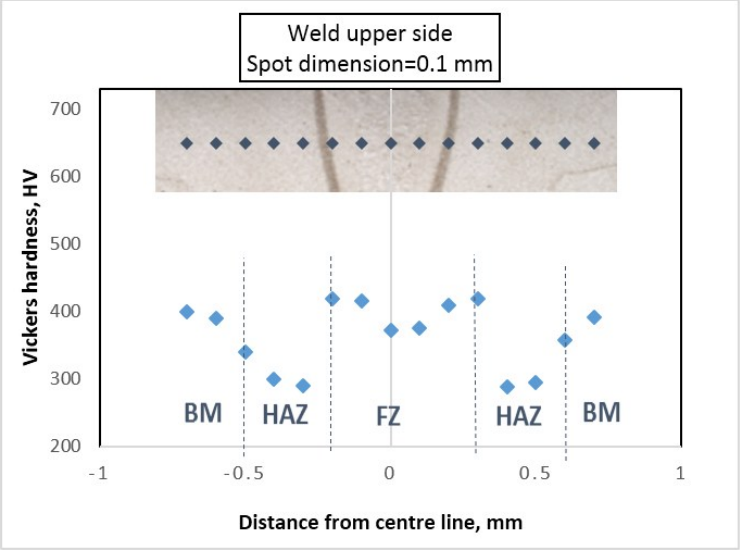

Figure 7-30 Proximity laser welding of lap joint, V=200 mm/s

Results of hardness test for middle side and lower side of the weld are presented in Figure 7-31 and Figure 7-32. The hardness test shows that in the lower parts of the lap joint in respect to the surface, lower HAZ and fusion zone exist. All in all very low HAZ equal to 0.4 mm and very small fusion zone is present in the part.

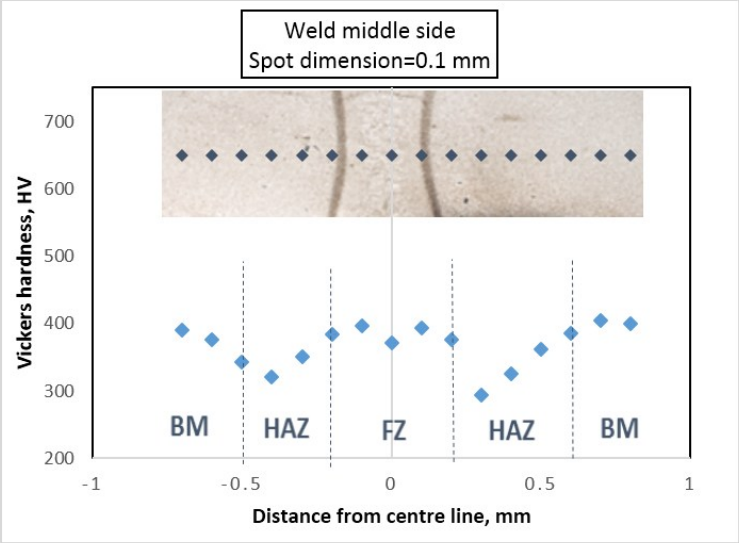

Figure 7-31 Proximity laser welding of lap joint, V=200 mm/s

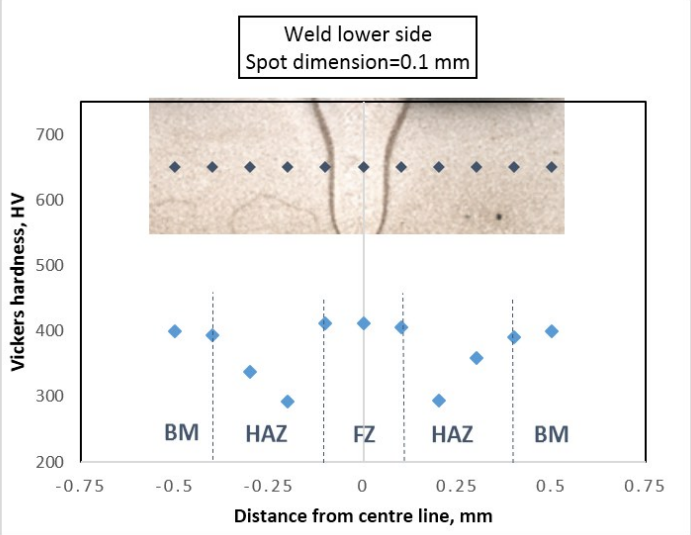

Figure 7-32 Proximity laser welding of lap joint, V=200 mm/s

7.1.4 Measuring the planarity of prototype

In principle, factors that significantly affect welding residual stress and distortion can be categorized into three types, namely, material properties, design-related parameters and fabrication- related variables. Material or material-related characteristics mainly include thermal conductivity, specific heat capacity, thermal expansion coefficient, Young's modulus, Poisson's ratio, yield strength, work hardening coefficient, thermodynamics and kinetics of phase transformation, and transformation plasticity [43]. During welding of steel, the heat source leads to rapid heating and melting of the material and the formation of a weld pool that subsequently cools and solidifies. Welding stresses arise due to the inhomogeneous cooling and in steel these stresses are caused by the effects of non-uniformly distributed cooling contractions [44].

One of the main objectives of this work is reducing the deformation of pipes which is directly related to heat input to the component. The heat input is equal to:

$$H(Kj) = \frac{p(kw)}{v(mm/s)} * l(mm)$$

The final experiment is done with 3 Kw power and 200 (mm/s), the length of each pipe is equal to 120(mm). The heat which is inputted in the component is equal to 1.8 Ki. The planarity of the component is measured before and after welding with height gauge (see Figure 7-33). For measuring the planarity each pipe is divided to 60 different points, the gap between each point is 2cm. The pipe is placed on a plane table, height of each point is measured and then all the numbers are subtracted from the average. This process repeated for three times (Ynorm1, Ynorm2 and Ynorm3). Normalized numbers are plotted. Y_{tot1} is calculated as the Average of three different normalized height (Ynorm1, Ynorm2 and Ynorm3) .The same measurement is done for the pipe after welding and normalized heights are evaluated (Y_{tot2}). Finally Y_{tot1} and Y_{tot2} are plotted in a separate plot.

Figure 7-33 Height gauge used for measuring planarity of pipes

Before welding, the difference between min and max value of height in is 2.04 mm. Trend of pipe height is plotted in Figure 7-34. The difference between maximum and minimum normalized height in different step of measurement and is reported in Table 7-1. The variances of averaged normalized measured heights (Y_{tot}) before welding is 0.4 mm.

	Y1norm	Y2norm	Y3norm	Y(tot)
Min	-1.06	-1.10	-1.03	-1.06
Max	0.96	0.98	1.02	0.98
Max-Min	2.03	2.09	2.06	2.04

Table 7-1 Measurement of planarity before welding

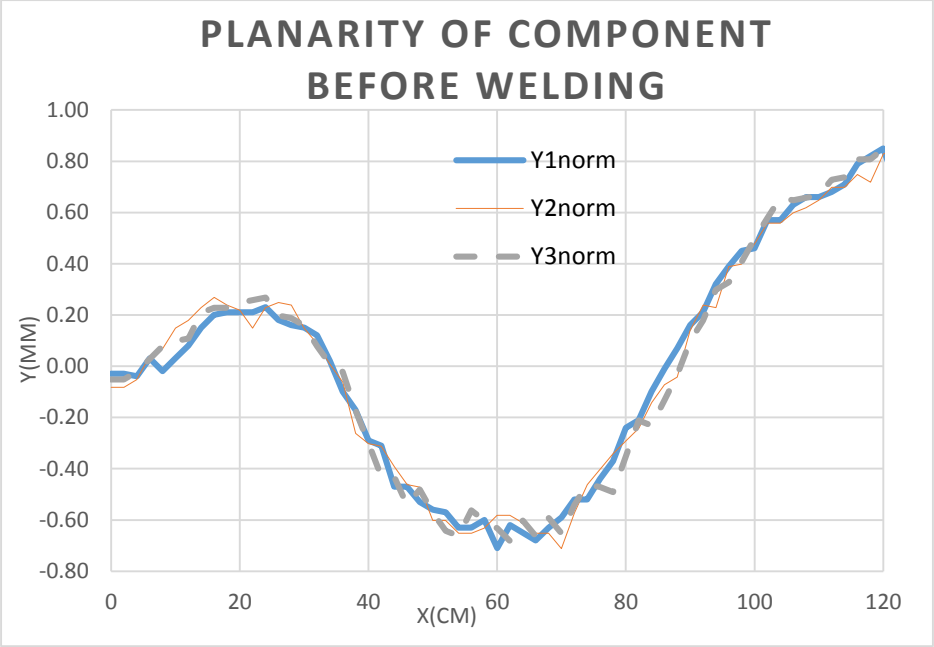

Figure 7-34 Planarity of component before proximity laser welding

After executing the welding, planarity is measured again. The same measurement is performed for three times. The difference between min and max value is 1.66 mm. Therefore in this case the planarity is even improved, Figure 7-35.

The difference between maximum and minimum normalized height in different step of measurement is reported in Table 7-2. The variances of averaged normalized heights (Y_{tot}) before welding is 0.16mm.

	Y1norm	Y2norm	Y3norm	YTOT
Min	-0.89	-0.94	-0.89	-0.88
Max	0.80	0.80	0.77	0.77
Max-Min	1.7	1.75	1.67	1.66

Table 7-2 Measurement of planarity after welding

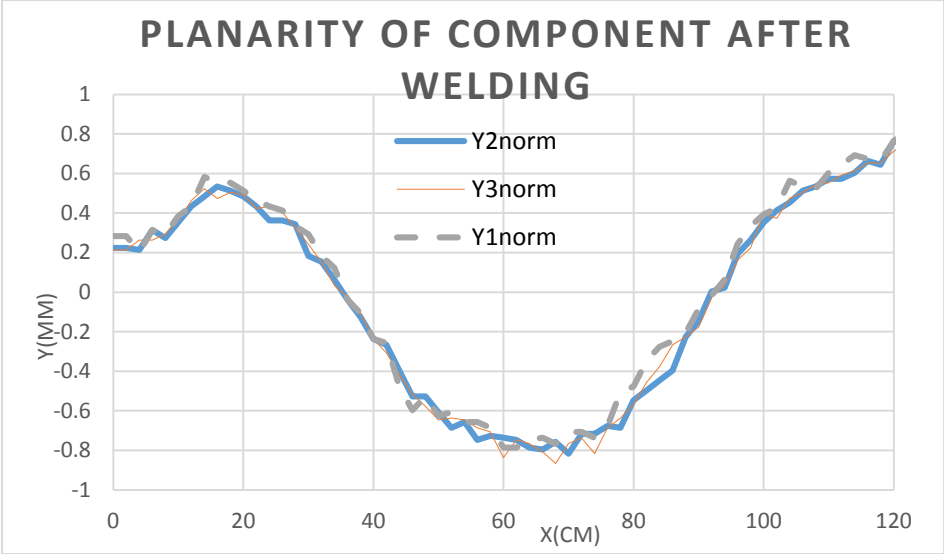

Figure 7-35 Planarity of component after proximity laser welding

In Figure 7-36 the comparison of planarity of pipe before and after welding is shown.

Y_{tot} is calculated as the Average of three different normalized height (Ynorm1, Ynorm2 and Ynorm3). It present that high speed laser welding, input very small amount of heat to the component and it is an outstanding solution for welding with minimum deformation in the component.

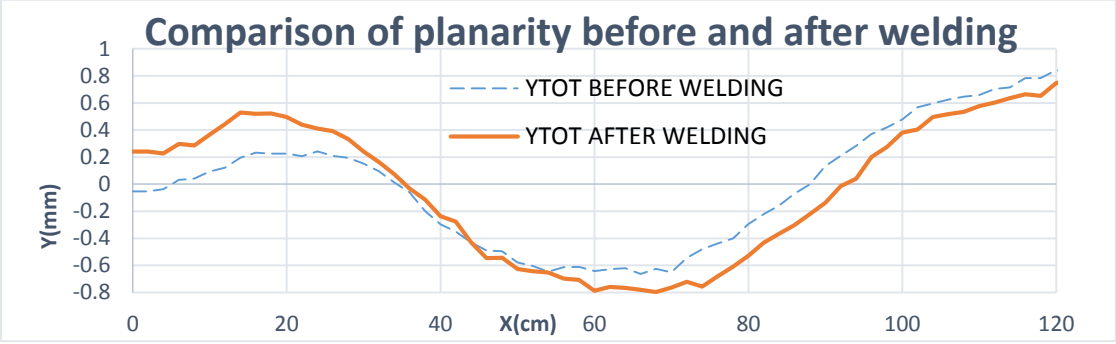

Figure 7-36 Comparison of planarity before and after proximity laser welding

7.2 Wobbling laser welding

The main objective of using laser welding with wobbling method (which is a very new and interesting technology of laser welding) in this experiment is studying the feasibility of using wobbling technique for different joint and also evaluating the effect of main parameters, particularly welding power and velocity. It is important to be taken in to account that remote welding with wobbling technique is the only choice for laser welding of butt joints without using of filler metal in order to compensate the gap.

7.2.1 Preliminary experiment for choosing proper velocity

In the first step bead-on-plate experiments were performed to obtain the appropriate laser parameters for welding with 3 kW power with the focus position on the surface. Three different velocities are tested in this step. No velocity more than 70 mm/s is tried since wobbling needs high energy in order to melt the material. At low velocity the pool is wide and large therefore it results in drop out. The micrograph of first three experiments is shown in Figure 7-37. In the two first tests the **drop out** defect is visible which is happened due to the high power and low velocity, Figure 7-38.

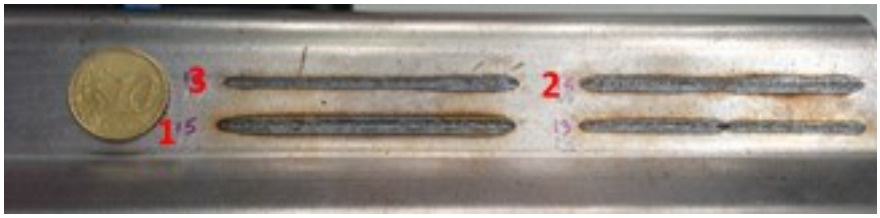

Figure 7-37 Welding on bop configuration, P=3Kw, V= 30 mm/s

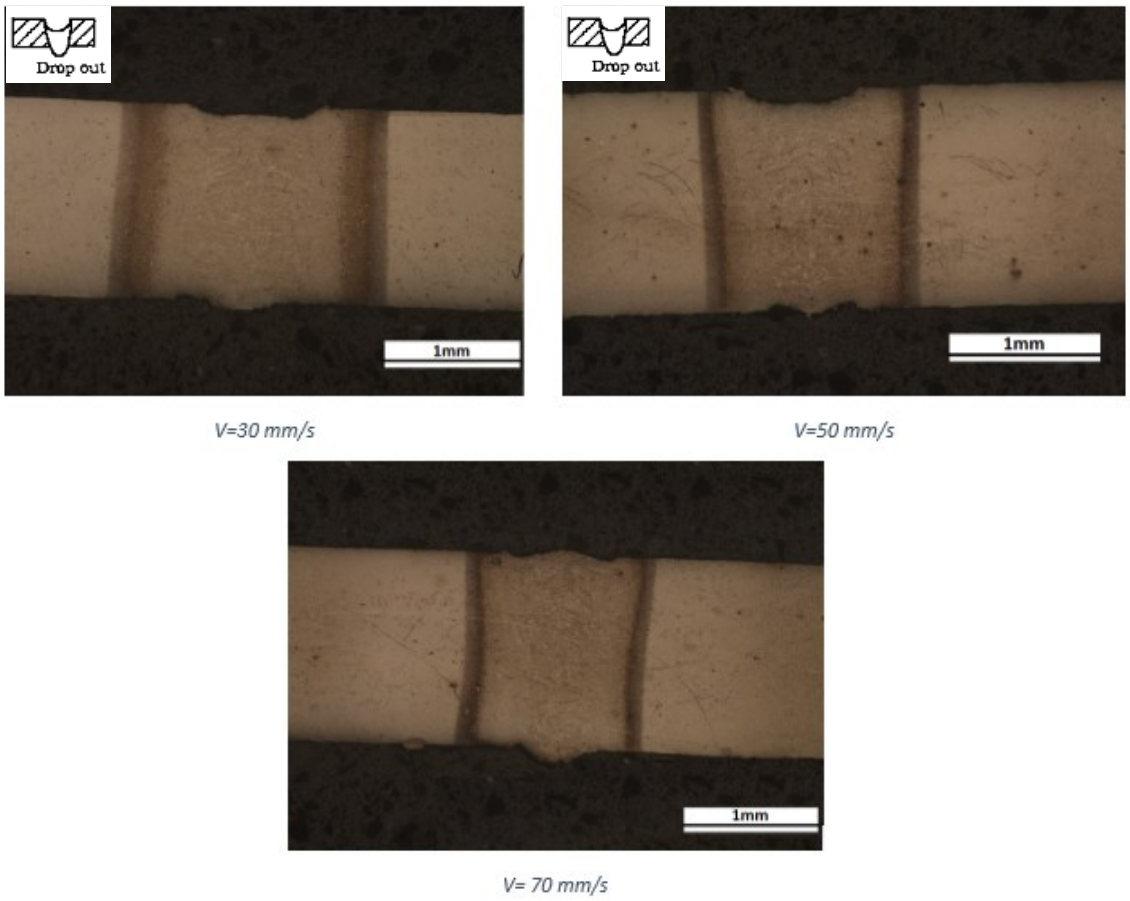

Figure 7-38 Welding on bop configuration, P=3Kw, V= 30 mm/s

7.2.2 Preliminary experiment on different joint configuration

Since the energy of drilling is needed for doing wobbling, the velocity of 30 mm/s is chosen for performing the second experiment test on different joints. Macrographs are shown in Figure 7-39.

Edge flange joint, P=3, V=30 mm/s

Butt joint, P=3Kw, V=30 mm/s

Lap joint, P=3, V=30 mm/s

Figure 7-39 Second step, No wobbling

Full penetration obtained in butt joint and lap joint butt as it is evident in the Figure 7-40 the material is drilled due to present of high power and low velocity.

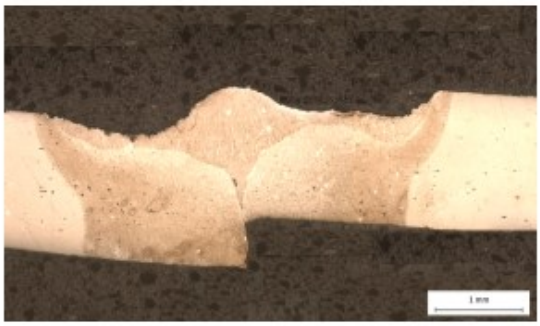

Butt joint, V=30 mm/s

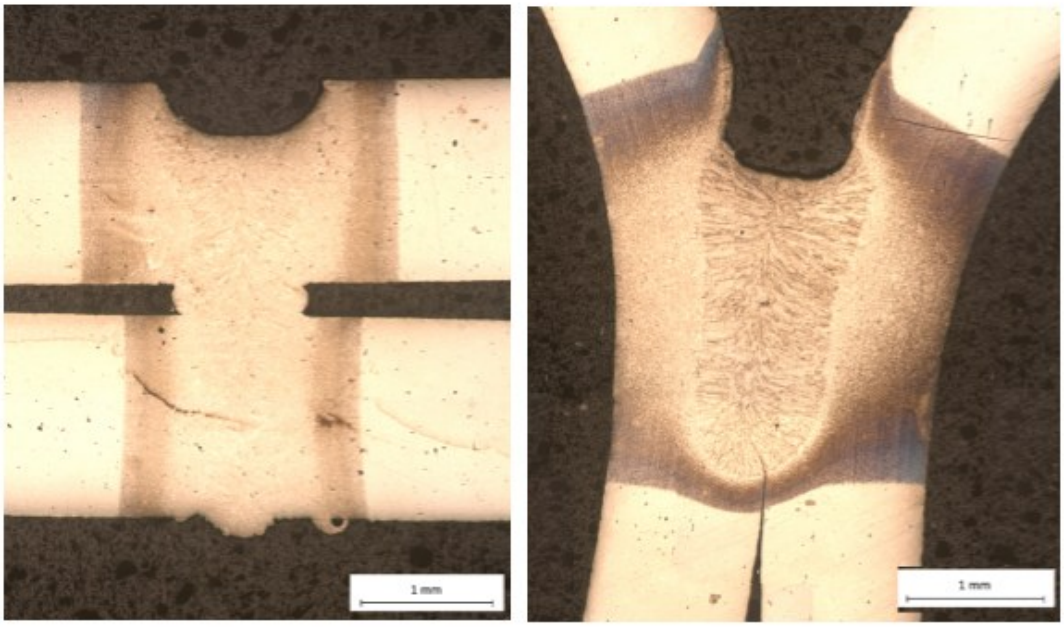

Lap joint, V=30 mm/s

Flange joint, V=30 mm/s

Figure 7-40 Remote laser wobbling, P=3Kw

Welding is performed without stirring the spot dimension, Butt in the lap joint no gap is present so it is welded properly, in order to weld joints with present of gap, in the next

experiment , two different PLU are tested on the material. Flange designs are common only in structural use. Since the weld does not penetrate completely through the joint thickness, it should not be used in stress or pressure applications [6].

7.2.3 Preliminary experiment with two levels of PLU

Third preliminary tests are performed with two different Values on the flanged joints, butt joints and lap joints. Micrographs and hardness tests are reported for each experiment. Flanged weld joints are shown in Figure 7-41. Hardness of weld is not decreased significantly and it's remain between 320HV, and 400 HV of hardness measured in the weld. As it is mentioned in the Proximity laser welding chapter Hardness of base metal is in range of 370-430. Also in wobbling laser welding since no filler metal is used Laser welds contains only martensitic microstructure but in wobbling method the fusion zone contains tempered martensite with corresponding hardness of 330 HV. Hardness of the HAZ decreased to 270 HV. Also in this case small heat affected zone equal to 1mm is obtained. Macrographs are shown in Figure 7-42.

Figure 7-41 Flanged joints wobbling test, P=3Kw, V= 30 mm/s

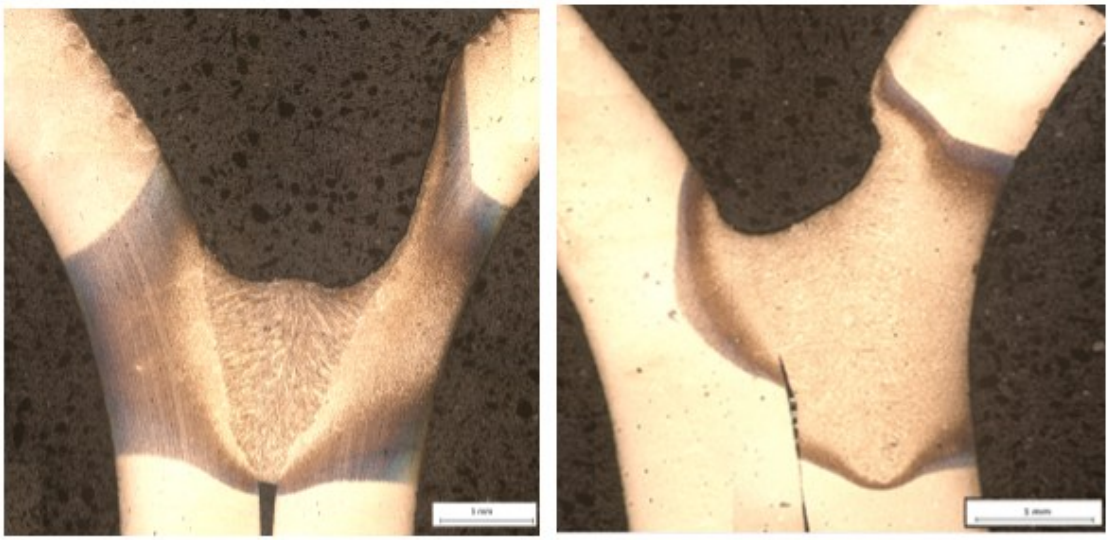

Figure 7-42 Flanged joints wobbling test, P=3Kw, V= 30 mm/s

Macrograph of lap joint welded with 20 PLU is shown in Figure 7-43. Hardness of weld is not decreased significantly and it's remained between 320HV, and 400 HV. As it is mentioned in the Proximity laser welding chapter, Hardness of base metal is in range of 370-430 HV. As it is mentioned at slow speeds the pool is large and wide and may result in drop out. In the both experiment which is done with 20 PLU and 40 PLU on the lap joint drop out defect is present. This problem can be solved with higher value of PLU. See Figure 7-45.

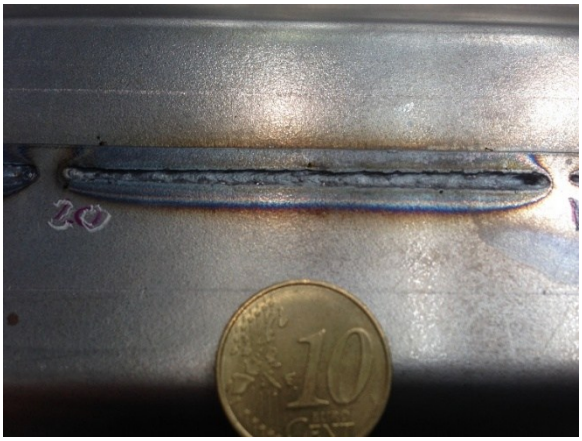

Figure 7-43, P=3 Kw, V=30 mm/s, Wobbling 20 PLU

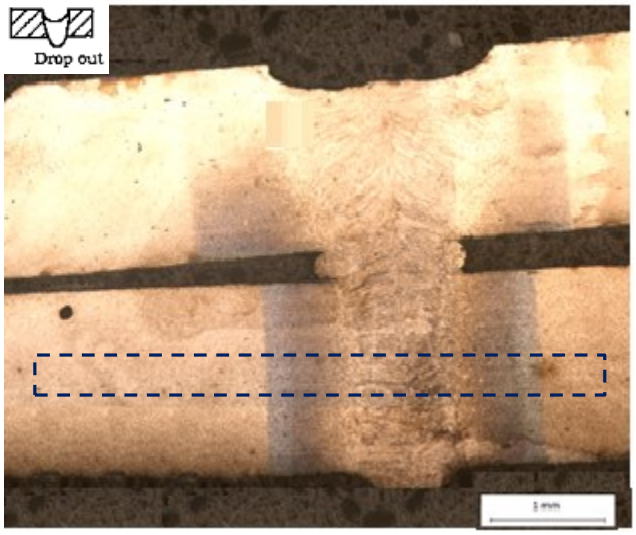

Figure 7-44 Lap joint, V=30 mm/s

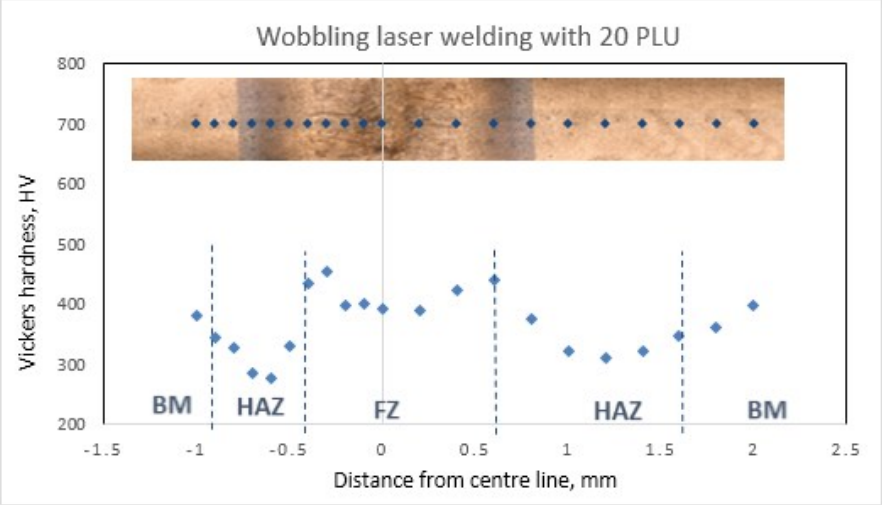

Figure 7-45 V=30 mm/s

Wobbling with 40 PLU is applied to another sample. Micrograph of lap joint welded with 3 Kw power and 30 mm/s is shown in Figure 7-46. Again the hardness in the fusion zone is not changed significantly, and length of HAZ is 2mm, Figure 7-48.The gap is present in lap joint since two sheets are not fitted precisely, Figure 7-47.

Figure 7-46 P=3 Kw, V= 30 mm/s

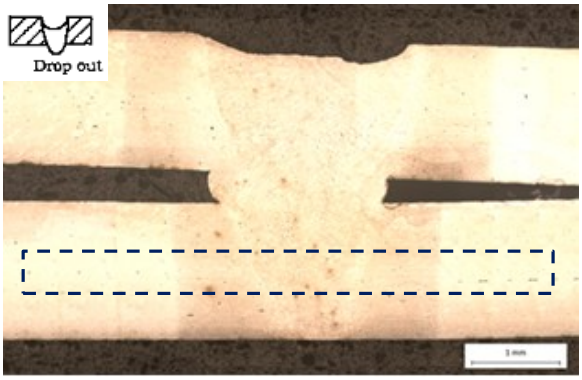

Figure 7-47 Lap joint, v=30 mm/s

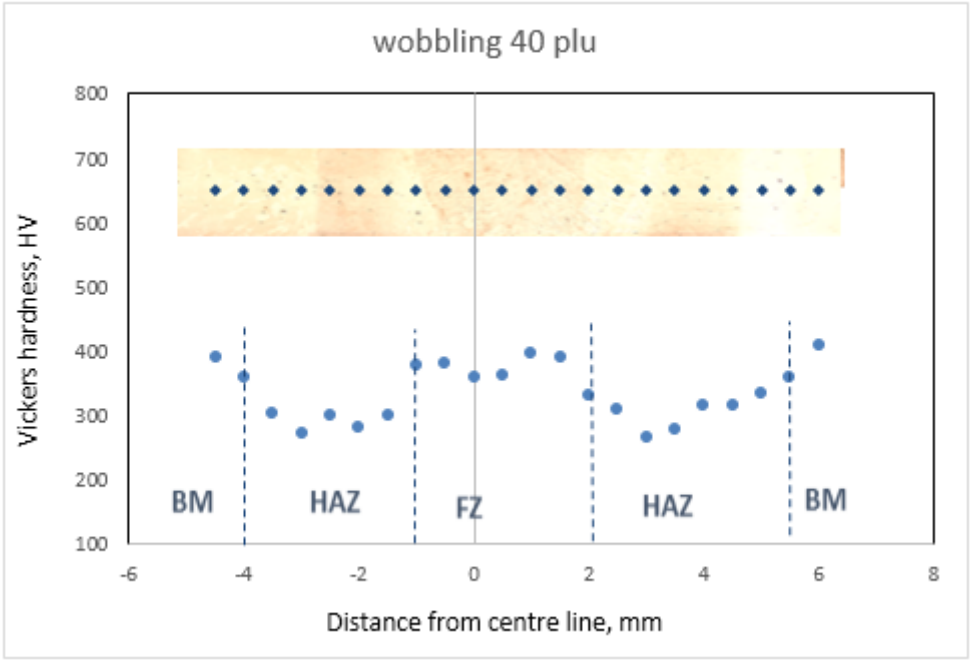

Figure 7-48 v=30 mm/s

Due to the present of big gap test n5 and n6 are not cut and sampled. The macrographs are showed in Figure 7-49.

Figure 7-49 Butt joint, P=3Kw, V=30 mm/s

7.2.4 Results and analysis of Welding on prototype

Values of hardness of upper and middle side of the sample are measured and shown in Figure 7-50. As it is mentioned in the Proximity laser welding chapter Hardness of base metal is in range of 370-430 HV. Also in wobbling laser welding since no filler metal is used Laser welds contains only martensitic microstructure but in wobbling method the fusion zone contains tempered martensite with corresponding hardness of 330 HV. Hardness of the HAZ decreased to 270 HV. Also in this case small heat affected zone equal to 1mm is obtained, Figure 7-51.

Figure 7-50 Prototype of wobbling test

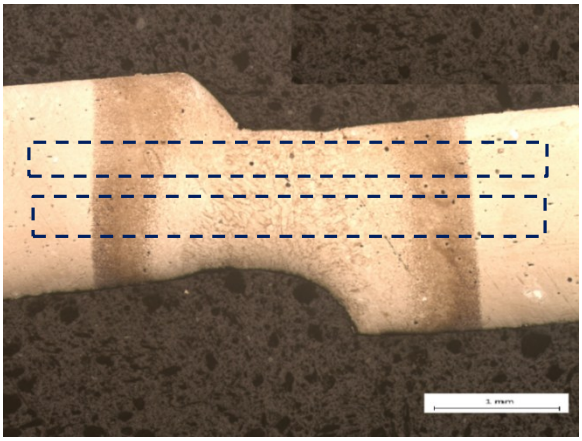

Figure 7-51 Micrograph of final test, P=3Kw

Wobbling with 80 PLU is applied to another sample. Micrograph of butt joint welded with 3 Kw power and 30 mm/s is shown in Figure 7-52. Again the hardness in the fusion zone is not decreased significantly, and length of HAZ is 1.5 mm.

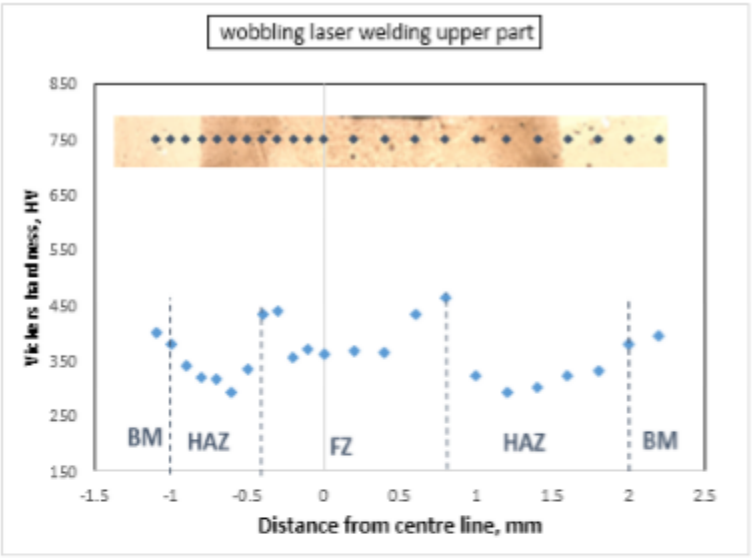

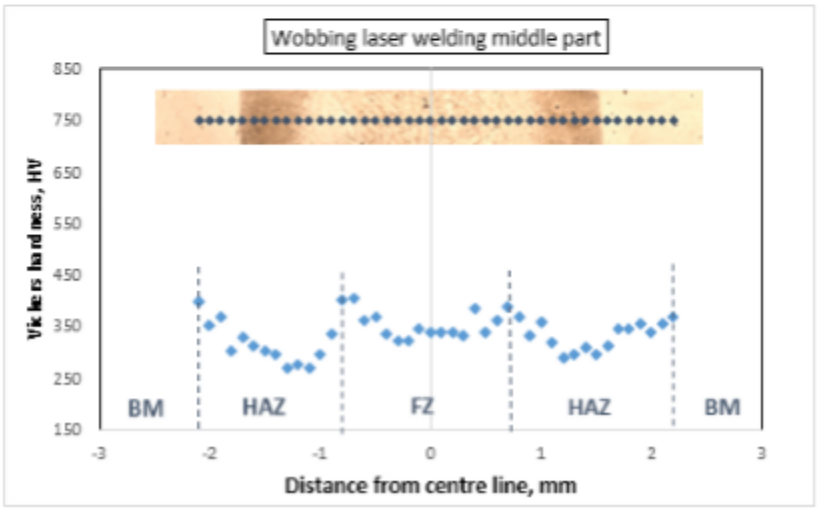

Figure 7-52 Hardness test with 80 PLU wobbling

Micro hardness is also evaluated for lower part of the component; also in this case micro hardness has the same trend. Hardness results are shown in the Figure 7-53 and Figure 7-54.

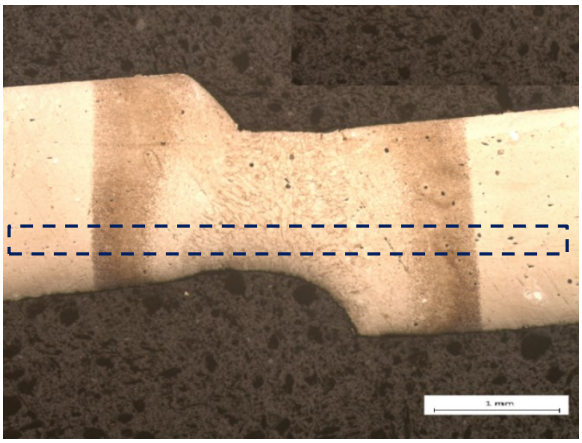

Figure 7-53 Wobbling welding, PLU=80 PLU

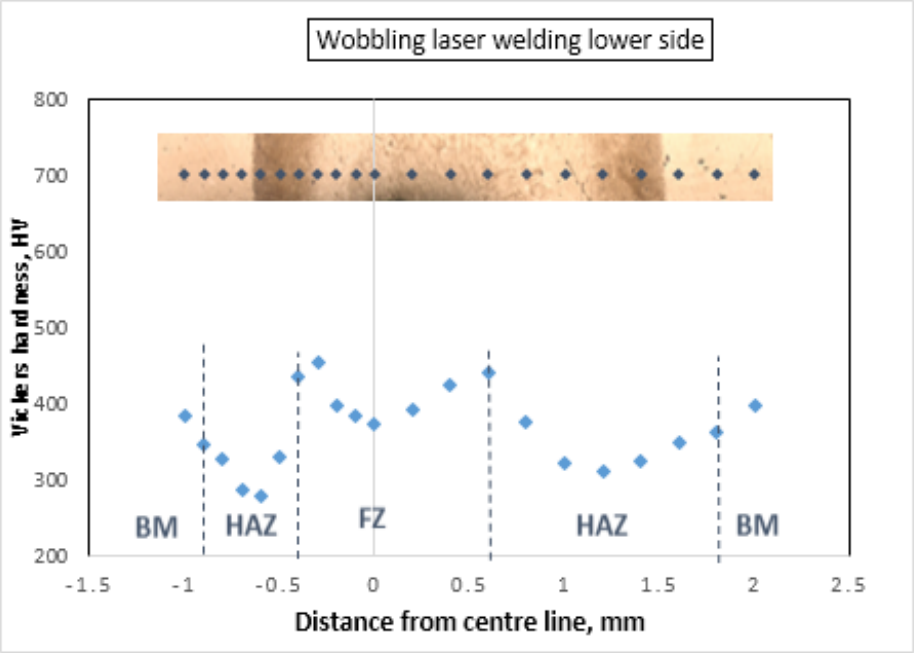

Figure 7-54 Hardness of final test with 80 PLU wobbling

7.2.5 Measuring the planarity of prototype

The basic concept of residual stress and deformation is explained in previous sections. It is explained that Welding stresses arise due to the inhomogeneous cooling and in steel these stresses are caused by the effects of non-uniformly distributed cooling contractions.

As mentioned before the heat input is calculated with$H(Kj) = \frac{p(kw)}{v(mm/s)} * l(mm)$.

In wobbling laser welding the test is performed with 3KW fiber laser with 30mm/s velocity and 80 PLU. The heat input in 20 mm weld length is 2Kj. So for the same length of proximity laser welding it will be 12 KJ. This value is more than 6 times of proximity laser welding pipe.

The same measurements as proximity welded pipe are done for the pipe welded with laser wobbling welding. All steps are repeated for three times. Before welding the difference between min and max value is 0.73 mm. the measurements are presented in Figure 7-55.

The difference between maximum and minimum normalized height in different step of measurement is reported in Table 7-3 and the variances of averaged normalized measured heights (Y_{tot}) before welding is 0.05 mm.

	Y1norm	Y2norm	Y3norm	YTOT
Min	-0.32	-0.31	-0.35	-0.33
Max	0.36	0.38	0.42	0.39
Max-Min	0.69	0.7	0.78	0.72

Table 7-3 Measurement of planarity before welding

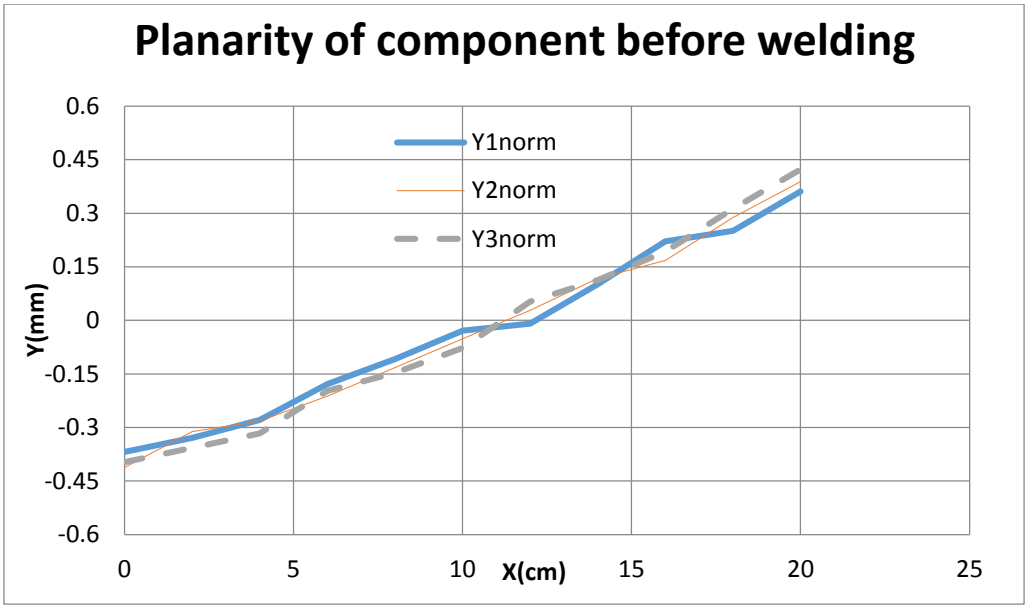

Figure 7-55 Planarity of component before wobbling laser welding

After executing the welding, planarity is measured again. The measurement is performed for three times. The difference between min and max value is 0.96 mm. As it is expected since we put more energy to the component in respect to proximity laser welding consequently more residual stress and deformation is obtained, Figure 7-56.

The difference between maximum and minimum normalized height in different step of measurement is reported in Table 7-4 and the variances of averaged normalized measured heights (Y_{tot}) before welding is 0.11 mm.

	Y1norm	Y2norm	Y3norm	YTOT
Min	-0.283	-0.314	-0.263	-0.28333
Max	0.697	0.666	0.667	0.676667
Max-Min	0.98	0.98	0.93	0.96

Table 7-4 Measurement of planarity after welding

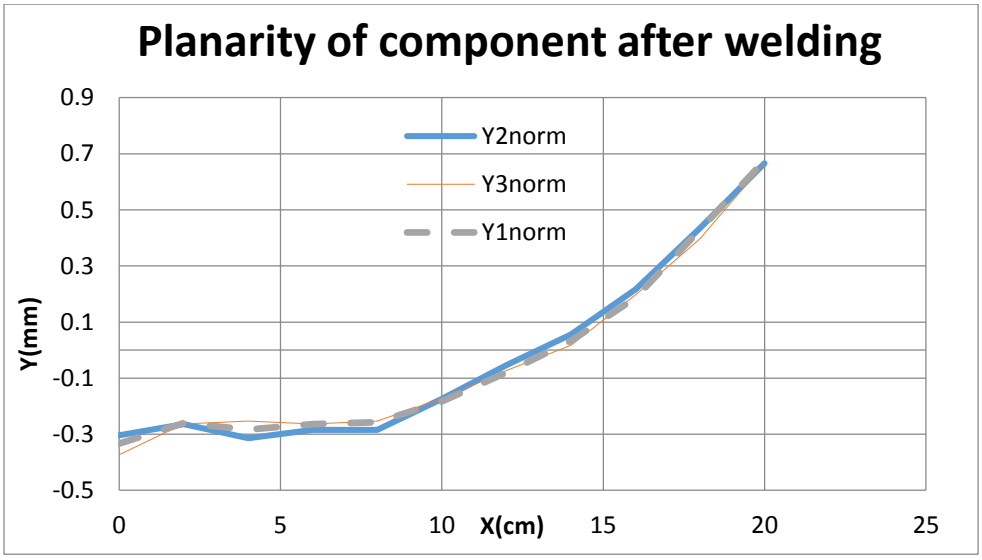

Figure 7-56 Planarity of component after wobbling laser welding

In Figure 7-57 the comparison of planarity of pipe before and after wobbling laser welding is shown. It presents that high speed laser welding; input very small amount of heat to the component and it is an outstanding solution for welding with minimum deformation in the component.

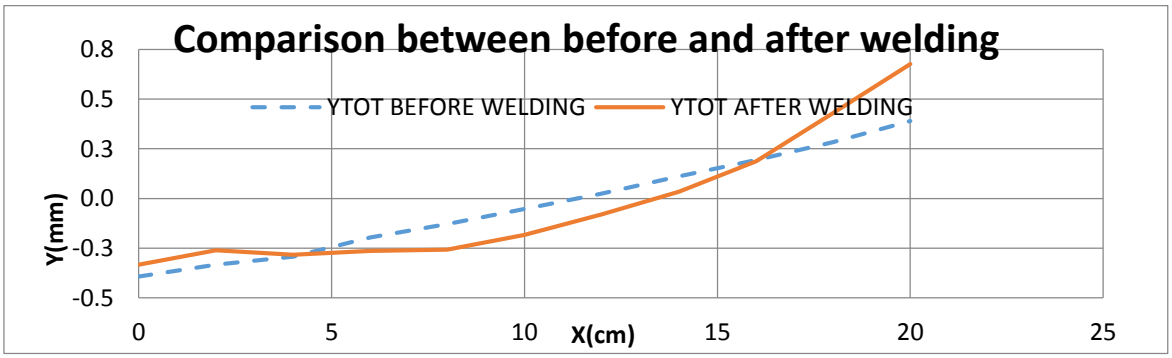

Figure 7-57 Comparison between before and after Wobbling laser welding

7.3 CMT welding result and analysis

Since the nature of welding with Cold Metal Transformation (CMT) is a rule based task and it is not knowledge based, fewer experiments are done in this step. In the first step of experiment $_{after}$ selecting the joint configuration, wire material and gas type for the program

prepared especially for the steel, other parameters e.g. WS (Welding Speed), current, WFS (Wire Feed Speed) and the voltage values are suggested by the machine.

7.3.1 Preliminary experiment with bead on plate configuration

The first experiment is done with bead on plate configuration; performing bead on plate welding is a proper way to have a better understanding of penetration of the weld and choosing good combination of process parameters to act welding.

First test is done with 12 (volt) and 175 A current. Velocity of welding is lower than laser welding and filler metal is used for welding. Micrograph of the first weld is shown in Figure 7-58 and Figure 7-59.

Figure 7-58 CMT welding V=10 mm/s

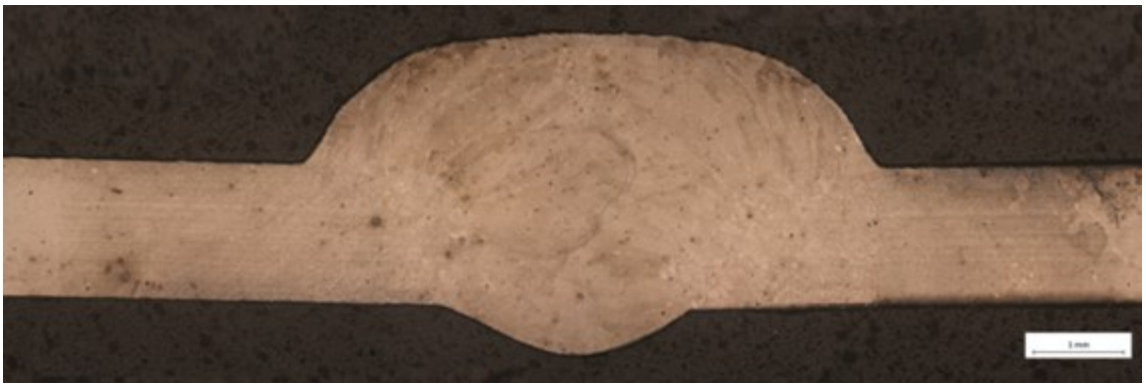

Figure 7-59 Velocity=10 mm/s

7.3.2 Preliminary experiment for selecting the proper velocity

The main goal of second experiment is modifying the travel speed in order to change the bead size and bead width. With increasing the travel speed both bead size and bead width decrease but it has no effect on penetration and little effect on the deposition rate. Two values of velocity are chosen for performing welding on the butt joint and flanged joint configuration. First experiment is performed with 12 voltage and 175 Ampere.

Figure 7-60 shows the micrographs of the first test. Unlike proximity Laser welding large heat affected zone equal to 2 mm is present in the material. As it is visible in the Figure 7-41, a hole is present in the weld. Values of hardness measured in the weld are shown in the Figure 7-61 and Figure 7-62.

Figure 7-60 CMT welding, V=20 mm/s

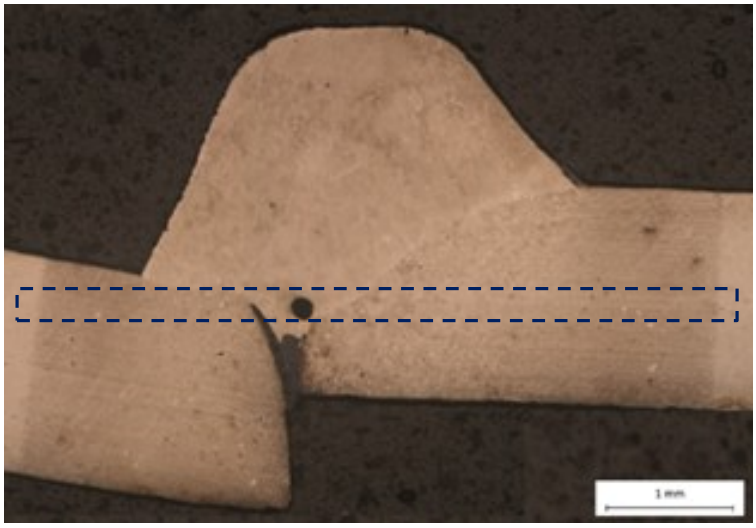

Figure 7-61 V=20 mm/s

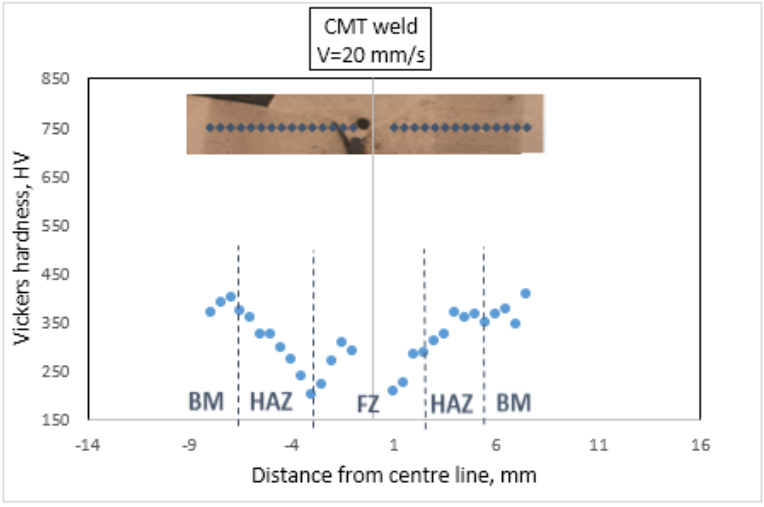

Figure 7-62 First CMT weld, V=20 mm/s

Second experiment is performed with 12 voltage and 175 Ampere. Figure 7-63 shows the micrographs of the first test. Also in this case large heat affected zone equal to 2.5 mm is present in the material. Values of hardness measured in the weld are shown in the Figure 7-64 and Figure 7-65.

Figure 7-63 CMT welding, V=20 mm/s

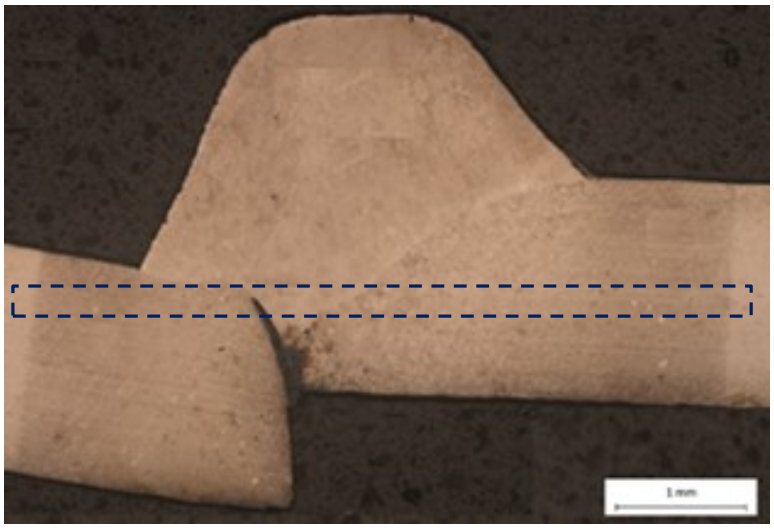

Figure 7-64 V=15 mm/s

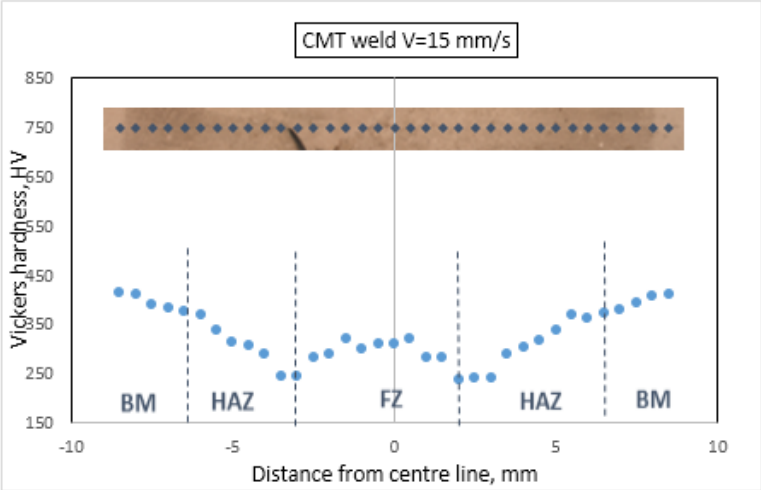

Figure 7-65 First CMT weld, V=15 mm/s

For welding flanged joint higher velocity is chosen in order to decrease the weld width and length to seal better the material. As it is mentioned changing the velocity has little effect in weld penetration in CMT welding. The corresponding hardness of fusion zone is equal to 280 HV and hardness of the filler metal is equal to 290 HV, Figure 7-66 and Figure 7-67.

Figure 7-66 CMT welding, V=20 mm/s

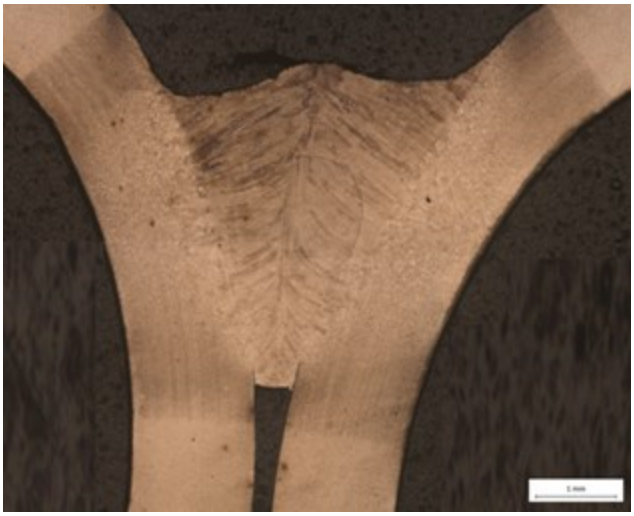

Figure 7-67 V=20 mm/s

Welding with velocity of 25 mm/s and 205 ampere is performed on the flanged joint as well. With increasing the travel speed both bead size and bead width decrease but it has no effect on penetration and little effect on the deposition rate. The tension is equal to 14 voltages, Figure 7-68 and Figure 7-69.

Figure 7-68 CMT welding, V=25 mm/s

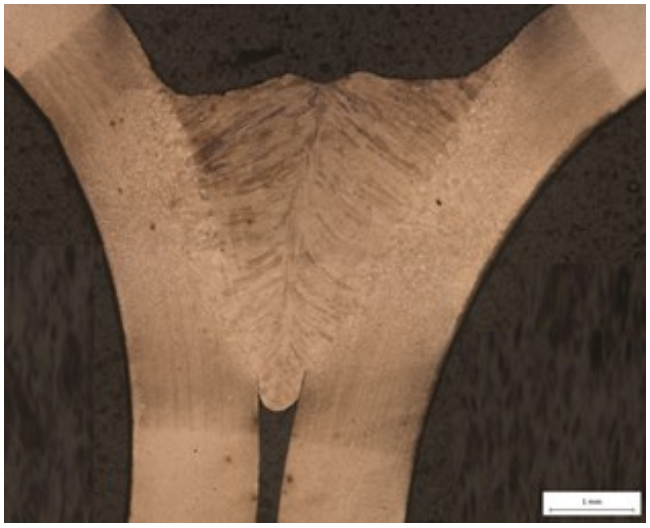

Figure 7-69 V=25 mm/s

7.3.3 Welding on prototypes

Due to the second preliminary test for obtaining the desired weld bead dimension an average value of velocities are chosen. The macrograph is shown in Figure 7-70.

Hardness of filler metal AWS, A, 5.28 is 290HV. The base metal of all pipes is the same and the corresponding hardness is between 370HV-430HV. Since weld contains filler metal microstructure degradation of material happens and in border of HAZ and FZ an area of coarser acicular microstructure of bainite with corresponding hardness of 230 is present. Hardness of the HAZ decreased to 220 HV. In this case large heat affected zone equal to 5mm is obtained, Figure 7-71 and Figure 7-72.

Figure 7-70 CMT welding, V=17 mm/s

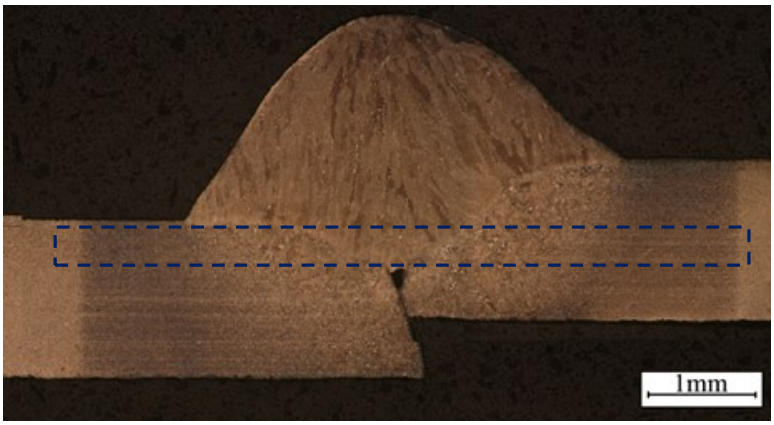

Figure 7-71 CMT welding of butt joint, V=17 mm/s

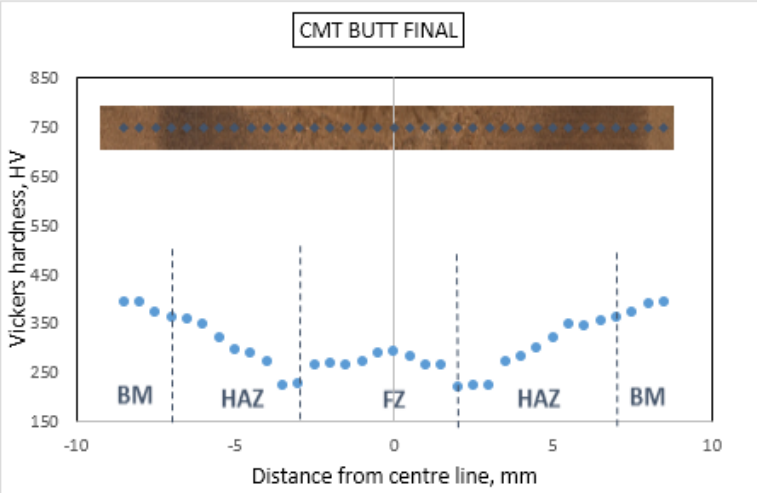

Figure 7-72 V=17 mm/s

Welding is also performed on the flanged joint with 22mm/s. The macrograph is shown in Figure 7-73. The value of hardness depends on how far is the point from fusion zone. The weld component in CMT welding is degraded by filler metal and hardness of fusion zone is dictated by filler metal as well. The second test is performed on both butt joint and flanged joint configuration. The current is equal to 205 (A), with the corresponding tension of 22 voltage. According to the hardness test, hardness test of fusion is 280 HV and heat affected zone is equal to 3 mm with hardness equal to 230 HV, Figure 7-74.

Figure 7-73CMT welding, V=22 mm/s

Figure 7-74 V=22 mm/s

Chapter 8: Cost-Tolerance modeling

In recent years unconventional welding process has been growing in the industries and market and their applications have continued to increase. However, very limited research work has been carried out to investigate their economic implications on tolerance allocation. This chapter reports cost relationships for non-traditional processes, including Proximity laser welding, Laser welding with wobbling technique and CMT welding. Docol M high strength steel (HSS) has been welded using the three processes to obtain cost-tolerance. An example is presented to illustrate the application and to compare the cost implication.

The welding cost can be broadly classified in to two categories, namely fixed and variable cost. For cost-tolerance, the fixed cost components such set-up cost is ignored since they do not vary with the tolerance. Thus, only the variable cost components will be considered. Machining cost components used in this work are adopted from [40].

The following are the variable costs that are common to Proximity laser welding, Laser welding with wobbling and CMT welding:

- ✓ **Machine**

This component consists of the machine depreciation rate and the machine overhead. The depreciation rate is calculated based on 9 hours of burn time per day, 240 productive days per year and an amortization period of 5 years. The machine overhead includes the cost of routine maintenance, the cost of unexpected breakdowns and services, and the cost of factory space used. This is estimated to be about 30% of the depreciation rate consequently it is calculated as: $M_M = €\ [\frac{Equipment\ price}{Amortization\ period*240*9} * (1 + Equipment\ price)]$

For laser welding machine cost is equal to 125000 (€) therefore the laser machine cost will be

$M_M = €\ [\frac{125000}{5*240*9} * (1 + 30\%)] = 40\ (€/h)$

But for CMT welding the cost of machine is less and equal to 30500 (€), subsequently the CMT welding machine is calculated from the same formula and it is equal to 7 ($€/h$).

Hence the machine cost of laser welding corresponding to the same amortization period is more than five times than CMT welding.

- ✓ **Labor**

This component is made up of the operator's wage rate and overhead. The operator's overhead includes training costs, employer's CPF contributions, medical and other fringe benefits. This is estimated as 60% of the wage rate. Accordingly the wage cost is estimated 15($€/h$) for both laser and CMT welding with overhead of 30%, consequently overall labor cost is calculated from this formula: M_L=Operators wage rate + Operators overhead.

M_L=15+15*30% ($€/h$) = 20 ($€/h$)

The labor cost is considered to be the same for laser welding and CMT welding and equal to 20 ($€/h$)

- ✓ **Electricity**

This is the cost of the electricity consumed by the machine in producing the part. Besides the above-mentioned components of the variable cost, there are other cost components that are unique to each process. The cost rate for electricity according to year 2014 in Italy is equal to 0.168($€/Kwh$). Considering 3Kw fiber laser consumption equals to 30 Kw. The formula for calculating electricity cost is equal to: M_P= (Cost rate) *(Consumed power), and for laser it's equal to $M_P(Laser)$=30*0.168=5 ($€/h$)

For CMT welding the power consumption is equal to:

Consumed power=Power source consumption +Robot consumed power

Therefore it is calculated as: M_P= (14*20+5000)*0.168/1000=0.88 ($€/h$)

Thus also Electricity cost of laser technology is way more than CMT welding.

- ✓ **Gas and wire electrode cost**

In CMT welding technology, gas cost and wire electrode cost must be taken in to account as well. Since laser welding is done without shielding gas and filler metal these costs are not considered in welding with laser technology. The consumption of gas and electrode can be slightly altered for different process. The gas and electrode consumptions are consistent

to real case which welding is performed. The formulas for calculating gas and electrode cost are:

Cost of gas/h, MG = (Cost per hour) × Gas flow.

Wire electrode cost= Mw = (Cost per roll/Length of wire) × Wire feed speed

The price of gas is equal to 0.006($\frac{€}{L}$) and gas flow in the process is equal to 21.5 l/min so overall gas price will be: MG= [0.006 x 21.5 x60 /h= 8($\frac{€}{h}$). The price of electrode per unit of meter is 60.00 ($\frac{€}{L}$) and welding is done with 8 m/min wire feed speed.

Taken as a whole the wire electrode cost will be: Mw= [60 * 8/14000] ($\frac{€}{\text{min}}$) = 2.05($\frac{€}{\text{h}}$)

As a result total welding cost for each process of welding can be obtained from the equations given below:

M_t(Laser) = $(M_{L+}M_{M+}M_P) * t_m$), t_m=Total time of operation. Fallowing this calculation overall cost for laser welding process in one hour will be 65 (€).

And overall cost of CMT laser welding process can be calculated from the equation given below:

M_t= $(M_{L+}M_{M+}M_P + M_G) * t_m$), t_m=Total time of operation

Therefore the welding cost with CMT technology will be 37($\frac{€}{\text{h}}$) and it is lower in respect to laser welding which is 65 (€).

Chapter 9: Conclusion

Laser welding is known to introduce considerably less heat input in to the material than conventional welding techniques. For the proximity laser welding coarsening in the HAZ is minimal, as well as the HAZ width (0.4 mm). The proper velocity range for 3Kw power proximity laser welding of Docol M is in the range of 100 mm/s- 200mm/s for different joint configuration.

Proximity laser welding with 3Kw power and 200 mm/s does not change the planarity of pipes and the planarity remains intact. On the other hand, softening and tempering took place in the HAZ. However, thanks to low amount of the heat introduced to the component the width of HAZ in Proximity laser weld is notably less than that in wobbling laser welds and CMT welds. The weld bead always showed higher hardness than that of wobbling laser welds and CMT welds. Hardness of laser welds is higher than other two technologies due to a greater temperature gradient and faster dissipation of heat. Even if the cost-tolerance/h of this technology is more than CMT welding, for high production rate the cost for unit will be less.

Bigger HAZ (1.5mm) is presented in Docol M joint welded with wobbling laser than in the HAZ of the proximity laser weld joint due to a lower welding speed and more heat input. The measurements of planarity show that the planarity changed in order of tenth of millimeter for 20 mm length pipe. On the contrary wobbling laser welding is a very new technology which permits access to areas not accessible with short focal length welding and makes welding possible in presence of big gap. The trend of hardness in wobbling laser weld is different from the proximity one. In the center of weld where the gap is present and the material is not available, the hardness decreases to 320 HV but the hardness in the border of HAZ and FZ has the same value of FZ in the proximity welding (405HV). Further investigation is needed on the weld bead of wobbling laser welding to understand the strength of weld bead, fatigue and other mechanical properties of the joint.

Consequently, in comparison with proximity laser welding and wobbling laser welding, CMT weld joints exhibit larger HAZ equal to 5mm (12 times more than proximity laser welds). Its grain structure is very coarse and due to present of filler metal is not purely martensite anymore and in border of HAZ and FZ an area of coarser acicular microstructure of bainite with corresponding hardness of 230 exists. The hardness is also depends on the

filler metal which is used for the welding process. In our case the hardness of filler metal (AWS/SFA A5.28 ER110) is equal to 290 HV which is more than HAZ hardness (220HV). The cost-tolerance of CMT welding is lower than other two technologies and it is not sensitive to the gap. More studies must be done on CMT welds in order to find out the mechanical properties of joint such as strength, tensile and fatigue properties.

References

1. Mallen, R.Z., Tarr, S., Dykeman, J, *Recent Applications of High Strength Steels in North American Honda Production.* http://www.autosteel.org/AM/ 2008.
2. Oscar Bjorklund, R.L., Larsgunnar Nilsson, *Failure of high strength steel sheets: Experiments and modelling.* Journal of Materials Processing Technology 2013: p. 1103–1117.
3. *www.ssab.com.* 2009.
4. L. Rizzo, L.t., *Improving and enlarging the application field of HSS and UHSS for automotive body Components by the integration of innovative technologies based on roll forming and stretch-bending processes* .European Commission, 2008: p. 25-35
5. Marciniak, Z.D., J. L.; Hu, S. J., *Mechanics of sheet metal forming. .* ISBN 2002: p. 75.
6. society, A.w., *welding joint.* 2009.
7. Encyclopedia, B.C., *Butt Joint welding.* 2003: p. 1997.
8. ASME, *Laser Beam Welding, Welding Fundamentals and Processes.* ASM Handbook 2011. **6**: p. 556–569.
9. T. Lienert, T.S., S. Babu, and V. Acoff, *Welding Fundamentals and Process.* ASM Handbook, 2011. **6A**.
10. Gahan, B.C., & Shiner, B, *New high-power fiber laser enables cutting-edge research.* Laser Technology 2004.
11. Diehl, R.E., *High-Power Diode Laser Fundamentals, Technology, Applications. .* Springer, 2000.
12. Quintino, L., Costa, A., Miranda, R., Yapp, D., Kumar, V., & Kong, C. J. , *Welding with high power fiber lasers - A preliminary study. .* Materials and Design (2007)(28): p. 1231-1237.
13. Thomy C, S.T., Vollertsen F, *Application of high-power fiberlasers for joining of steel and aluminium alloys.* Proceedings of the third international WLT-conference on lasers in manufacturing, 2005: p. 27-32.
14. R. Miranda a, A.C.a., *, L. Quintino a, D. Yapp b, D. Iordachescu, *Characterization of fiber laser welds in X100 pipeline steel* Materials and Design 2009. **30**: p. 2701–2707.
15. Mei Lifang a, Yan Dongbing a, Yi Jiming a, Chen Genyu b, Ge Xiaohong, *Comparative analysis on overlap welding properties of fiber laser and CO 2 laser for body-in-white sheets* Materials and Design 2013. **49**: p. 905–912.
16. S., R., *Laser welding efficiency and cost – CO2, YAG, Fiber and disc lasers.* ICALEO, 2004.
17. Ceglarek D, H.W., Zhou S, Ding Y, Kumar R, Zhou Y., *Time-based competition in manufacturing: stream-of-variation analysis (SOVA) methodology – review.* International Journal of Flexible Manufacturing Systems 2004, 2004. **16**(1): p. 11-44.

18. Maropoulos PG, C.D., *Design verification and validation in product lifecycle.* CIRP Annals – Manufacturing Technology 2010. **59**(2): p. 740-759.

19. Gábor Erd sa*, Z.K., András Kovácsa, József Váncza,, *Planning of remote laser welding processes.* Procedia CIRP 2013: p. 222 – 227.

20. R.S. Sharma, P.M., Journal of Materials Processing Technology 2011: p. 1888– 1897.

21. Rajashekhar S. Sharma, P.M., *Weldability of advanced high strength steels using an Yb:YAG disk laser.* Journal of Materials Processing Technology, 2011. **211**: p. 1888–1897.

22. Ream, S.L., *Disc and fiber gain ground.* Laser Focus World 2005. **20**(2).

23. Quintino, L., Costa, A., Miranda, R., Yapp, D., Kumar, V., Kong, C.J., *Welding with high power fiber lasers – preliminary study.* Materials and Design 2007. **28**: p. 1231–1237.

24. Yousuke Kawahito1, M.M.a.S.K., *Elucidation of high-power fibre laser welding phenomena of stainless steel and effect of factors on weld geometry.* Applied Physics 2007. **40**(19).

25. Kim, J.-K., Lim, H.-S., Cho, J.-H., Kim, C.-H, *Bead-on-plate weldability of Al 5052 alloy using a disk laser.* Journal of Achievements in Materials and Manufacturing Engineering 2008. **28**(2): p. 187–190.

26. Swift-Hook, D., Gick, A, *Penetration welding with lasers* Welding Journal 1973(52): p. 92.

27. Steen, W., Dowden, J., Davis, M., Kapadia, P, *A point and line source model of laser keyhole welding.* Journal of Physics D: Applied Physics 1988(21): p. 1255–1260.

28. Dowden, J.M., Davis, M., Kapadia, P, *The flow of heat and the motion of the weld pool in penetration welding with a laser.* Journal of Applied Physics, 1985(57): p. 4474–4479.

29. Kaplan, *A model of deep penetration laser welding based on calculation of the keyhole profile.* Journal of Physics 1994. **27**(9).

30. Huntington, C.A., Eagar, T.W., *Laser welding of aluminum and aluminum alloys.* Welding Journal 1982. **4**(62): p. 105.

31. Lankalapalli, K., Tu, J., Gartner, M, *A model for estimating penetration depth of laser welding processes. Journal of Physics D: Applied Physics* Journal of Physics D: Applied Physics, 1996: p. 1831.

32. Zhao, H., White, D.R., DebRoy, T, *Current issues and problems in laser welding of automotive aluminum alloys.* International Materials Reviews 1999. **44**(6): p. 238–266.

33. Fronius, B., *CMT process–A Revolution in Materials-Joining Technology.* 2004.

34. Hasselberg, T.P., *A Feasibility Study of "Cold Metal Transfer" on Nickel Base Superalloy Inconel 718™.* Rensselaer Polytechnic Institute Hartford, Connecticut, 2009: p. 11_13.

35. Ohio, E.D.L.O., *Welding, Brazing, and Soldering.* ASM International, 2007. **6**.

36. Brien, *American Welding Society.* Welding Handbook, 1991. **2**.

37. Bruckner, J., *"Cold Metal Transfer Has a Future Joining Steel to Aluminum.".* American Welding Society, 2005.
38. Ohio, D.L.O., *Welding, Brazing, and Soldering* ASM International, 2007. **6**.
39. Polak V., D.P., *ANALYSIS OF MODERN METHODS IN WELDING TECHNOLOGY OF TECHNICAL MATERIALS* Department of Technology and Automobile Transport, Faculty of Agronomy, Mendel University in Brno, Zemedelska 1, 613 00 Brno, Czech Republic
40. www.ABB.com/it.
41. Americanfillermetal, www.amfiller.com, 2013.
42. D.Tabor, *The Hardness of Metal.* Oxford university press, 2000.
43. Totten G, H.M., Inoue T., *residual stress and deformation of steel.* ASM International, 2002.
44. Pilipenko, *Computer simulation of residual stress and distortion on thick plates in multielectrode submerged arc welding.* Norwegian University of Science and Technology, 2001.